Title
Genes that control cell migration and cell polarity in C. elegans

Author
Harris, Jeanne Marie

Publication Date
1996

Peer reviewed|Thesis/dissertation

Genes that Control Cell Migration and Cell Polarity in C. elegans

by

Jeanne Marie Harris

DISSERTATION

Submitted in partial satisfaction of the requirements for the degree of

DOCTOR OF PHILOSOPHY

in

Cell Biology

in the

GRADUATE DIVISION

of the

UNIVERSITY OF CALIFORNIA

San Francisco

Date **University Librarian**

Degree Conferred: . . . . . .

Preface

I want to thank Cynthia Kenyon for her advice and encouragement throughout the course of my graduate career. Even when things weren't working, her firm belief that the *egl-20* gene was one of the most interesting things ever to happen to a worm made it easier to keep on with the project. I also appreciate the freedom Cynthia gave me to explore whatever interested me. The scientific independence that I developed as a result of this freedom is one of the most important things that I will take with me after graduation. The second thing I will always be indebted to Cynthia for is her patience and persistence in teaching me how to write a scientific paper. Together, my thesis committe, Cynthia Kenyon, Lou Reichardt, Yuh Nung Jan and Barbara Meyer, were instrumental in steering me through graduate school. They encouraged me to recognize what I had accomplished and to set realistic goals for what I had left to do. Their perceptive questions and reliable scientific insight helped guide my project.

Without the support and help of the members of the Kenyon lab I would never have finished this thesis. The Kenyon lab was an exciting place to work filled with many warm and caring people. Their help on evenings and weekends, moving worms and changing washes made it possible for me to do science around the constraints of daycare hours. I would especially like to thank Steve Salser, Julin Maloof, Craig Hunter, Lee Honigberg, Deborah Cowing, and Bruce Wang for much technical help, advice, and encouragement and for many wonderful discussions. My thanks also to Gregg Jongeward and Jennifer Whangbo, who have continued this project.

Throughout graduate school, my family has been a constant source of support and encouragment. Their interest in my chosen field, the people I work with and the my graduate school hurdles has helped me to complete

this work. I would like to especially thank my parents for telling me that I could do whatever I set my mind to. Their interest and encouragement has been very precious to me. I would also like to thank my aunt and uncle for their generous support and their unflagging interest in my work. My brother's scientific curiosity and questioning mind have been the source of many great discussions about my work and science or life in general.

My husband, Rama, has transformed my graduate school experience. I can't imagine the last 6 years without him. He is a wonderful companion and sounding board and a great person to talk to about experiments and lab worries. Rama's support and interest have made graduate school a joy. Finally, I would like to thank my daughter, Anna. Her presence in my life has put graduate school in perspective. Nothing has ever been the same since she was born - and I can't imagine my life without her.

Chapter 2 has been accepted to Development and Chapter 5 is being prepared for submission to Development.

Abstract

Genes that Control Cell Migration and Cell Polarity in *C. elegans*

What directs migrating cells to positions far from their birthplace? How is the polarity of asymmetric cells determined? What regulates the position-specific expression of the most widely-conserved members of the animal anterior/posterior patterning system, the Hox genes? In my analysis of *C. elegans* development, I found that the gene *egl-20* is required for all of these developmental events. *egl-20* activity directs the migrating QL neuroblast to express the Hox gene *mab-5*, which determines its direction of migration. Independent of its effect on Hox gene expression, *egl-20* also guides migrating Q descendants to more anterior positions in the body. I have shown that *egl-20* must regulate the production or response of local cell-cell signals to activate expression of the Hox gene *mab-5* in the V6 epidermal cell, and determine the anterior/posterior polarity of the V5 epidermal cell. Curiously, the same three genes, *mig-14*, *mig-1* and *lin-17*, interact with *egl-20* to regulate both expression of *mab-5* in a migrating cell and A/P polarity of a stationary cell. These observations suggest that stationary and migratory cells may share a system for determining position and orientation along the anterior/posterior axis.

Table of Contents

List of Tables

List of Figures

Chapter 1: Introduction

Introduction

The *C. elegans egl-20* gene plays a role in many different aspects of anterior/posterior (A/P) patterning: in particular, direction of cell migration and orientation of cell polarity. In *egl-20* mutants, certain neural cells that normally migrate towards the posterior now migrate towards the anterior. In addition, other migrating cells now migrate to positions shifted posteriorly to normal. I have found that the change in direction of migration is due to the failure of these cells to express the Hox gene, *mab-5*, but that the posterior shift in the migration stopping points is independent of the activity of any of the Hox genes of known function. Mutations in *egl-20* can also reverse the orientation of certain asymmetric cell divisions along the A/P axis. I have found that signals from neighboring cells can influence the orientation of polarity in an *egl-20* mutant, suggesting that *egl-20* may be a component of a signal/response pathway. Similarly, mutations in *egl-20* affect the response of the V6 epidermal cell to signals from its neighbor, T. In *egl-20* mutants, V6 is no longer able to activate the Hox gene *mab-5* in response to extracellular signals.

Proper regulation of cell migration, orientation of cellular asymmetry and Hox gene expression are all essential aspects of the development of other metazoans. These different processes all function to organize and pattern the developing body. Although the function of a single gene, *egl-20*, in these three processes underscores their similarities, cell migration, cell polarity and Hox gene regulation are very different events. In this chapter, I will review each one separately.

I. Cell Migration

Cell migrations play an important role in the development of all animals, from the concerted movements of large populations of cells at gastrulation to the organization of different cell types during organogenesis. The role of cell migration is perhaps most evident in the development of the nervous system. In vertebrates the entire peripheral nervous system is derived from cells that migrate out of the neural crest. In the CNS, the complex layered arrangement of the mammalian forebrain is formed when postmitotic cells from the germinal layer of the cortex migrate out towards the pial surface of the brain. Different types of neurons stop at different points, thus forming the many layers of the cerebrum. Cell migrations are also essential for patterning the nervous systems of invertebrates. In *Drosophila*, cell migrations fine-tune the pattern of neurons in the CNS and bring glial cells into the developing eye (Choi and Benzer, 1994). In the nematode *C. elegans*, several neurons, including both mechanosensory neurons and motoneurons, and also neuroblasts migrate, sometimes over long distances, to reach their final positions. In *Hydra*, interstitial cells migrate up through the body column to the head and peduncle, where they give rise to neurons (Teragawa and Bode, 1995).

What determines what direction cells migrate and where they stop? Molecules both inside and outside these cells must be responsible for guiding and directing their migration through specific regions of the animal. Although axon elongation involves cell growth, and cell migration does not, there are many aspects of these two processes that are analogous, and I will consider them both together. The migrations of both cells and axons can be guided by several distinct mechanisms: chemoattraction/repulsion, adhesion/anti-adhesion, and perhaps even endogenous electrical fields. Motoneurons in the chick and nematode migrate up gradients of an

attractant, a netrin (Kennedy *et al.*, 1994; Serafini *et al.*, 1994). Repulsive cues can guide the growth cones of chick retinal axons in the tectum and guide trochlear motor neurons away from the floor plate of the neural tube (Colamarino and Tessier-Lavigne, 1995; Dodd and Schuchardt, 1995; Tessier-Lavigne, 1995). The attractant could even be an electrical field, since neurites have been shown to grow towards the cathode and endogenous electrical fields have been observed in developing quail embryos (McCaig, 1988; Hotary and Robinson, 1990). The role of adhesion in cell migration and axon outgrowth has been well-studied. Integrin receptors serve as a structural link with neighboring cells or the extracellular matrix (ECM), but also as a signalling unit that recruits other components to focal adhesions and reorganizes the actin cytoskeleton (Clark and Brugge, 1995; Huttenlocher *et al.*, 1995). Downstream from the integrins, the *rho* subfamily of small GTP-binding proteins regulate focal adhesion formation and changes in actin polymerization, and tyrosine kinase activity has been shown to regulate both focal adhesion formation and adhesive release (reviewed in(Huttenlocher *et al.*, 1995). Intriguingly, some reports also suggest that localized proteolysis, or its inhibition, can also regulate the ability of cells to migrate (Monard, 1988; Chen, 1992) and possibly influence the direction of migration (Hawkins and Seeds, 1989), perhaps by locally modifying either the ECM or adhesive contacts.

Once mobilized, how are migrating cells and growth cones instructed that they have reached their target? This question of how cells know where they are is often too tightly connected to how they got there for these two processes to be treated separately. For example, the chemoattractant that guides the migration may be the same molecule that tells the migrating cells or axons that they have reached their target. Similarly, although repulsive factors often

direct migrating cells or growing axons to turn or migrate in the opposite direction (Colamarino and Tessier-Lavigne, 1995), such factors could conceivably cause the cell or axon to stop, if they were confined to a narrow track (either by fasciculation or adhesion) and were unable to migrate in any other direction than the source of the repulsive factor. Similarly, an anti-adhesive domain of S-laminin appearsc to act as a motoneuron-selective stop signal at the neuromuscular junction (Porter *et al.*, 1995), and too much adhesion may inhibit the release of contacts required in cell migration, and thus prevent cells from moving (Giancotti and Ruoslahti, 1990; Dimilla *et al.*, 1993). Alternatively, the migrating cell or growth cone might receive a signal to differentiate and stop migrating. This signal could be secreted by the target, thus effectively trapping the cell or axon by preventing it from migrating any further. Another variation is that the target cells could secrete a molecule which allows the cells near it to survive, while those farther away die. In this way nerve growth factor can act both as a chemoattractant and as a neurotrophic factor to both attract axons and then keeps the cells that extended those axons alive (Anton *et al.*, 1994; Behar *et al.*, 1994; Donovan *et al.*, 1995; Seedorf, 1995).

Clearly, for many migrating cells and growth cones the process of guidance and target recognition are indistinguishable. In some cases, however, target recognition could be a second event, independent of guidance, with the migrating cell or growth cone stopping in response to a specific molecule made by the target cell. In yet other cases, there may be no target recognition, and the positioning of migrating cells or axons may be due to other factors. For example, the guidance system that directed the migration of these cells or growth cones might fail to operate at a certain point, leaving the cells or axons stranded in a certain region of the body: the adhesive

gradient might run out, the chemoattractant or repulsive factor might no longer be secreted, or any of these molecules might be degraded or masked. Alternatively, the migrating cells and axons might differentiate in such a way that they could no longer recognize or respond to guidance cues. If the guidance system acted fairly reproducibly from animal to animal, then these cells and axons would always end up in the same region of the body, relatively near the same set of cells every time.

Several cells, both neuronal and mesodermal, migrate during *C. elegans* development (Sulston and Horvitz, 1977; Sulston *et al.*, 1983). As in vertebrates, some cells are guided by an attractive signal, others perhaps by a repulsive signal. For example, the migrations of the sex myoblasts in hermaphrodites are guided by an attractive signal from the developing gonad mediated by an FGF receptor (Devore *et al.*, 1995). Similarly, ventral-directed axonal and cell migrations in *C. elegans* are guided by an attractive signal, a netrin, encoded by the *unc-6* gene (Hedgecock *et al.*, 1990; Ishii *et al.*, 1992). In contrast, the dorsal-directed migrations of many axons may be guided by a repulsive effect of the UNC-6 netrin, much as its vertebrate homolog netrin-1 guides the axons of trochlear motor neurons in the spinal cord (Colamarino and Tessier-Lavigne, 1995). In addition to the FGF and netrin signalling systems, other molecules known to be required for cell migration in other organisms have been shown to be required for cell migration in *C. elegans*, such as a rac family member (Ilan Zipkin and Cynthia Kenyon, unpublished data) and a beta-integrin (Gettner, 1994).

In addition to molecules known to be required for cell migration in other organisms, genetic and molecular analysis of cell migration in *C. elegans* has revealed a role for the Hox genes in controlling the migratory fate of certain neuroblasts and neurons (Salser and Kenyon, 1991; Clark *et al.*, 1993; Wang *et*

al., 1993). In an organism as small as *C. elegans*, many different guidance cues may be located in the same region of the body. The Hox genes may act to restrict which set of cues a migrating cell may respond to.

In conclusion, cell migration in *C. elegans* appears to require similar molecules and mechanisms to migrations in vertebrates. In addition, the single-cell resolution and ease of genetic analysis make it possible to identify new roles for previously identified genes in the migration of specific cells.

II. Hox gene regulation

The Hox genes are a group of related homeotic genes homologous to the *Antennapedia* and Bithorax clusters of *Drosophila*, responsible for patterning the anterior/posterior (A/P) body axis. These genes are expressed in spatially restricted patterns along the A/P axis of such evolutionarily diverse organisms as *C. elegans*, crustaceans, flies, frogs, chicks and humans (Krumlauf, 1994; Lawrence and Morata, 1994). This spatial restriction is important, because Hox genes function cell-autonomously to specify cell fate (Krumlauf, 1994; Lawrence and Morata, 1994). What genes are responsible for this precise and highly reproducible pattern of gene expression? In *Drosophila*, proper expression of the Hox genes appears to depend on the earlier A/P patterning system involving the gap, pair-rule, and segment polarity genes (Lawrence and Morata, 1994). Interactions between the Hox genes themselves also regulate their expression. After these genes establish the initial pattern of Hox gene expression, the polycomb and trithorax group genes act to maintain the OFF or ON state, respectively (reviewed in (Orlando and Paro, 1995; Pirrotta, 1995; Simon, 1995; Tamkun, 1995).

The pattern of Hox gene expression is a highly dynamic and specific process: individual Hox genes can turn on and off within a cell or cell lineage

as the organism develops (Salser and Kenyon, 1996). This fine a level of gene regulation is easiest to study in an animal like *C. elegans*, where single-cell resolution is possible. It seems likely that this cell-specific change in Hox gene expression must be due to genes other than the gap and pair-rule genes which appear to affect broad swaths of cells in defined regions of the body. These genes could either act by directly activating or repressing specific Hox genes, or by inactivating the maintenance system.

In *Drosophila*, positional information appears to play a large role in regulating Hox gene expression (Krumlauf, 1994). Although any individual Hox gene in *C. elegans* is expressed by cells of a specific body region only, A/P position has not yet been shown to regulate expression of a Hox gene in *C. elegans*. In fact, Cowing and Kenyon (unpublished data) have demonstrated that expression of the *Antennapedia* homolog, *mab-5*, does not require posterior positioning of the expressing cell. Local cell-cell interactions play a role in regulating expression of *mab-5* in the V cells, epidermal blast cells in the *C. elegans* lateral hypodermis (Waring and Kenyon, 1990; Waring and Kenyon, 1991; Salser and Kenyon, 1996) and Salser and Kenyon, unpublished data) and may refine the pattern of *lin-39* expression in vulval precursor cells (Julin Maloof and Cynthia Kenyon, unpublished data). Similarly, (Hursh *et al.*, 1993) have demonstrated that the *Drosophila* Hox gene, *Ubx* is activated by the *dpp* gene, arguing that cell-cell signals may regulate Hox gene expression in *Drosophila* as well.

Many genes that regulate expression of the *C. elegans* Hox gene *mab-5* have been identified. Some of these genes have *Drosophila* homologs that also regulate Hox gene expression: *pal-1* is homologous to the gap gene *caudal* (Waring and Kenyon, 1991) and *egl-5* to the Hox gene AbdB (Salser *et al.*, 1993; Wang *et al.*, 1993) and *lin-22* to the primary pair-rule/proneural gene *hairy*

(Wrischnik, 1995). Other *C. elegans* mutants, however, demonstrate that genes not primarily involved in A/P polarity can also act to regulate Hox genes. For example, *lin-17*, homologous to the *Drosophila* tissue polarity gene *frizzled* (H. Sawa and R. Horvitz, pers. comm.), and *unc-40*, a potential netrin receptor with immuoglobulin and fibronectin type III domains (S. Chan, M-W Su, H. Zheng, J. Culotti and E. Hedgecock, pers. comm.), all are required to activate *mab-5* in the migrating QL neuroblast (see Chapter 2 and Appendix). The sequence of many other Hox gene regulators, such as *egl-20*, *mig-14* and *mig-1* have not yet been determined. Further analysis of these and other genes will help us to understand how Hox gene expression is regulated at the level of single cells.

III. Orientation of cell polarity

The generation of cellular asymmetry, the mechanism by which a mother cell divides to produce two different daughter cells, has been the focus of many studies over the years. However, the question of how that asymmetry is oriented has only recently begun to be addressed. In many cases, the orientation of an asymmetric cell division is predictable. What distinguishes one end of a cell from another? There are two possibilities: the cell could be born with an inherent asymmetry, or it could be sensitive to an environmental asymmetry.

The unicellular organisms *Caulobacter crescentus* and *Saccharomyces cerevisiae* both divide to produce two daughters with different fates. In each case, the orientation of this asymmetry can be predicted based on the site of the previous cell division. When the *Caulobacter* cells divide, one pole of each daughter cell is composed of newly synthesized material deposited during septation. When that daughter cell divides, the daughter that inherits

the more recently synthesized pole will develop into a swarmer cell, while the other daughter will develop as a stalk cell (Marczynski and Shapiro, 1995). Similarly, in *S. cerevisiae* haploids, the GTP-binding protein Bud1p (Rsr1p) recognizes a mark present at the site of the last cell division. Bud1p then assembles a large complex of signalling proteins at that site, including Cdc42p and Cdc24p, which subsequently initiate formation of a new bud at that location (reviewed in (Drubin and Nelson, 1996). Thus, for both *Caulobacter* and budding yeast, a molecular mark left at the site of a previous cell division generates an internal asymmetry that orients the polarity of the next asymmetric cell division.

An inherent asymmetry may also direct the orientation of the asymmetric division of the P1 cell, the posterior cell of a two-cell *C. elegans* embryo. The site of the previous cell division appears to be the location of a special actin-associated structure (Waddle *et al.*, 1994). A signal located in the vicinity of this structure appears to orient the P1 spindle, thus determining the orientation of P1 cell division and ensuring the segregation of germline determinants to the posterior daughter (Hyman, 1989). Thus for the P1 cell as well, the location of the previous cell division appears to play a major role in determining the orientation and polarity of its subsequent division.

An asymmetry present in the evironment can also provide information to distinguish one region of a cell from others. For example, the developing zygote of the brown alga, *Fucus*, is thought to be polarized by a localized Ca^{++} current, generated by a gradient of light, as the cell floats in the water (Quatrano *et al.*, 1979; Kropf *et al.*, 1988). Similarly, the dorsal/ventral polarity of the *Drosophila* oocyte, and later the embryo, is generated by a series of signals back and forth between the developing oocyte or embryo and its

neighboring somatic cells, the follicle cells (Shupbach and Roth, 1994; Gavis, 1995).

The above examples are all of individual cells; how is polarity determined within a tissue? Classic studies by Peter Lawrence revealed pattern reversals in insect epidermis following wounding. The gradient model that he proposed to explain tissue polarity has, until recently, been the most widely accepted (reviewed in(Lawrence, 1992). More detailed analysis of tissue polarity in the fly eye now suggests that local cell-cell signalling may determine the orientation of cell polarity in that tissue (Ma and Moses, 1995; Wehrli and Tomlinson, 1995; Zheng *et al.*, 1995). Further support for this model comes from the observation that *wnt* family members, *wingless* in *Drosophila* and *lin-44* in *C. elegans*, play a role in determining the orientation of polarized cells along the body (Herman and Horvitz, 1994; Theisen *et al.*, 1994; Herman *et al.*, 1995). Members of the *wnt* family are signalling molecules that act locally, perhaps only on adjacent cells, via components of cell junctions such as *armadillo*, the *Drosophila* plakyglobin homolog (Burrus, 1994; Klingensmith and Nusse, 1994). The local, directional non-autonomy associated with patches of *frizzled*(-) tissue in the fly wing are consistent with interruption of a signal that gets transmitted cell to cell along the proximal/distal axis of the wing (Vinson and Adler, 1987). Thus, it seems likely that local cell-cell signals may play a large role in determining tissue or cell polarity in both *Drosophila* and *C. elegans*.

Several genes have been identified in *C. elegans* that when mutated reverse the polarity of certain asymmetric cell divisions. Mutations in *lin-44*, a *wnt* family member, act non-autonomously to reverse the polarity of certain asymmetric cell divisions in the tail (Herman and Horvitz, 1994; Herman *et al.*, 1995). Mutations in *lin-17*, a frizzled homolog (H. Sawa and R.

Horvitz, pers. comm.), and *lin-18* reverse the polarity of cell divisions in the developing vulva (Ferguson and Horvitz, 1985). *lin-17* activity also appears to be required for the orientation of asymmetric cell divisions in many other tissues, including the somatic gonad and the male tail (Sternberg and Horvitz, 1988). In addition, *lin-17* function appears to be required for the generation of cellular asymmetry, since many asymmetric cell divisions now divide symmetrically in *lin-17* mutants (Sternberg and Horvitz, 1988). None of these genes appears to be required for orientation of all asymmetric cell divisions, although the *lin-44* mutation analyzed appears to eliminate gene function (Herman *et al.*, 1995). Since 807 out of 949 nongonadal cell divisions in *C. elegans* are asymmetric, and the polarity of most are constant, it seems likely that yet unidentified genes must also play a role in orientation of cell asymmetry in *C. elegans*.

Why is correct orientation of cell polarity so important? Positioning daughter cells with different fates in different environments may be more important in an organism as simple as *C. elegans*. In *C. elegans*, which has many different cell fates, but only 1059 non-germline cells, each cell makes an important contribution to the development of the organism. For example, polarity reversals in the vulval lineages cause abnormal morphogenesis, leading the formation of two adjacent vulvas, neither of them wild-type. Also, in tissues where there are lots of locally-acting inductive interactions, such as in the developing male tail, being in the right spot may be essential for a cell to develop properly. Mutations that cause polarity reversals in the male tail, such as *lin-17* and *lin-44* mutations, often have severely abnormal development and are unable to mate (Herman and Horvitz, 1994; Chamberlin and Sternberg, 1995). In other organisms, however, tissue development can be more flexible, and adjust to the altered division pattern.

For example, although the *tangled-1* mutation causes abnormal division orientation in the maize leaf, overall leaf shape is normal at all stages of growth, suggesting that for this organism, generation of organ (leaf) shape does not depend on the precise spatial control of cell division (Smith *et al.*, 1996).

Summary

In the following chapters I show that the *C. elegans* gene, *egl-20*, is required for several aspects of wild-type development: regulation of cell migration, orientation of cell polarity and activation of Hox gene expression.

I found that in *egl-20* mutants, the migrations of certain neurons and neuroblasts are abnormal: for example, the descendants of the neuroblast QL migrate towards the anterior instead of the posterior. In Chapter 2 I demonstrate that this change in direction of migration of the QL descendants is due to a failure to activate the Hox gene *mab-5* in the QL neuroblast and its descendants. Together with Lee Honigberg and Naomi Robinson, I showed that *egl-20* is a member of a group of four genes, which also include *mig-14*, *mig-1* and *lin-17*, that are all required for activation of *mab-5* in QL and its descendants. I also show that *egl-20* affects another aspect of cell migration. In *egl-20* mutants, the descendants of the neuroblast QR migrate towards the anterior as in wild-type, but stop short of their final wild-type positions. In Chapter 2, I demonstrate that this is not due to a defect in motility, but rather to a change in guidance: in *egl-20* mutants, migrating Q descendants seek out positions posterior to normal. Unlike its affect on direction of QL descendant migration, this *egl-20* phenotype does not act through any of the *C. elegans* Hox genes with known functions, *mab-5*, egl-5 or lin-39. Lee Honigberg has shown that *mig-14* also affects this aspect of cell migration and thus functions

with *egl-20* to regulate two different aspects of cell migration. To learn more about the different roles of *egl-20*, *mig-1* and *lin-17* in Q descendant migration, I analyzed the migrations of the Q descendants in animals that were mutant for two of these genes (presented in Chapter 3).

egl-20 is required to activate expression of the Hox gene *mab-5* in QL and its descendants but is not generally required for expression in other cells (see Chapter 2). In *pal-1(e2091)* mutants, the epidermal blast cell V6 does not express *mab-5*. However, *mab-5* can be activated in this cell in response to neighbor ablation (S. Salser, C. Hunter and C. Kenyon, unpublished data). Together with Craig Hunter in the lab, I showed that *egl-20* function is required for neighbor ablation to activate *mab-5* in V6 in *pal-1* mutants (Chapter 4). Analysis of the fates of V6 descendants in operated *pal-1; egl-20* mutants suggests that *mab-5* may come on at a later stage, in an *egl-20*-independent way.

In addition to its effects on cell migration and Hox gene expression, I found that *egl-20* affects the anterior/posterior (A/P) polarity of certain epidermal stem cells, in particular, that of V5. In wild-type animals, V5 divides with a characteristic polarity. This polarity can be reversed in *egl-20* mutants. In Chapter 5, I show that signals from posterior seam cell neighbors reverse the polarity of V5 in *egl-20* mutants, and signals from anterior seam cell neighbors restore wild-type polarity. Jennifer Whangbo in the lab has shown that when both anterior and posterior neighbors are ablated in *egl-20* mutants, the polarity of the V5 cell division is wild-type. Interestingly, V5 polarity is not sensitive to neighbor ablation in wild-type animals. This suggests that there are at least two ways to determine V5 polarity in *egl-20* mutants, and that the wild-type function of *egl-20* is to block either the generation of or response to signals from neighboring seam cells.

Together with Jennifer Whangbo, I have shown that mutations in the cell migration genes *lin-17*, *mig-1*, and *mig-14* suppress or enhance the *egl-20* V5 polarity reversal (Chapter 5). *lin-17*, homologous to the *Drosophila* tissue polarity gene, frizzled, is also required for the generation or orientation of many asymmetric cell divisions. We found that a *lin-18* mutation, which has a subset of the *lin-17* phenotypes, also suppresses the *egl-20* V5 polarity reversal, but not as strongly. Ablation analysis suggests that these genes are likely to act in the seam-cell signalling pathway, and not in the seam-cell independent pathway, since isolated V cells divide with wild-type polarity in these mutants. Since *egl-20* and *mig-14* also act to determine the stopping points of certain migrating cells along the A/P axis, these observations suggest that stationary and migratory cells may share a system for determining position and orientation along the anterior/posterior axis.

In order to better understand how and where *egl-20* acts, I initiated the cloning of the *egl-20* gene (Chapter 6). I used genetic and molecular markers to map *egl-20* to an interval of approximately 100 kilobases. To help identify the location of the *egl-20* gene in that interval, I designed a screen to identify *egl-20* mutations caused by large deletions (2-8kb). This cloning effort is being continued by Gregg Jongeward and Jennifer Whangbo. Molecular analysis of the *egl-20* gene should help us to understand how this gene can function in such diverse developmental events as cell migration, cell polarity and A/P pattern formation.

Chapter 2:

Neuronal Cell Migration in *C. elegans*: Regulation of Hox Gene Expression and Cell Position

Prepared for submission to Development.

This work was done in collaboration with Lee Honigberg and Naomi Robinson. Lee Honigberg performed all the analysis of the *mig-14* mutations and analyzed ALM, CAN, M and muIntR migrations in *mig-1* mutants. Lee

also developed and performed laser-induced heat shock of a single cell. Naomi Robinson followed the migrations of QL and its descendants in *mig-1* mutants and constructed and analyzed the *mig-1; mab-5(gf)* double mutant strain. In addition, Naomi constructed the *egl-20; mig-13* double mutant and the *mab-5; egl-20; mig-13* triple mutant strains. All the remaining data is my work, as is the writing.

Summary

In *C. elegans*, the Hox gene *mab-5*, which specifies the fates of cells in the posterior body region, has been shown to direct the migrations of certain cells within its domain of function. *mab-5* expression switches on in the neuroblast QL as it migrates into the posterior body region. *mab-5* activity is then required for the descendants of QL to migrate to posterior rather than anterior positions. What information activates Hox gene expression during this cell migration? How are these cells subsequently guided to their final positions? We address these questions by describing four genes, *egl-20*, *mig-14*, *mig-1* and *lin-17*, that are required to activate expression of *mab-5* during migration of the QL neuroblast. We find that two of these genes, *egl-20* and *mig-14*, also act in a *mab-5*-independent way to determine the final stopping points of the migrating Q descendants. The Q descendants do not migrate toward any obvious physical targets in wild-type or mutant animals. Therefore, these genes appear to be part of a system that positions the migrating Q descendants along the anteroposterior axis.

INTRODUCTION

Cell migrations play an important role in development. Concerted movements of large numbers of cells help to establish the different tissue layers during gastrulation, and the migrations of individual cells contribute to tissue organization and body pattern. For example, cells of the vertebrate neural crest migrate from their birth place over the neural tube to different locations throughout the body, generating widely distributed neuronal and non-neuronal tissues. Invertebrates such as *Hydra*, *C. elegans*, and *Drosophila* all require cell migration to develop normally (Hedgecock *et al.*, 1987;

Teragawa and Bode, 1990; Montell, 1994). For cell movement to be a reproducible part of development, the migrations of these cells must be guided. Some cells migrate towards a visible target which supplies a guidance cue; for example, germ cells are attracted to and migrate towards the genital ridge in mammals (Godin *et al.*, 1990). However, many migrating cells stop at positions that are not associated with any obvious physical structures.

A number of genes required for cell migration have been identified in the nematode, *C. elegans*. Dorsal/ventral (D/V) migrations in *C. elegans* are guided by the netrin UNC-6 (Hedgecock *et al.*, 1990; Ishii *et al.*, 1992), in a highly conserved process that has also been shown to guide D/V migrations of axons in the developing vertebrate nervous system (Kennedy *et al.*, 1994; Serafini *et al.*, 1994). The guidance of migrations along the anteroposterior (A/P) axis in *C. elegans* has been shown to involve the gene *vab-8*, which is required for the posterior migration of cells and axons (Wightman *et al.*, 1996). However, in general, the guidance of cells along the A/P axis is less well-understood.

We have chosen to focus on the migrations of the neuroblasts QL and QR, which migrate along the A/P body axis in *C. elegans*. The Q cells are similar to neural crest cells in that they delaminate from an epidermal epithelium and go on to populate regions of the body with sensory neurons (Sulston and Horvitz, 1977; Chalfie and Sulston, 1981). The Q cells and their descendants migrate to highly reproducible positions in a relatively uniform region of the body. QL and QR are born in the same A/P position on opposite sides of the animal, QL on the left and QR on the right. Although they undergo an identical sequence of cell divisions, the two Q cells and their descendants migrate in opposite directions: QL and its descendants migrate

towards the posterior whereas QR and its descendants migrate towards the anterior (Sulston and Horvitz, 1977) (Fig. 2.1).

The *C. elegans* Hox genes *lin-39* and *mab-5* play important roles in regulating the migrations of cells in the Q lineages. *lin-39*, the *C. elegans Sex combs reduced* homolog that specifies cell fates in the mid-body region, is required for the anterior migration of the QR descendants (Clark *et al.*, 1993; Wang *et al.*, 1993). *mab-5*, the *C. elegans Antennapedia* homolog that specifies cell fates in the posterior body region, is required for the posterior migration of the QL descendants (Chalfie and Sulston, 1981; Kenyon, 1986). Salser and Kenyon (1991) have shown that *mab-5* acts as a switch to determine the direction of migration. If *mab-5* is ON, the Q descendants migrate towards the posterior; if *mab-5* is OFF, the Q descendants migrate towards the anterior (Salser and Kenyon, 1991; Fig. 2.1). Here, we extend these results by using a laser microbeam to activate a *heat-shock-mab-5* fusion gene (Salser and Kenyon, 1991) exclusively within a migrating cell. Our findings, together with previous genetic mosaic analysis (Kenyon, 1986) argue that *mab-5* acts within migrating Q descendants to determine their direction of migration.

The state of *mab-5* expression within QL or QR determines whether their descendants will migrate to anterior or posterior positions. However, additional information is required to specify the final positions of these cells, since each QL descendant migrates to a characteristic position in the posterior and each QR descendant migrates to a characteristic position in the anterior. There are no obvious cellular targets located at these stopping points.

To understand better how these cells find their characteristic positions along the A/P axis, we have identified and characterized mutants in which cells in the Q lineage migrate to incorrect positions. Here we show that four of these genes, *egl-20*, *mig-14*, *mig-1* and *lin-17*, are required to turn on the Hox

gene *mab-5* in the migrating QL cell. When these gene activities are reduced or eliminated, QL and its descendants do not express *mab-5* and consequently migrate towards the anterior. Two of the genes, *egl-20* and *mig-14*, also act in a *mab-5*-independent way to determine the final stopping points of the migrating Q descendants along the A/P axis. Whether or not cells in the Q lineage are provided with *mab-5* activity, in the absence of *egl-20* or *mig-14* gene activities, they migrate to positions shifted posterior to the positions that they would otherwise seek: Cells that would migrate posteriorly go too far and cells that would migrate anteriorly stop short. In addition, cells that would remain stationary migrate posteriorly, and cells that would only migrate a short distance anteriorly instead reverse direction and migrate posteriorly. Thus, in addition to activating *mab-5* expression in the migrating QL cell, *egl-20* and *mig-14* appear to participate in a guidance system that determines the final stopping points of cells in the Q lineage. Together, these four genes provide entry points into understanding how migrating cells are positioned along the body axis.

MATERIALS AND METHODS

General Procedures, Nomenclature, and Strains

Methods for routine culturing and genetic analysis are described in (Brenner, 1974) and (Sulston and Hodgkin, 1988). Analyses were performed at 25°C, unless otherwise noted. The wild-type strain N2 is the parent of all strains used with the exception of *egl-20(n1437)*, which was isolated in an MT2878 background (G. Garriga, pers. comm.). Mutations not described in this paper are described by (Hodgkin *et al.*, 1988) or are noted below.

Mutations used:

LG I: *lin-17(n671), lin-17(n677), lin-17(e1456)* (Ferguson and Horvitz, 1985) *mig-1(e1787), mig-1(mu72), mig-1(n687), mig-1(n1354), mig-1(n1652),* (Desai et al., 1988) *lin-6(e1466), dpy-5(e61), jeIn1[mec-7-lacZ+pRF4(rol-6d)]* (Hamelin et al., 1992)

LG II: *mig-14(mu71), mig-14(k124)* (pers. comm. Kiyoji Nishiwaki), *rol-1(e91), unc-52(e444).*

LG III: *mab-5(e1239), mab-5(e2088), mab-5(e1751gf)* (Hedgecock et al., 1987; Salser and Kenyon, 1991), *pag-1(ls2)* (Guofeng Xie and Eric Aamodt, pers. comm.)

LG IV: *unc-24(e138), dpy-20(e1282), egl-20(n585), egl-20(n1437),* (Desai et al., 1988) *egl-20(mu25), egl-20(mu27), egl-20(mu39), unc-31(e169), muIs6 [lin-39-lacZ + pRF4(rol-6d)]* (Wang et al., 1993).

LG V: *him-5(e1490)*

LG X: *mig-13(mu31)* (Robinson, 1995) *muIs5 [lin-39-lacZ + pRF4(rol-6d)]* (Wang et al., 1993), *muIs9[hs-mab-5 + C14G10(unc-31^{+})]* (Salser et al., 1993).

Rearrangements: *eDf19 , tDf3 , tDf4* (Ahn and Fire, 1994), *jDf1, jDf2, jDf4* (Jacobson et al., 1988)

Isolation of mutants with misplaced QL descendants

mig-14(mu71) and *mig-1(mu72)* were isolated in a screen for mutants with misplaced Q descendants. In order to visualize the Q descendants using a dissecting microscope, we used a *mec-7-lacZ* fusion, which is expressed in the touch receptor neurons AVM (QR.paa) and PVM (QL.paa) (Hamelin *et al.*, 1992) and an X-gal staining protocol that does not kill the eggs inside a stained hermaphrodite (Xie *et al.*, 1995). EA23 *jeIn1*[*mec-7-lacZ*+pRF4(*rol-6d*)]; *pag-1(ls2)* hermaphrodites were mutagenized with ethyl methanesulfonate (EMS; (Brenner, 1974). (*pag-1(ls2)* increases the intensity of *mec-7-lacZ* expression;

Guofeng Xie and Eric Aamodt, pers. comm.) 3500 F2's from these animals were screened for the absence of a staining cell in the posterior where PVM is normally found.

egl-20(mu25) is an EMS-induced allele isolated in a screen using Nomarski optics to visualize animals with misplaced Q descendants. *egl-20(mu39)* was isolated in a screen for EMS-generated mutations affecting the expression of a *mab-5-lacZ* fusion gene, which will be described elsewhere (Maloof and Kenyon, unpublished data).

egl-20(mu27) was isolated in a non-complementation screen. EMS-mutagenized *him-5(e1490)* L4 males were mated to *unc-24(e138) egl-20(n585)* hermaphrodites. Approximately 2100 F1 non-Unc L4 hermaphrodites were picked away from their male siblings, grown to adulthood and screened for the Egl phenotype. Their progeny were screened for a QL.(d) migration (Mig) defect. Since *unc-24(e138) egl-20(n585)/eDf19* are viable, fertile and Egl, we should be able to identify and recover complete loss-of-function alleles in this screen.

Forty-eight percent of *mab-5(e2088)/+; egl-20(n585)/+* animals have QL.pa daughters in anterior positions (i.e. in the V1-V3 region; n=56). To rule out the possibility that these new mutations were unlinked non-complementing mutations, we mapped *mu25*, *mu27* and *mu39* to the *egl-20* region, using *unc-24(e138)* and *dpy-20(e1282)* (see next section; data not shown).

Genetic Mapping

egl-20. The *egl-20* gene maps to LG IV (Trent *et al.*, 1983). We mapped *egl-20* between the genes *unc-24* and *dpy-20*. From heterozygotes of genotype *unc-24(e138) + dpy-20(e1282)/ + egl-20(n585) +*, 9/14 Dpy non-Unc recombinants

and 8/20 Unc non-Dpy recombinants segregated Mig progeny. We also found that the deficiency *eDf19* failed to complement *egl-20(n585)* (data not shown).

mig-14. *mig-14(mu71)* was mapped to the right arm of LGII using STS markers (Williams *et al.*, 1992). Three-factor mapping placed it between *rol-1* and *unc-52*: from *rol-1(e91) unc-52(e444)/mig-14(mu71)* heterozygotes, 4/25 Rol non-Unc recombinants segregated Mig progeny. None of the known deficiencies in the region (*jDf1, jDf2, jDf4*) delete *mig-14*.

mig-1. Two-factor map data had placed *mig-1* on the left arm of LGI (Hodgkin *et al.*, 1988). Three-factor mapping was used to further define the map position of *mig-1*. From heterozygotes of genotype + *lin-6(e1466) dpy-5(e61)/ mig-1(e1787)* + +, 21/21 Dpy non-Lin recombinants segregated Mig animals. *lin-17*, whose QL.(d) cell mutant phenotype is similar to that of *mig-1* mutants, also maps to the left arm of LGI. However, deficiencies *tDf3* and *tDf4*, which delete the *lin-17* locus, both complement *mig-1(e1787)* (data not shown). Together, these data suggest that the map position of *mig-1* is to the left of *lin-6*, consistent with the two-factor map data, and confirm that *mig-1* and *lin-17* are two distinct genes.

Genetic analysis of gene activity

egl-20. Four of the five *egl-20* alleles, *n585, n1437, mu25,* and *mu27* have similar phenotypes at 20° C; namely, severe QL.(d) migration defects and HSN migration defects. At 25° C, *mu25* has a weaker QL.(d) migration defect (see Table 2.2). The QL.(d) migration defects are less severe in *egl-20(mu39)* mutants (see Table 2.2), which also fail to exhibit some of the other *egl-20* mutant phenotypes such as crumpled spicules, incomplete migration of rays 1 and 2 into the tail, and the A/P reversal of cells in the V5 lineage (data not shown). Placing the allele *n585* in trans to a deficiency for the region, *eDf19*,

did not increase the severity of the QL.(d) defect, the HSN defect or the polarity reversal, suggesting that the *n585* mutation may completely eliminate gene activity. Although placing the weak allele *mu39* in trans to either *n585* or *eDf19* increased the penetrance of the QL.(d) and HSN migration defects to approximately the same degree, the polarity reversal phenotype was more severe in *mu39/eDf19* worms (data not shown). Thus the *n585* allele, although it is a strong reduction of function allele, may not represent the *egl-20* null phenotype.

To generate *egl-20* heterozygotes for gene dosage analysis (see Table 2.2), hermaphrodites of genotype *unc-24(e138) egl-20* were crossed with N2 males, and their non-Unc progeny were scored. *eDf19* heterozygotes were identified as non-Unc, non-Dpy progeny from an *eDf19/unc-24(e138) dpy-20(e1282)* strain. As a control, *unc-24(e138) dpy-20(e1282)* hermaphrodites were crossed to N2 males and their non-Unc, non-Dpy progeny scored.

***mig-14, mig-1* and *lin-17*.** The alleles of *mig-14*, *mig-1* and *lin-17* that we studied are all recessive (Ferguson and Horvitz, 1985; Desai *et al.*, 1988); data not shown). Both alleles of *mig-14*, *mu71* and *k124*, have a QL.(d) migration defect that is more than 95% penetrant (Fig. 2.3 and data not shown), although some of the other migration defects appear to be more severe in *k124* than *mu71* (K. Nishiwaki, pers. comm. and data not shown). The QL.(d) migration defects in *mig-1* and *lin-17* mutants are less penetrant than those of *egl-20* and *mig-14* mutants, and some alleles of *mig-1* have no associated QL descendant migration defect at all. The positions of the QL.pa daughters are anterior to wild type in greater than 75% of worms homozygous for the *mig-1* alleles *e1787* (Fig. 2.3), *n687* and *mu72*, but less than 2% of worms homozygous for *n1354* and *n1652* (data not shown; Maloof and Kenyon, unpublished data). All *lin-17* alleles examined, *n671*, *n677*, and *e1456*, have

similar QL.(d) migration phenotypes. However, the *lin-17(n671)* and *n677* mutations, reported to be the most severe *lin-17* alleles with respect to vulva formation (Ferguson and Horvitz, 1985), are both temperature sensitive for the QL.(d) migration defect (data not shown). Interestingly, the *e1456* allele, reported to be weaker than *n671* and *n677* for other phenotypes (Ferguson and Horvitz, 1985), exhibits the migration defect at lower temperatures (data not shown). Thus, it is difficult to infer what the *lin-17* null phenotype might be and whether any of these alleles are null.

Scoring the positions of the Q.pa daughters

The positions of the Q.pa daughters were determined in late L1 after the descent of the last P nucleus into the ventral nerve cord. The positions of the QL descendants along the A/P axis were determined relative to that of the stationary Vn.p and Vn.a epidermal cells. Although QL/R.paa and its sister QL/R.pap migrate to different A/P positions, they are generally very close together. Since it was not always possible to determine which cell was which without observing the division of Q.pa, the positions of both cells were plotted on the same graphs. By convention, anterior is always to the left in all graphs and diagrams. All strains were examined at 25°C except *mig-14(mu71); mab-5(e1751gf)* which was examined at 20°C.

Direct observation of Q lineage migrations

Worms were mounted for long-term observation as described by (Sulston and Horvitz, 1977). Unhealthy strains were observed at lower temperatures: *mig-1(e1787)* and *mig-14(mu71); mab-5(e1751gf)* mutants at 20°C, and *mab-5(gf); egl-20(n585)* mutants at 22.5°C. All other strains were observed at 25°C.

Determination of Mab-5-like phenotypes

We examined *egl-20(n585)*, *mig-14(mu71)*, *mig-1(e1787)* and *lin-17(n671)* mutants at 25° for other Mab-5 phenotypes (Kenyon, 1986). Tissues examined were: adult coelomocytes in hermaphrodites, and spicules, hooks and sensory rays 1-6 in males. More than 20 worms of each genotype were examined for each phenotype.

***egl-20*, *mig-14*, and *mig-1*.** All tissues examined were essentially wild-type, except the coelomocytes and spicules in *egl-20* mutants, which were often missing (20/43) or crumpled (16/26).

***lin-17*.** *lin-17* mutations are known to cause many asymmetric cell divisions to become symmetric or to adopt a reversed polarity. The lineage of the M mesoblast was abnormal in *lin-17* mutants (Sternberg and Horvitz, 1988), however, we found that 21 out of 25 animals produce adult coelomocytes, unlike *mab-5* mutants. Male tails have few rays, often with severely abnormal morphology (Hodgkin *et al.*, 1988) and data not shown), but, unlike *mab-5* mutants, do not contain alae instead (data not shown). *lin-17* mutations affect the formation of the hook and the spicules; however, the defects in these structures are due to different developmental abnormalities in *lin-17* and *mab-5* mutants (Kenyon, 1986; Sternberg and Horvitz, 1988).

Antibody staining of whole mount larvae

Larvae were fixed and stained with a rabbit polyclonal antisera to MAB-5 as described in (Salser and Kenyon, 1996). The DNA stain DAPI, which labels all nuclei, was used to confirm the identity of both *mab-5* immunoreactive and non-immunoreactive cells.

Single-Cell Activation of *hs-mab-5*

To induce *heat-shock-mab-5 (hs-mab-5)* expression in a migrating Q.(d) cell, we heated it using a laser microbeam. Experiments were performed as described by (Stringham and Candido, 1993) except that laser strength was calibrated daily by inserting neutral density filters in the laser light path until 15-25 pulses were needed to burst an *E. coli* cell. We then further attenuated the laser by placing a glued stack of 10 or 12 microscope slides perpendicular to the laser's path. The laser was focused on a single cell for 3 minutes at a pulse rate of 2.5 Hz. After testing several different integrated lines carrying *hs-mab-5*, we chose the strain CF301 *mab-5(e2088); unc-31(e169); him-5(e1490); muIs9*[*hs-mab-5* + C14G10(*unc-31*$^{+}$)] (Salser *et al.*, 1993) because of its high sensitivity and low background in whole-animal heat-shocks. Animals were kept at 20°C throughout the experiments. 3.5-4 hour old L1 larvae were mounted on agarose pads containing 2 mM azide to immobilize them. After laser treatment, animals were allowed to recover for 1 hour on a seeded NG plate and then were remounted on agarose pads. The migrating cells were followed until QR.a or QR.ap had remained stationary for at least 2 hours, usually about 8 hours total. Reversals were defined as migrations in which QR.a or QR.ap moved towards the posterior and passed more than one nucleus in the surrounding epidermis. The data presented in Figure 2.2 represents all experiments carried out once conditions were found that caused QR.a migration reversals. To insure that the reversals were dependent on the laser heat-shock of QR.a, we carried out controls in parallel in which animals were mounted on azide for the same amount of time but without laser pulsing. Controls in which QR.a was targeted in N2 (wild-type) worms were also done in parallel. We found that the laser intensity necessary for inducing QR.a reversals had the side-effect of delaying or blocking the division of QR.a. This effect was independent of *mab-5*, however, because

focusing the laser on QR.a in wild-type worms also delayed or blocked the division but did not induce reversals.

RESULTS

Wild-type Q lineage migrations

The QR and QL neuroblasts are born at the same time, in the same A/P position on opposite sides of the animal (Sulston and Horvitz, 1977). These cells each undergo an identical sequence of divisions (Fig. 2.1) to produce one mechanosensory neuron (AVM/PVM), one putative interneuron (SDQR/SDQL), a ciliated neuron (AQR/PQR) and two cells that undergo programmed cell death (Sulston and Horvitz, 1977; Chalfie and Sulston, 1981; White *et al.*, 1986). Approximately one hour after the worm hatches, QL and QR begin their migrations: QL towards the tail and QR towards the head. Shortly before QL reaches the end of its migration, it starts to express the Hox gene *mab–5*. Both QL's anterior daughter, QL.a, and its posterior daughter, QL.p, express *mab-5*, as do all their descendants. In contrast, QR and its descendants never express *mab-5* (Salser and Kenyon, 1991) (Fig. 2.1). In mutants lacking *mab-5* activity, QL still migrates towards the tail, but its daughters migrate towards the head, just as the daughters of QR do in wild type (Fig. 2.1) (Kenyon, 1986; Salser and Kenyon, 1991). In animals that express *mab-5* ectopically, such as *mab-5(gf)* mutants (Hedgecock *et al.*, 1987; Salser and Kenyon, 1991) or animals carrying *heat-shock-mab-5* (Salser and Kenyon, 1991), QR still migrates towards the head, but now QR.p and its descendants stop and QR.a and its descendants migrate towards the tail, just as QL.p, QL.a and their descendants do in wild type (Fig. 2.1). In this paper, we will refer to

the daughters of QL and QR and all of their subsequent descendants collectively as QL.(d) and QR.(d) cells.

Previous mosaic analysis has shown that *mab-5* activity is required within the AB.p branch of the *C. elegans* lineage for QL's descendants to migrate posteriorly (Kenyon, 1986). Since QL is derived from AB.p, this finding is consistent with *mab-5*'s acting cell autonomously. To demonstrate that *mab-5* activity within a migrating Q.(d) cell is sufficient to direct its posterior migration, we used an attenuated laser microbeam to activate *hs-mab-5* within a single cell (see Materials and Methods). We found that focusing the laser beam on the anteriorly migrating QR.a cell, but not surrounding cells, caused QR.a to reverse direction and migrate towards the posterior (Fig. 2.2). Despite the fact that in wild-type animals all three QL-derived neurons express *mab-5*, each cell comes to occupy a characteristic position along the body axis (Fig. 2.1). Similarly, all three QR-derived neurons fail to express *mab-5*, yet each of them migrates to a different characteristic position (Fig. 2.1). Thus, although *mab-5* expression plays an important role in determining whether these cells ultimately reside in the posterior or the anterior of the body, it does not appear to be sufficient to specify their precise locations.

Genes affecting Q descendant migration: Overview

In this paper we describe four genes that affect the migrations of the Q.(d) cells along the A/P body axis. A number of mutants had been identified previously in which the descendants of QL were located in anterior body regions (Hedgecock *et al.*, 1987; Way *et al.*, 1992)(Hedgecock *et al.*, 1987; Way *et al.*, 1992; G. Garriga and C. Bargmann, pers. comm.), and we identified additional mutants with this phenotype (Fig. 2.3A; see Materials and Methods). We find that mutations in *egl-20*, *mig-1*, *mig-14*, and *lin-17* can cause the Q.(d) cells,

which normally migrate posteriorly, to reverse direction and migrate anteriorly instead. In addition, mutations in two of these genes affect another aspect of cell positioning that affects both the QL.(d) and QR.(d) cell migrations: namely, that subsequent anterior migrations are shortened and posterior migrations are lengthened. We will discuss these two different mutant phenotypes in turn, beginning with the change in direction of migration.

Mutations in *egl-20, mig-1, mig-14,* and *lin-17* reverse the direction of migration of QL's descendants

The QL.(d) cells in *egl-20, mig-1, mig-14,* and *lin-17* mutants migrate towards the anterior just as they do in *mab-5* mutants (Fig. 2.3A). Are these reversals due to a failure of the *mab-5* switch? If *mab-5* activity in QL were blocked, one would expect QL to migrate posteriorly, but its descendants to migrate anteriorly, as they do in *mab-5* mutants (Fig. 2.1). To ask whether QL migrated posteriorly in these mutants, we observed its migration in living animals using Nomarski microscopy. We found that in these mutants QL migrated towards the posterior, as in wild type, but its descendants migrated towards the anterior, as in *mab-5(-)* mutants (Fig. 2.3B). Thus, these four genes, *egl-20, mig-1, mig-14,* and *lin-17,* were likely to function in the *mab-5* pathway.

Mutations in *egl-20, mig-14, mig-1* and *lin-17* prevent MAB-5 expression in QL

In principle, the QL.(d) cells could migrate anteriorly in these mutants either because they fail to express *mab-5,* or because they fail to respond correctly to *mab-5.* To distinguish between these two possibilities, we first used polyclonal antisera against *mab-5* protein (MAB-5) (Salser *et al.,* 1993) to determine

whether QL and its daughters, QL.a and QL.p, produced MAB-5. We found that although QL.a and QL.p always expressed *mab-5* strongly in wild-type worms, they produced no detectable MAB-5 in *egl-20(n585)* and *mig-14(mu71)* mutants (Fig. 2.4 and Table 2.1).

The effect on *mab-5* expession at this stage seemed to be fairly specific for QL.a and QL.p: surrounding cells (V6, P9/10, P11/12, M and the seven most posterior juvenile motoneurons) appeared to produce MAB-5 as in wild type (data not shown). We also found that in general, *mab-5*-dependent cell fates in four other tissues (the hermaphrodite M-derived coelomocytes, male spicules, rays 1-6 and hooks) (Kenyon, 1986) were normal in *egl-20, mig-14* and *mig-1* mutants (exceptions are described in Materials and Methods). These tissues were defective in *lin-17* mutants, but had a phenotype that differed from that of *mab-5* mutants (see Materials and Methods). Therefore these genes are not required globally for *mab-5* expression.

When we examined MAB-5 expression in *mig-1(e1787)* and *lin-17(n671)* mutants, we found that the QL daughters showed weak or no MAB-5 staining in 83% and 48% of the worms, respectively (Fig 2.4 and Table 2.1). As in *egl-20* and *mig-14* mutants, staining appeared normal in surrounding cells. Since these *mig-1* and *lin-17* mutants have an incompletely penetrant migration defect, the QL.(d) cells that remain in the posterior in *mig-1* mutants could do so as a result of *mab-5* activity. To test this, we removed *mab-5* activity using a *mab-5* null mutation, *e1239* (Salser and Kenyon, 1996). We found that the QL.pa daughters were located in the anterior in 98% (n=67) of the *mig-1(e1787); mab-5(e1239)* double mutants. The same was true for *lin-17(n671); mab-5(e1239)* double mutants constructed and analyzed previously by Way et al. (1992). These observations indicate that the QL descendants that remain in

the posterior in *mig-1* and *lin-17* mutants do so largely as a result of *mab-5* activity.

If the QL.(d) cells in *mig-1* and *lin-17* mutants migrate incorrectly because they fail to express MAB-5, then they would be expected to migrate correctly if provided with MAB-5. To test this, we used a *mab-5* gain-of-function mutation, *e1751gf*, a regulatory mutation that causes ectopic production of MAB-5 (Salser and Kenyon, 1991; Salser *et al.*, 1993). In *e1751gf* mutants, both QL and QR produce MAB-5, and both the QL and QR descendants migrate to posterior positions (Hedgecock *et al.*, 1987; Salser and Kenyon, 1991) (Fig. 2.5). We found that in double mutant combinations between *mab-5(e1751gf)* and *egl-20, mig-1* or *mig-14* mutations, the QL.pa descendants remained in the posterior (Fig 2.5). This shows that the QL.(d) cells in *egl-20, mig-1,* and *mig-14* mutants can respond correctly to MAB-5. This finding, together with the MAB-5 expression data, indicates that the QL.(d) cells migrate towards the anterior in *egl-20, mig-1,* and *mig-14* mutants because they fail to express MAB-5.

We were unable to maintain *lin-17(n671); mab-5(e1751gf)* double mutants because the animals were very sick. However, the frequency of QL daughters in *lin-17* mutants that have little or no MAB-5 staining correlates well with the percentage of QL descendants that migrate into the anterior, as it does for *mig-1* mutants (Table 2.1), and the QL.(d) cells that remain in the posterior require *mab-5* activity to do so (Way *et al.*, 1992). Together, these observations suggest that a lack of *mab-5* expression in the QL.(d) cells causes them to migrate into the anterior.

The *egl-20, mig-1, mig-14* and *lin-17* mutations examined are likely to be reduction- or loss-of-function alleles

What is the wild-type function of these four genes in QL.(d) migration? To address this question, it was necessary to determine whether these mutations were likely to be loss-of-function or gain-of-function mutations. To do this, we asked whether these mutations were dominant or recessive, and, where possible, how the phenotypes were affected by changes in gene dosage (see Materials and Methods). We found that the *egl-20* allele *n585* is semi-dominant due to haploinsufficiency (Table 2.2) and behaves as a strong reduction-of-function mutation by genetic criteria (see Materials and Methods). The alleles of *mig-14*, *mig-1* and *lin-17* that we studied were all found to be recessive. For each of these genes, more than one allele caused a QL.(d) migration defect (see Materials and Methods). Thus, the simplest explanation for all these mutations is that they reduce or eliminate gene function, and therefore function during normal development to activate *mab-5* expression in QL.

In *egl-20* and *mig-14* mutants the anterior migrations of the QR descendants are shortened

In addition to their failure to express *mab-5* in QL, *egl-20* and *mig-14* mutants also exhibit a second migration phenotype. In the wild type, the three QR-derived neurons each stop at unique and characteristic positions in the anterior, just as the three QL-derived neurons do in the posterior. Interestingly, we found that in *egl-20* and *mig-14* mutants, the final positions of most of the QR.pa daughters were consistently shifted posteriorly relative to wild type (Fig 2.6, column 1). When we observed the QR.(d) migrations in living animals using Nomarski microscopy, we found that, in general, these cells stop migrating prematurely (Fig. 2.7A). We also noticed a similar alteration in the QL.(d) migrations: in *egl-20* or *mab-5; egl-20* double mutants

the final positions of these cells were generally shifted significantly posteriorly relative to the positions in the anterior that they would come to occupy in *mab-5(lf)* mutants (Fig. 2.3 and data not shown). Since the Q.(d) migrations of *egl-20* and *mig-14* mutants are not the same as those of *mab-5(lf)* mutants, the *egl-20* and *mig-14* mutant phenotypes cannot be completely explained by a loss of *mab-5* expression in the QL lineage. Because *egl-20* and *mig-14* influence *mab-5* expression in the QL lineage, in the following sections we will describe the shortening of the anterior migrations on the right side only, where cells in the QR lineage do not express *mab-5*.

The shortening of the anterior migrations of the QR descendants in *egl-20* and *mig-14* mutants is not due to a defect in motility

What causes the QR descendants to stop short in *egl-20* and *mig-14* mutants? These cells may be specifically defective in anterior migration, or they may simply be unable to migrate well in any direction. Alternatively, these mutations may direct cells to migrate to positions shifted posterior to normal. To distinguish between these possibilities, we asked what effect *egl-20* or *mig-14* mutations would have on a mutant in which QR.p did not migrate at all. In worms carrying the *mab-5* gain-of function mutation, *e1751gf*, QR.p and its descendants do not migrate and QR.a and its daughter migrate towards the posterior (Fig. 2.7). We found that when an *egl-20* or *mig-14* mutation was introduced into this strain, the QR.p cell now migrated towards the tail (Fig. 2.7), thus shifting the positions of the QR.pa daughters towards the posterior (Fig. 2.6, column 3). This meant that a loss of *egl-20* or *mig-14* activity could cause a normally stationary cell to migrate posteriorly. We also observed that in *mab-5(gf); egl-20* double mutants, QR.a and its daughter, QR.ap, now migrated further posteriorly than in the *mab-5(gf)* single mutant (Fig. 2.7A,

black triangles). This new finding is not consistent with the hypothesis that *egl-20* mutants are defective in cell motility. Instead, they imply that *egl-20* and *mig-14* mutations cause cells to migrate to positions located posterior to their normal stopping points.

In another mutant, *mig-13(mu31)*, QR.p and its descendants only migrate a short distance to the anterior (Robinson, 1995) (Fig. 2.7B). The *mu31* mutation is recessive and the severity of the phenotype does not increase in trans to a deficiency (Robinson, 1995). Thus, the wild-type function of *mig-13* is probably to allow QR.(d) cells to migrate anteriorly. Since mutations in *egl-20* and *mig-14* shift the positions of the QR.pa daughters toward the posterior in wild-type, *mab-5(lf)* and *mab-5(gf)* mutants, we wondered whether they would shift the QR.p descendants toward the posterior in a *mig-13* mutant as well: specifically, might they cause the QR.p cell to actually reverse direction and migrate posteriorly? We found that the positions of the QR.pa daughters in *mig-13* mutants carrying *egl-20* or *mig-14* mutations were consistently shifted posterior relative to the *mig-13* single mutants (Fig. 2.6, column 4), and some, most strikingly in the *egl-20; mig-13* double mutant, were actually posterior to the birthplace of QR (denoted by asterisks at the bottom of Fig. 2.6). We followed the migrations of QR and its daughters in both *egl-20; mig-13* and *mig-14; mig-13* double mutants and found that QR.p always migrated in the reverse direction, towards the posterior, whereas in *mig-13* single mutants, QR.p either stopped or migrated towards the anterior (Fig. 2.7B). These observations indicate that loss of *egl-20* or *mig-14* activity can cause a QR.(d) cell to change its direction of migration from anterior to posterior.

In the wild type, posterior migration of Q.(d) cells requires *mab-5* activity. Is *mab-5* required for the posterior migration caused by *egl-20* mutations? To ask whether the posterior migration of these cells required *mab-5* activity, we

constructed and analyzed *mab-5(e2088); egl-20(n585); mig-13(mu31)* triple mutants. We found that in these mutants QR.p migrated towards the posterior in 3 out of 4 animals. This observation indicates that *mab-5* is not absolutely required for posterior migration.

The known Hox gene functions are not responsible for the shortened migrations of the QR descendants in *egl-20* and *mig-14* mutants

Both *egl-20* and *mig-14* mutations affect the expression of the Hox gene *mab-5*. Could the posterior shift in the positions of the QR.pa daughters in *egl-20* and *mig-14* mutants be explained by altered activities of the Hox genes? Of the four *C. elegans* Hox genes, three, *lin-39*, *mab-5* and *egl-5*, are known to be required for wild-type Q.(d) migrations (Kenyon, 1986; Costa *et al.*, 1988; Chisholm, 1991; Clark *et al.*, 1993; Wang *et al.*, 1993). There are no mutations in the fourth gene, *ceh-13*, and its function is unknown (Shaller *et al.*, 1990; Clark *et al.*, 1993; Wang *et al.*, 1993).

The Hox gene *lin-39* is required for patterning the central body region and for the anterior migrations of QR and its descendants (Clark *et al.*, 1993; Wang *et al.*, 1993) In *lin-39* mutants, the anterior migrations of QR and its descendants are shortened. To determine whether reduced *lin-39* activity in *egl-20* and *mig-14* mutants is responsible for shortening anterior QR.(d) migrations, we first examined the expression of a *lin-39-lacZ* fusion gene (Wang *et al.*, 1993) in *egl-20* and *mig-14* mutants. *lin-39-lacZ* is normally expressed in both QL and QR (Wang *et al.*, 1993) and we found that its expression in both cells was unaffected by *egl-20* or *mig-14* mutations (data not shown). Second, we examined the QR.(d) migrations in a double mutant containing *egl-20(n585)* and a *lin-39* null allele, *mu26*, (Wang *et al.*, 1993), and J. Maloof and C. Kenyon, unpublished data). If the shortened anterior migrations of the QR.(d)

cells in *egl-20* mutants were due to a loss of *lin-39* activity, then the migrations in the *lin-39; egl-20* double mutant should be the same as those in the *lin-39* single mutant. We found that the positions of the QR.pa daughters in the double mutant were further posterior than in the *lin-39(mu26)* single mutant (data not shown). Since the presence of an *egl-20* mutation shortened the anterior-directed migrations of the QR.(d) cells in a *lin-39* null mutant, the failure of these cells to migrate to their normal positions in *egl-20* mutants cannot be explained simply by a loss of *lin-39* activity.

Another possibility is that the QR.(d) cells did not migrate as far anteriorly as normal because they misexpressed the Hox genes *mab-5* or *egl-5*. These two genes are required for the posterior migrations of the QL.(d) cells: *mab-5* 100% of the time (Kenyon, 1986; Salser and Kenyon, 1991) and *egl-5* approximately 9% of the time (Chisholm, 1991). To test whether ectopic *mab-5* or *egl-5* activity could be responsible for the shortened anterior migrations and lengthened posterior migrations of the QR descendants in *egl-20* and *mig-14* mutants, we made double mutants between *mab-5(e2088)* or *egl-5(n945)* and *egl-20(n585)* or *mig-14(mu71)*. We found that neither Hox mutation rescued the shortened QR.(d) migrations of *egl-20* and *mig-14* mutants (Fig. 2.6 and data not shown). These observations demonstrate that the posteriorly shifted positions of the QR.pa daughters in *egl-20* and *mig-14* mutants are not due to ectopic *mab-5* or *egl-5* activity.

The phenotypes of mutations in *egl-20* and *mig-14* are additive

We examined the positions of the QR.pa descendants in *mig-14(mu71); egl-20(n585)* double mutants, and found that they were shifted even further posterior than either single mutant (Fig. 2.8). Further genetic and molecular analysis of these alleles should help us to determine whether these genes

function in the same or in parallel pathways to determine the stopping points of the migrating QR.(d) cells.

Effect of *egl-20, mig-14, mig-1* and *lin-17* mutations on other cell migrations

To ask whether these mutations affected other cell migrations, we examined the positions of the migratory cells HSN, ALM, CAN, muIntR, ccLa/p, ccRa/p, and M (Fig. 2.9). Mutations in *egl-20, mig-14, mig-1* and *lin-17* affected a few migrating cells but did not produce a consistent posterior shift. Since we have not examined the position of every cell in these mutants, the possibility remains that *egl-20, mig-14, mig-1* and *lin-17* may also play a broader role in cell migration than we have so far determined.

DISCUSSION

Our experiments address two important questions: First, what initiates expression of a Hox gene in a migrating cell, and second, what directs migrating cells to their final positions? We have identified four genes required to activate *mab-5* in QL. Two of these genes, *egl-20* and *mig-14*, are also required independently of *mab-5* activity to position the migrating Q descendants correctly along the A/P axis.

Activation of the Hox gene *mab-5* within the migrating QL neuroblast

egl-20, mig-14, mig-1 and *lin-17* act in the same pathway as the Hox gene *mab-5* to direct descendants of QL to migrate towards the posterior. All four of these genes act upstream of *mab-5*, and mutations in these genes appear to affect *mab-5* expression primarily in QL. None of these mutations appear to affect *mab-5* expression or activity globally; thus they are not likely to be general activators of *mab-5* unless their functions in other cells are redundant

with other factors. These genes could act either at the level of transcription or of protein stability; however, the latter possibility seems less likely since mutations in these genes also block appearance of B-galactosidase in QL.a and QL.p in worms carrying *mab-5-lacZ* fusions containing only the first seventeen amino acids of the MAB-5 protein (Salser and Kenyon, 1991); data not shown).

How might *egl-20*, *mig-14*, *mig-1* and *lin-17* act to turn on *mab-5*? One possibility is that these genes are part of a system that creates left/right (L/R) asymmetries since, in wild type, QL but not QR expresses *mab-5*. Alternatively, these genes could be part of a system that is involved with the establishment of, or the response to, A/P positional information. In this model, the asymmetric initial migration would place QL and QR in different A/P positions, creating an A/P difference in addition to a L/R asymmetry. Signals present in QL's new posterior location would then instruct it to turn on *mab-5*, allowing the A/P patterning system to distinguish the fate of QL from that of QR. Finally, it is possible that these genes act to specify aspects of Q cell fate in a manner independent of either A/P or L/R position.

One of these genes, *lin-17*, is required for many asymmetric cell divisions. For example, in *lin-17* mutants, many cells that normally divide to generate two different cell types (A and B) instead generate two similar cells (A and A) (Sternberg and Horvitz, 1988; Way *et al.*, 1992). Although QL's ability to express *mab-5* is altered in *lin-17* mutants, it does not adopt the fate of its sister, an epidermal cell called V5. It is not clear how, or if, these two roles of *lin-17* are related. Molecular analysis of *lin-17*, as well as *egl-20*, *mig-14* and *mig-1*, should help to understand how *mab-5* gene expression is activated during the migration of QL.

The *egl-20* and *mig-14* genes influence the stopping points of the migrating Q descendants along the A/P axis

Two of the genes required for *mab-5* activation in QL, *egl-20* and *mig-14*, are also required in a *mab-5*-independent process to position cells correctly along the body axis. Mutations in these two genes cause the Q descendants to stop at positions that are further posterior than wild-type (Fig. 2.6). This shift is not due to misregulation of the Hox genes *mab-5*, *lin-39*, or *egl-5*. Nor is the posterior shift due to a defect in motility, since mutations in *egl-20* and *mig-14* lengthen posterior-directed migrations, cause a non-migratory cell to migrate posteriorly, and reverse the direction of an anteriorly migrating cell (Fig. 2.7). The *egl-20* and *mig-14* mutations we have analyzed all appear to reduce or eliminate gene function. Thus, it appears that the wild-type function of *egl-20* and *mig-14* is to allow the QR.(d) cells to migrate to more anterior positions.

In migrations directed by signals from target cells, the attraction of migrating cells or growth cones to a specific target determines both their direction of migration and their stopping or turning point. In contrast, the Q.(d) cells do not migrate towards any apparent target, and yet they stop at precise positions. This situation is reminiscent of the targeting of chick retinal axons to specific positions in the optic tectum. Axons from cells in different regions of the retina map to specific locations on a tectum that morphologically appears relatively uniform. Graded expression of cell-surface molecules across the tectum may direct the migrating growth cones to different locations (reviewed in Tessier-Lavigne, 1995). If a similar graded signal guides the Q descendants, then *egl-20* and *mig-14*'s role in it must be relatively specific for Q.(d) cell migration, since many other A/P migrations are unaffected by mutations in these genes (Fig. 2.9).

Positioning migrating Q descendants along the A/P axis

How might *egl-20* and *mig-14* instruct the migrating Q.(d) cells where to stop? There are at least three possibilities. 1) The Q.(d) cells might seek out specific positional values, perhaps defined by a specific concentration or combination of guidance molecules whose composition changes with position along the A/P axis. Mutations in *egl-20* and *mig-14* could act by shifting positional values, or the cell's perception of these values, towards the posterior (Fig. 2.10A). This model could also explain the failure of QL to turn on *mab-5* if the decision to activate *mab-5* is based on a positional cue that is shifted out of the range of QL in *egl-20* or *mig-14* mutants. 2) Opposing forces within the Q.(d) cells "push" or "pull" the migrating cells in both an anterior and a posterior direction. During this "tug-of-war", the relative strength of two opposing forces determines the final position of the migrating cell along the A/P axis (Fig. 2.10B). For example, if anterior and posterior migration were mediated by different receptors binding to two different external guidance cues, mutations in genes like *egl-20* and *mig-14* could act by increasing the relative concentration of "posterior-directing" receptor molecules in the plasma membrane, and thus tip the balance toward posterior migration (Fig. 2.10). Thus the wild-type function of *egl-20* and *mig-14* would be to increase the activity or levels of proteins required for anterior migration or decrease the activity or levels of proteins required for posterior migration. 3) Mutations in *egl-20* and *mig-14* might disrupt fine-scale A/P patterning, in the manner of *Drosophila* segment polarity mutants (Howard, 1990; Ingham, 1991). *C. elegans* is not a segmented animal, but there are repeating patterns of cells along the body (for a discussion, see Kenyon and Wang, 1991). In this model, other gene products would guide Q.(d) cells to the correct region of the body,

and then *egl-20* and *mig-14* would position them correctly within each metameric unit (Fig. 2.10C). Interestingly, mutations in *egl-20* can reverse the A/P polarity of certain epidermal cells (J. H. and C. K., unpublished data) and cells in the Q lineage (Fig. 2.3, legend), much as mutations in segment polarity genes do in the fly (Ma and Moses, 1995; Wehrli and Tomlinson, 1995).

Why do *egl-20* and *mig-14* mutations cause posterior shifts in the positions of cells in the Q lineage but not in the positions of all cells that migrate along the A/P axis? Migrations along the D/V axis are coordinately affected by *unc-5* and *unc-6* mutations, and migrations along the A/P axis, including the Q.(d) cells, are coordinately affected by mutations in *vab-8*. The reason for the specificity of *egl-20* and *mig-14* is not clear; however, it makes us favor the possibility that these genes act to establish the response of cells in the Q lineage to extrinsic signals rather than in establishing cell extrinsic guidance information. However, it remains possible that there are cell-extrinsic migratory signals specific for Q.(d) cells.

A new look at *mab-5*'s role in cell migration

Our analysis of the *egl-20* and *mig-14* mutant phenotypes suggests a new interpretation of *mab-5*'s role in cell migration. The starting point for the experiments presented here was the hypothesis that *mab-5* acts as a migration switch: if *mab-5* is on, the Q.(d) cells migrate towards the posterior, if *mab-5* is off, the Q.(d) cells migrate towards the anterior. In this model, it was assumed that *mab-5* acts to specify the direction of migration. Thus it was somewhat surprising to find that *mab-5* is not absolutely required to migrate posteriorly (in *mig-13; egl-20* double mutants; Fig. 2.7b).

This analysis of *egl-20* and *mig-14* mutations suggests the possibility that cells in the Q lineages are instructed to migrate to specific positions rather than in

specific directions. In *egl-20* and *mig-14* mutants the target positions adopted by migratory cells are shifted posteriorly. In some cases this positional shift involves a change in the direction of cell migration from anterior to posterior (Fig. 2.7). Perhaps this type of guidance system, that is, specifying cell position rather than direction of migration, governs Q.(d) cell migration. If so, then other mutants that alter the migrations of the Q.(d) cells would also act by respecifying target position rather than altering the direction of migration. Perhaps *mab-5*, rather than directing cells to migrate in a specific direction (i.e. towards the posterior), acts by directing cells to migrate to specific positions: positions that just happen to be posterior to the cells' starting points. Another observation, that intermediate levels of *mab-5* (as in a *mab-5*/+ heterozygote) direct cells to intermediate positions (Salser and Kenyon, unpublished data), also suggests that *mab-5* may not act as a simple ON/OFF-type directional switch. Further analysis of *egl-20*, *mig-14*, *mig-1* and *lin-17* , both genetic and molecular, should provide a greater understanding of how guidance information is encoded in this system.

Acknowlegdments

We thank members of our lab for discussions and comments on the manuscript and Raffi Aroian and Marc Tessier-Lavigne for comments on the manuscript. We would also like to thank Kiyoji Nishiwaki for *mig-14(k124)*, Martie Chalfie for the *mec-7-lacZ* transgenic worms, Guofeng Xie and Eric Aamodt for the *pag-1* mutant and advice on the *mec-7-lacZ* screen and Gian Garriga for several *mig-1* mutants and the outcrossed *egl-20(n1437)* strain. Thanks to Judy Silber and Julin Maloof in the the Kenyon lab for the *egl-20* alleles *mu25* and *mu39*, to rotation students Monica Gerber and Martha Stark for constructing two double mutant strains and assisting in their analysis and

to Steve Salser for much patient assistance and advice on the beta-galactosidase and antibody staining protocols. Some *C. elegans* strains were provided by the *Caenorhabditis* Genetics Center which is funded by the NIH National Center for Research Resources (NCRR). This work was supported by NIH grant GM37053 and a grant from the Packard Foundation to C.K.

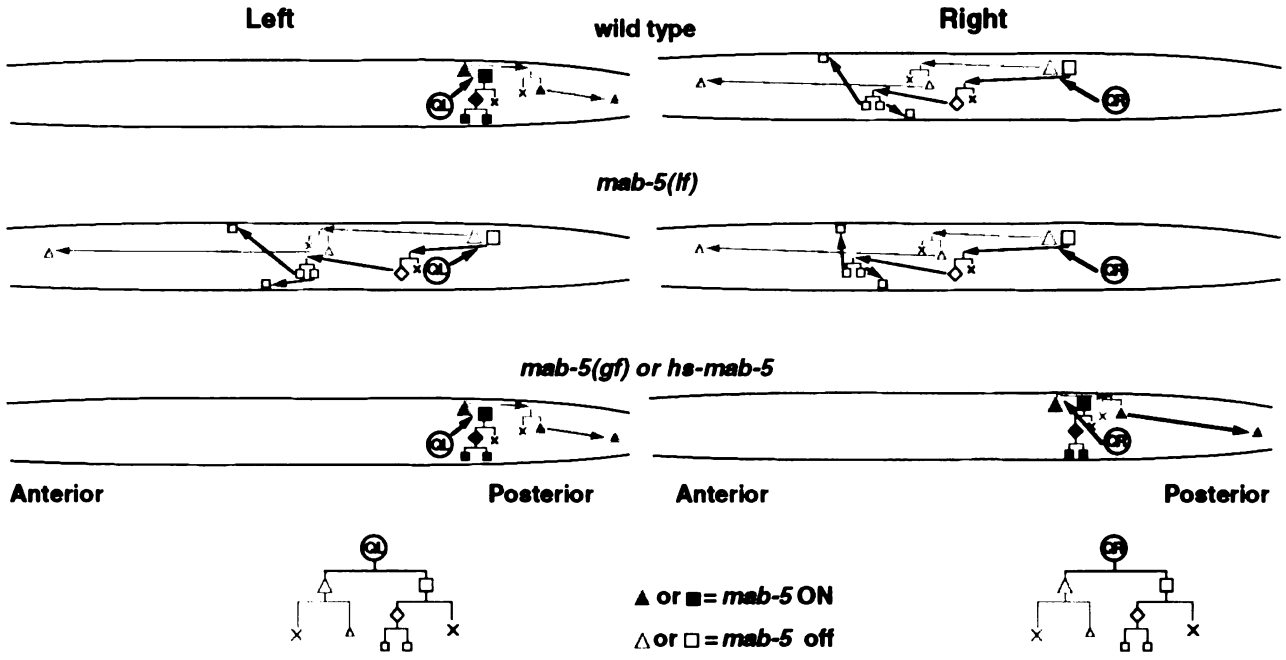

Fig. 2.1. Migration of the Q neuroblasts and their descendants in wild type (Sulston and Horvitz, 1977; Chalfie and Sulston, 1981), *mab-5(lf)* (Kenyon, 1986; Salser and Kenyon, 1991) and *mab-5(gf)* (Salser and Kenyon, 1991) mutants. Data are from Salser and Kenyon, (1991). Each cell in the lineage is denoted by a different shape (see lineage diagrams at bottom of figure): QL/R, circle; QL/R.a, large triangle; QL/R.ap (PQR/AQR), small triangle; QL/R.p, large square; QL/R.pa, diamond; QL/R.paa (PVM/AVM) and QL/R.pap (SDQL/R), small squares. Cells undergoing programmed cell death are marked with an x. Cell migrations are indicated by arrows. All cells divide and migrate along the A/P axis except for the daughters of anteriorly migrating QR.pa cells, which migrate dorsoventrally as well. The divisions of cells other than QL or QR are symbolized by cell lineage diagrams. In all figures, anterior is to the left. Filled symbols indicate *mab-5* expression as determined by antibody staining (S. Salser and C. Kenyon, unpublished data; see Fig. 4). This pattern is the same as that determined using *mab-5*-lacZ (Salser and Kenyon, 1991). The brief expression of MAB-5 in the QL neuroblast just before division is not depicted.

A.

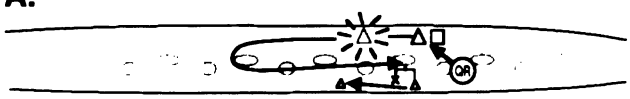

B.

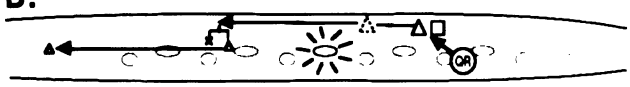

C.

genotype	targeted cell	QR.a reversed
hs-mab-5	QR.a	18/38
"	"nearby" hypodermal cell (V3)	0/9
"	"distant" hypodermal cell (V1,V2,V6, or P1-2)	0/8
"	dorsal syncytial nucleus	0/5
"	QR.p	0/2
"	none	0/17
wild-type	QR.a	0/16

Fig. 2.2. Laser activation of hs-mab-5 in QR.a as it migrates anteriorly causes the cell to reverse direction and migrate posteriorly. During the anterior migrations of QR.a and QR.p, an attenuated laser beam was focused on a single nucleus for three minutes in order to activate mab-5 expression and the resulting cell migrations were observed during the

the following 8-10 hours (see Materials and Methods). The symbols indicating cells in the QR lineage are the same as those in Fig. 2.1. The QR.p lineage (square) was unaffected and is omitted. Gray ovals show Vn.a and Vn.p hypodermal cells and correspond to the horizontal axis of Figure 2.3. The targeted cell is indicated with radiating lines. (A) Sample lineage from a *mab-5(e2088); muIs9(hs-mab-5)* animal in which the laser was focused on QR.a (red triangle). QR.a continued to migrate anteriorly, then reversed direction and migrated toward the posterior, divided as QR.a normally does, and then migrated a short distance to the anterior (presumably due to decay of the *hs-mab-5* activity (Salser and Kenyon, 1991). (B) Sample lineage from *mab-5(e2088); muIs9(hs-mab-5)* animal in which the laser was focused on a nearby cell, V3.p. At that time, QR.a (dashed triangle) was just dorsal of V3.p but was unaffected, continuing its normal anterior migration pattern. (C) Summary of all laser heat-shock experiments. In all cases the laser was focused on cells on the right side of the animal during the time that QR.a was migrating anteriorly (between V3 and V4). The targeted "Nearby" hypodermal cells were: V3, V3.a, and V3.p (n= 3, 2 and 4, respectively). "Distant" hypodermal cells were: V1, V2, V2.a, V2.p, V6, and P1/2 (n= 1, 1, 1, 1, 2 and 2, respectively). Dorsal syncytial nuclei were: the hyp7 nucleus between V2 and V3 (n=4) and the hyp7 nucleus between V1 and V2 (n=1). Using the positions of the Vn.a and Vn.p cells as a ruler (see horizontal axis for Fig. 2.3, in which each tick mark is defined as one unit) the distance migrated toward the posterior in the QR.a reversals ranged from 4 to 13 units, mean = 7.9.

Fig. 2.3. The migrations of the QL descendants in wild-type and *mab-5(e2088)*, *egl-20(n585)*, *mig-14(mu71)*, *mig-1(e1787)* and *lin-17(n671)* mutants. The positions of the QL descendants along the A/P axis were determined relative to that of the stationary Vn.p and Vn.a epidermal cells, shown at the bottom of the figure (see Materials and Methods). (A) Final positions of the QL.pa daughters, AVM and SDQL, at 25°C. The asterisk above V5.a marks the birthplace of QL. Fifty animals of each genotype were scored. (B) The migrations of QL and its descendants in representative animals of each genotype. The migrating cells were followed in living animals using Nomarski (DIC) optics. The different cells are depicted by different shapes (see lineage diagram at bottom of figure) as described in Fig. 2.1. The cells in the Q.p branch of the lineage are labelled blue and in the Q.a branch are labelled pink.

We observed the complete migrations in 5 *egl-20*, 3 *mig-14*, and 4 *mig-1* mutants. Data for wild-type and *mab-5* mutant migrations are from Salser and Kenyon (1991). Illustrated lineages are representative. The following variation was seen: ***egl-20.*** QL.p did not migrate at all in one *egl-20* mutant, although its daughter, QL.pa, did. QL.pa migrated anteriorly in 3/5 animals and did not migrate at all in the other two. In one animal, QL.ap did not migrate into the head but stopped in the body, just posterior to V1.p. In addition, in one animal, the polarity of the QL.a division was reversed: QL.aa migrated and QL.ap died. The migration of QL.aa in this animal was quite unusual; first it migrated anteriorly past three nuclei, then changed direction and migrated posteriorly past four nuclei, then changed direction again and migrated anteriorly past seven nuclei to a position just adjacent to V3.a, where it stopped. ***mig-14.*** In one animal QL.ap did not migrate into the head,

but stopped in the body between V1.a and V1.p. ***mig-1.*** In one *mig-1* mutant the QL.(d) cells migrated as in wild type. ***lin-17.*** *lin-17* mutants were not observed continuously, since their development at 25°C, where the Mig defect is observed, is greatly retarded. Instead, the initial migration of QL was observed and then the final positions of the QL.pa descendants were scored the following day. In all 8 *lin-17* mutants examined QL migrated towards the posterior; in four of those animals the QL.pa daughters migrated to positions anterior to wild-type.

In *egl-20*, *mig-14*, *mig-1* and *lin-17* mutants, but not in *mab-5* mutants, the migration of QL towards the posterior was lengthened, so that it divided next to P9/10 or even V6 instead of over V5 (see positions of QL.a and QL.p in Fig. 2.4). *egl-20* L1 larvae are slightly Dumpy, so distances between cells are shorter, but the other three mutants are of normal length.

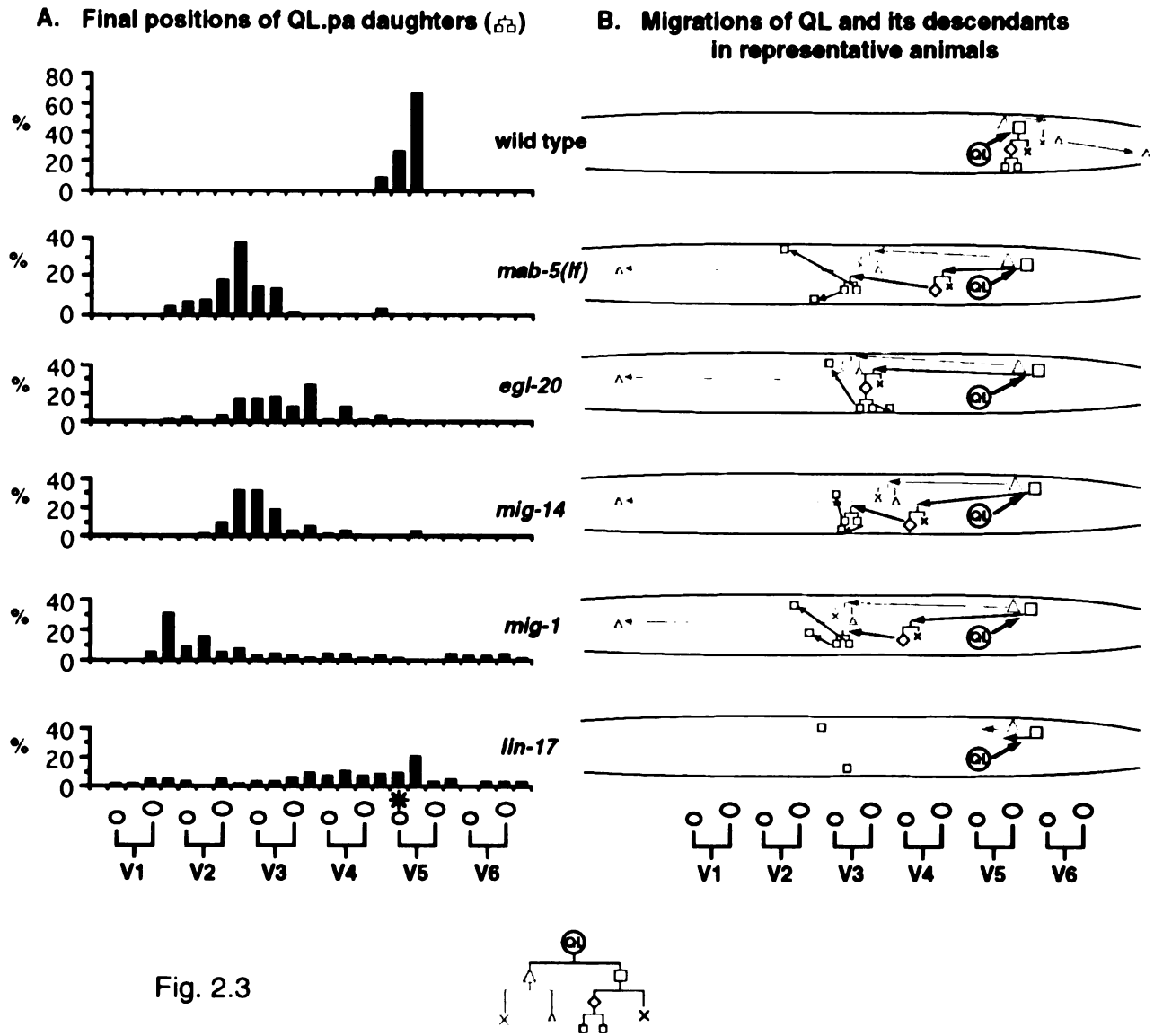
A. Final positions of QL.pa daughters (♂♂)
B. Migrations of QL and its descendants in representative animals
wild type
mab-5(lf)
egl-20
mig-14
mig-1
lin-17
%
80
60
40
20
0
V1
V2
V3
V4
V5
V6
QL

Fig. 2.3

Fig. 2.4. MAB-5 expression in QL.a and QL.p. Whole mount larvae, 3-6 hours post-hatching (raised at 25°C), were stained with polyclonal anti-MAB-5 antisera and the DNA stain DAPI (Salser *et al.*, 1993). At this time, QL has just divided and both daughters stain brightly with anti-MAB-5 antisera in wild type (top panels). In the *egl-20*, *mig-14* and *mig-1* mutants depicted above, QL.a and QL.p did not stain with anti-MAB-5 antisera. The *lin-17* mutant shown here demonstrates the faint MAB-5 staining occasionally seen in QL.a and QL.p in *mig-1* and *lin-17* mutants. The DNA stain DAPI labels all nuclei. Some other MAB-5-immunureactive cells are labeled for reference: arrow indicates V6, left arrowhead indicates P9/10, right arrowhead indicates P11/12.

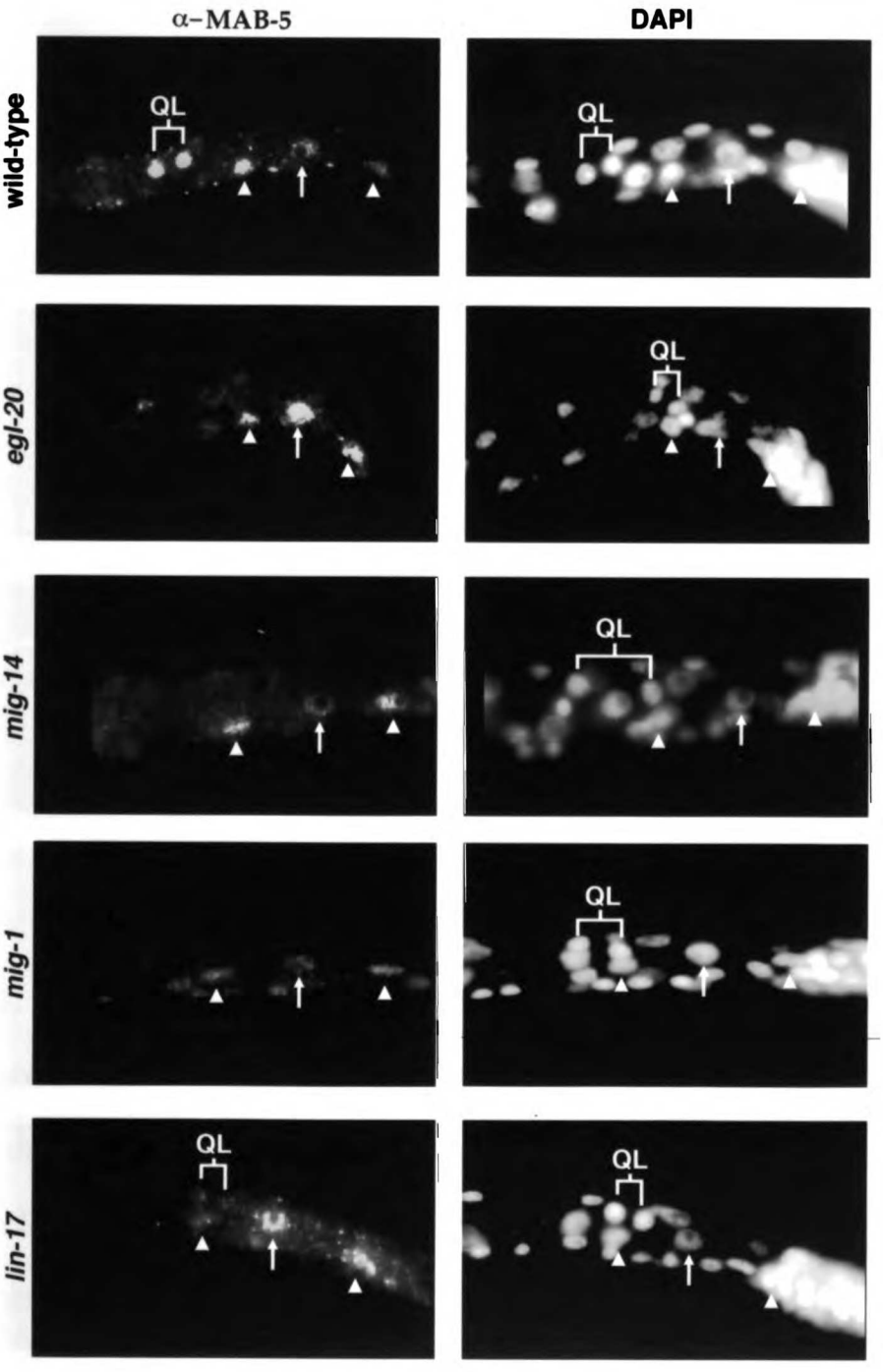

Fig. 2.4

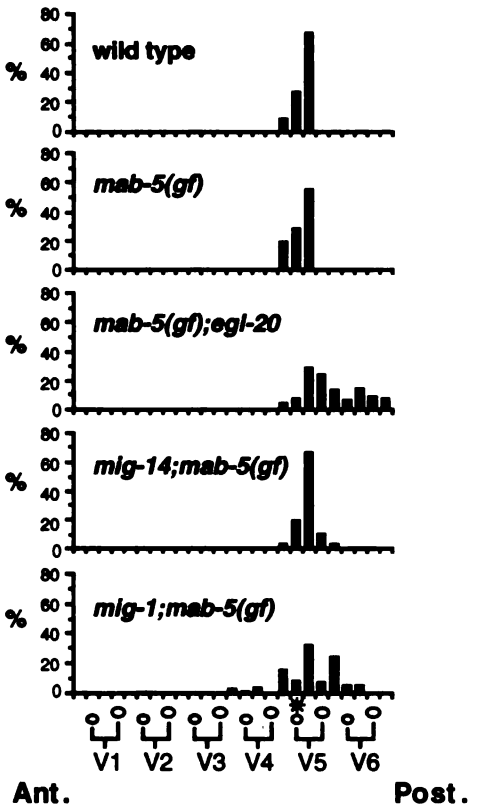

Fig. 2.5. A *mab-5(gf)* mutation suppresses the anterior migrations of the QL.(d) cells in *egl-20, mig-14* and *mig-1* mutants. Final positions of the QL.pa daughters (small blue squares in Figs 1 and 3) in worms carrying *mab-5(e1751gf)* alone and in combination with *egl-20(n585), mig-14(mu71)* and *mig-1(e1787)*. The positions in wild type are shown for comparison. The star above V5.a marks the birthplace of QL. n=35 for *mig-14; mab-5(gf)*. n=50 for all other genotypes.

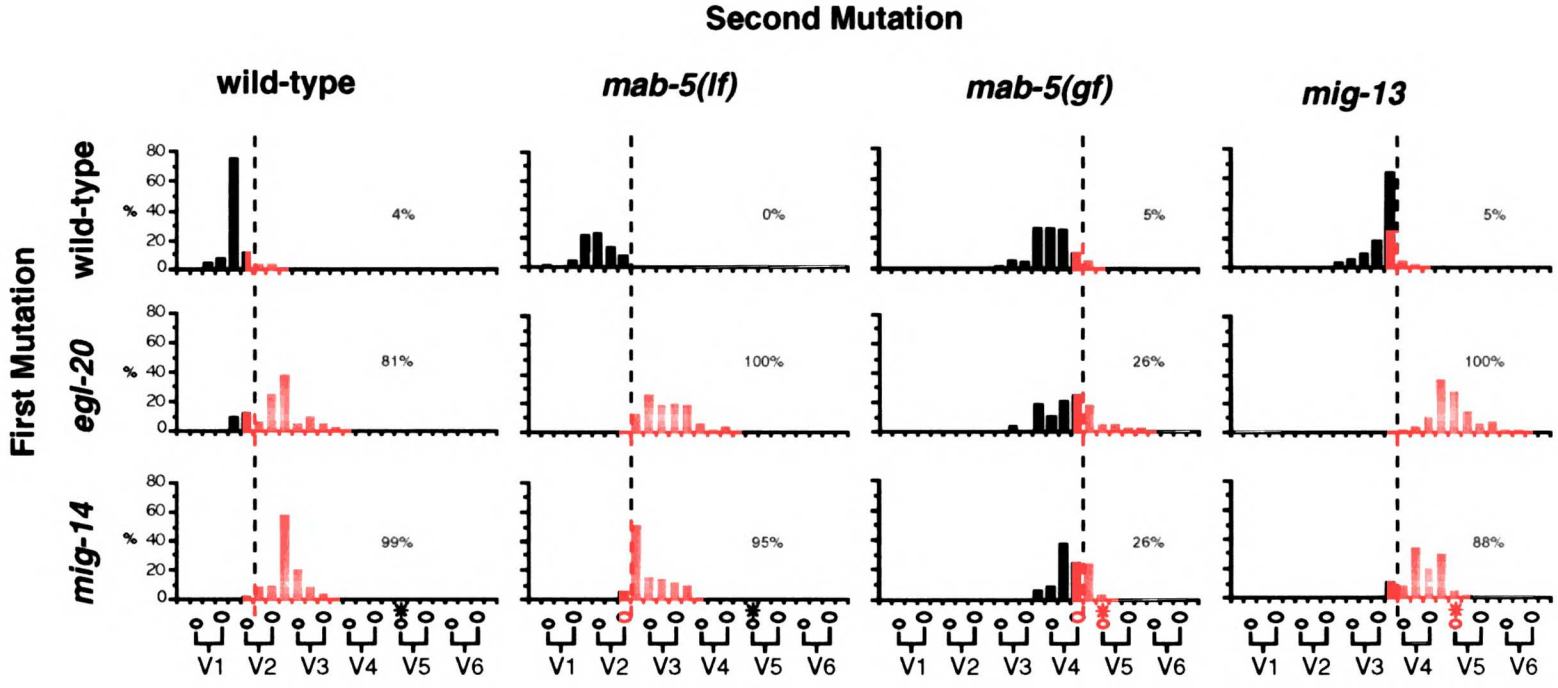

Fig. 2.6. Posteriorly-shifted positions of the QR.pa daughters (small blue sqares in Figs 1 and 7A) in *egl-20(n585)* and *mig-14(mu71)* mutants and in double mutant combinations. The asterisk above V5.a marks the birthplace of QR. n≥50 animals of each mutant genotype except: *mab-5(lf)*, n=35; *mig-14; mab-5(gf)*, n=37; and *egl-20; mig-13*, n=42. A dashed line is drawn through each column of graphs to make it easier to compare the distribution of positions in worms of different genotypes. The lines are drawn such that for each column, the final positions of the QR.pa daughters in 95% or more of control worms (top histogram of each column) are anterior to this line. The percentage of worms of each genotype with QR.pa descendants posterior to the line are noted at the right of each histogram.

Fig. 2.7. The migrations of QR and its descendants. The migrating cells were observed using Nomarski (DIC) optics. (A) QR lineage migrations in representative wild-type and mutant worms. Cells in the lineage are denoted by different shapes, as described in Fig. 2.1 (see lineage diagram at bottom of Part A). The final positions of the QR.pa daughters are labelled blue. The QR.p cell and its migration are labelled red. We observed the complete migrations in 2 *egl-20*, 3 *mig-14*, and 3 *mab-5gf; egl-20* mutants. The data for the wild-type and *mab-5gf* mutant migrations are taken from Salser and Kenyon (1991). Diagonal line near tail marks the position of the anus. (B) The migrations of QR.p (red square and arrow in part A) in wild-type and mutant animals. Each arrow represents the migration of QR.p in a different animal. Only cells that passed both a Vn.a/p nucleus and an internuclear interval were defined as having migrated posteriorly. QR.p cells that did not migrate are indicated with a red circle. The asterisk above V5.a marks the birthplace of QR. The dashed line is for reference and marks the average birthplace of QR.p.

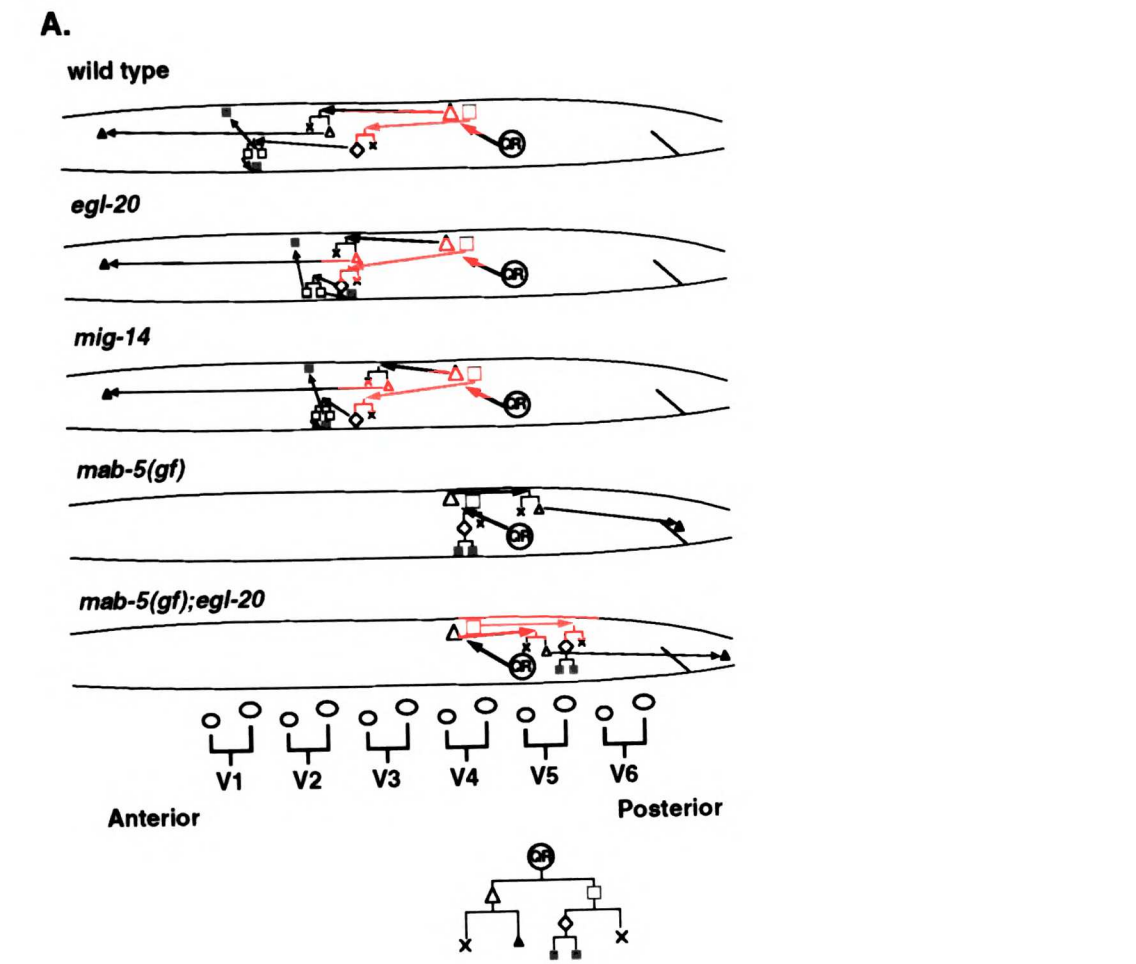
A.
wild type
egl-20
mig-14
mab-5(gf)
mab-5(gf);egl-20
V1
V2
V3
V4
V5
V6
Anterior
Posterior
B.
Second Mutation
wild-type
mab-5(gf)
mig-13
mab-5(lf);mig-13
First Mutation
w.t.
egl-20
mig-14
n.d.
n.d.

Fig. 2.7

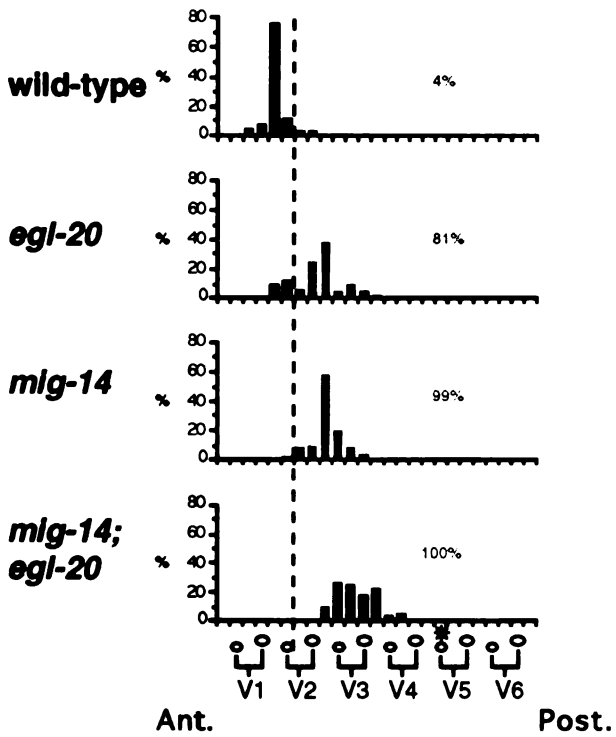

Fig. 2.8. *mig-14(mu71)* and *egl-20(n585)* mutations together shift the final positions of the QR.pa daughters even further posteriorly. The asterisk above V5.a marks the birthplace of QR. The dashed line is drawn such that the final positions of the QR.pa daughters in greater than 95% of wild-type worms are anterior to this line. The percentage of worms of each genotype with QR.pa daughters posterior to the line are noted at the right of each histogram. n > 50 animals of each genotype.

Fig. 2.9. Other cell migrations in wild-type and mutant worms. Cell positions in N2 at 20°C are defined as wild-type (data not shown). (A) The final positions of migratory cells in wild-type worms at 20°C. Range of final positions indicated beneath cell name was determined by examining over 20 worms. Each worm has two HSN, ALM and CAN neurons, one per side, but only one M and muIntR cell, both found on the right side (Sulston and Horvitz, 1977). There are also two pairs of juvenile coelomocytes found in different A/P positions (Sulston and Horvitz, 1977): ccLa/p on the left side and ccRa/p on the right side. Final positions of all cells were determined relative to the positions of the Vn.p and Vn.a cells (bottom of Part A) except for M and muIntR, which were determined relative to the positions of the undivided V and P cells and then extrapolated onto this diagram of a later developmental stage. The migrations of all these cells occur during embryogenesis, prior to Q cell migration. Arrows indicate direction of migration. Diagonal line near tail marks the position of the anus. (B) The percentage of worms grown at 25°C which have misplaced migratory cells. Note the effect of temperature on some migrations in wild-type animals. n, number of sides scored. a. Mostly anterior to wild type. p. Mostly posterior to wild type. The HSN position observed in *egl-20* and *mig-1* mutants at 25°C is similar to that observed by Garriga et al in worms grown at 20°C (Garriga *et al.*, 1993). The position of M is unaffected by mutations in *mab-5* (data not shown). **Other migration defects.** In addition to the defects described above, all four mutants have variable defects in the migrations of the distal tip cells (Kiyoji Nishiwaki, pers. comm and J. H., L. H., N. R., and C. K., data not shown). Also, in *mig-14(mu71)* mutants, the position of the neuron BDU,

A.

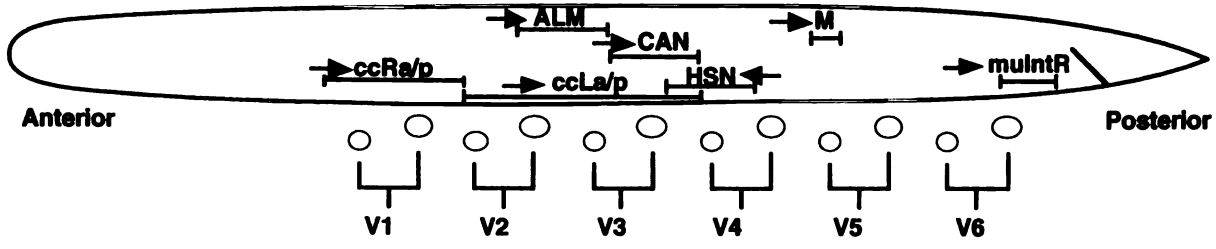

B.

Mig. Cells	% misplaced (n) wild type	*egl-20(n585)*	*lin-17(n671)*	*mig-1(e1787)*	*mig-14(mu71)*
HSN	4% (99)	81% (98) P	18% (77) a,P	38% (97) P	95% (43) P
ALM	0% (50)	5% (38)	10% (21)	2% (40)	26% (50) P
CAN	8% (50)	5% (40)	0% (22)	0% (40)	2% (50)
muIntR	0% (40)	2% (42)	0% (40)	6% (31)	0% (25)
ccLa/p	0% (38)	10% (47)	6% (40)	10% (40)	4% (23)
ccRa/p	3% (43)	18% (41) a	10% (41)	10% (40)	6% (33)
M	18% (34) a	68% (34) a	20% (40) a,P	35% (31) P	40% (25) a

Fig. 2.9

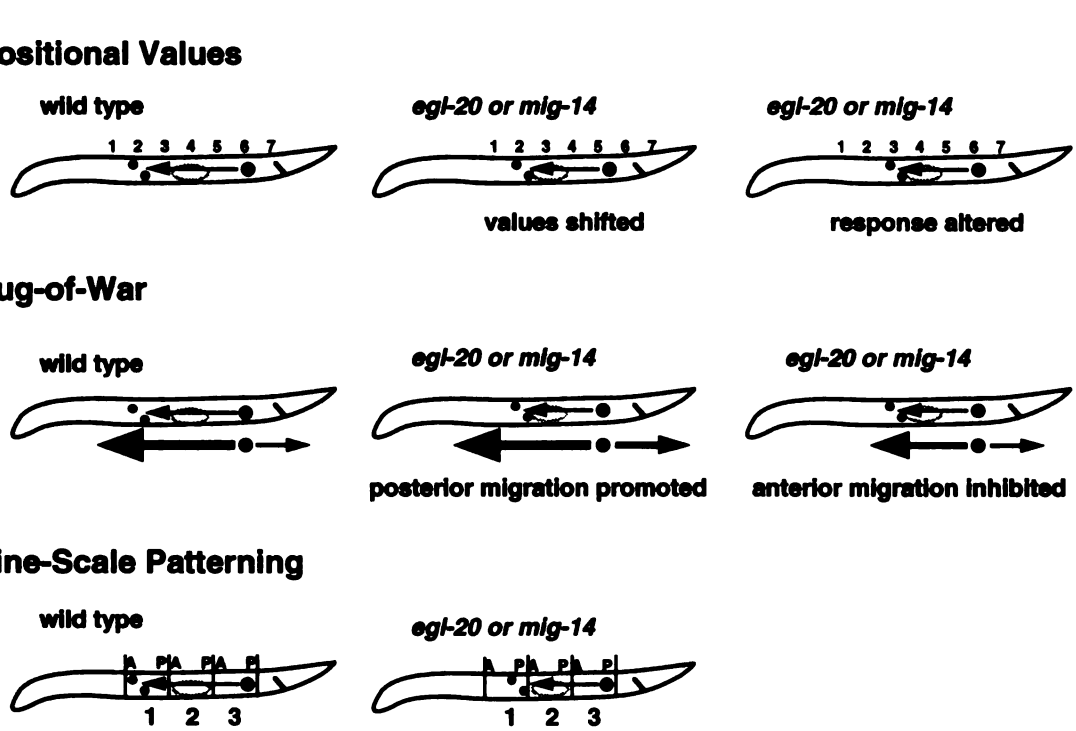

Fig. 2.10. Alternative models to explain the posterior shift in *egl-20* and *mig-14* mutants. Large circle indicates the birthplace of QR. Arrows indicate the sum of the QR and QR.(d) migrations. Small circles indicate the positions of the QR.pa daughters. The position of the gonad primordium, represented by the grey oval, is not shifted in *egl-20* and *mig-14* mutants and can thus be used as a reference point for Q.(d) cell position. 1. Positional Model. The QR.(d) cells seek out specific positional values. *egl-20* and *mig-14* mutations either shift positional values toward the posterior (values shifted) or direct cells to migrate to more posterior positional values (response altered). In the former case, the cells continue to migrate to their wild-type positional value, but that value is now in a more posterior position in the worm. 2. Tug-of-War Model. Proteins involved in anterior- and posterior-directed migrations compete for control of the QR.(d) cells. *egl-20* and *mig-14* mutations act by increasing the relative activity levels of proteins that promote posterior-directed migrations. 3. Fine-scale Patterning Model. QR.(d) cells migrate to the correct region of the body, then *egl-20* and *mig-14* help to position these cells correctly within that region. Mutations in *egl-20* and *mig-14* disrupt fine-scale patterning, for example, by locally reversing A/P polarity.

	A. *mab-5* Ab staining in QL.a and QL.p				B. Position of QL.pa desc.	
genotype	**% bright**	**% faint**	**% none**	**(n)**	**% posterior**	**(n)**
wild type	**98**	2	0	(94)	**100**	(50)
egl-20(n585)	**0**	0	100	(27)	**4**	(50)
mig-14(mu71)	**0**	0	100	(31)	**2**	(50)
mig-1(e1787)	**17**	11	72	(72)	**15**	(50)
lin-17(n671)	**52**	27	21	(52)	**48**	(50)

Table 2.1. Correlation of MAB-5 expression in QL.a and QL.p with posterior positions of the QL.pa daughters. Different worms were examined for MAB-5 expression and final positions. n, number of sides scored. All worms were grown at 25°C. (A) The percentage of worms with QL.a and QL.p staining brightly with antisera to MAB-5 (see Materials and Methods). All worms were fixed at 3-6 hours after hatching except for *mig-14* mutants which were fixed at 3.5-4.5 hours. Staining was only scored in animals in which QL had divided. (B) The percentage of animals in which the final position of the QL.pa descendants was posterior to V4.p. Data taken from Fig. 2.3.

genotype		% QL desc. anterior	n
egl-20	*(n585)*	96%	50
	mu27	100%	25
	n1437	96%	36
	mu25	83%	35
	mu39	66%	25
	eDf19/+	9%	123
egl-20	*(n585)/+*	7%	100
	mu27/+	5%	114
	n1437/+	3%	107
	mu25/+	3%	181
	mu39/+	0%	114
control	+/+	0%	279

Table 2.2. Gene dosage analysis of *egl-20*: strong *egl-20* mutations are haploinsufficient for the QL descendant migration defect. The positions of the QL.pa daughters were scored in L2 and late L1 larvae. Positions were scored as anterior if they were anterior to the V4.pp or V4.ppa nuclei in L2 or the posterior end of the V4.p nucleus in L1. *egl-20* heterozygotes were generated using the *unc-24(e138)* mutation to distinguish self- from cross-progeny (see Materials and Methods). The *eDf19* deficiency is maintained in trans to *unc-24(e138)* and *dpy-20(e1282)*. As a control, we examined *unc-24(e138) dpy-20(e1282)/+ animals.* n, number of animals scored for each genotype. The percentage of QL.pa daughters that migrate into the anterior in *egl-20* heterozygotes is significantly different from that of control animals according to the two-tailed Fisher Exact Test for all *egl-20* alleles except *mu39* (*eDf19*, P= 0.000004; *n585*, P=0.0002; *mu27*, P=0.001; *n1437*, P=0.04; *mu25*, P=0.02, *mu39*, P=1.00).

Chapter 3: Interactions between genes required for *mab-5* activation

Abstract

The known regulators of the *C. elegans Antennapedia* homolog, *mab-5*, all appear to be tissue-specific. In addition to their affect on *mab-5* expression, these genes all affect other aspects of development, such as cell migration, cell polarity and neural differentiation. To learn more about the role of these genes during development, I made and analyzed double mutant combinations between mutations in *egl-20, mig-1, lin-17* and *lin-22*.. My analysis did not uncover a role for any of these genes in a previously unidentified tissue, but, it did reveal some surprising interactions between the genes which regulate Q descendant migration. Our findings suggest that the interactions between *egl-20, mig-1* and *lin-17* may be quite complex, both in their effect on Q descendant migration and on *mab-5* regulation.

Introduction

The Hox genes are expressed in spatially restricted patterns along the A/P axis of such evolutionarily diverse organisms as *C. elegans*, crustaceans, flies, frogs, chicks and humans. This spatial restriction is important, because Hox genes function cell-autonomously to specify cell fate (Krumlauf, 1994; Lawrence and Morata, 1994). What genes are responsible for this precise and highly reproducible pattern of gene expression? In *Drosophila*, proper expression of the Hox genes appears to depend on the earlier A/P patterning system involving the gap, pair-rule, and segment polarity genes (Lawrence and Morata, 1994). Interactions between the Hox genes themselves also regulate their expression. After these genes establish the initial pattern of Hox gene expression, the polycomb and trithorax group genes act to maintain the

OFF or ON state, respectively (reviewed in (Orlando and Paro, 1995; Pirrotta, 1995; Simon, 1995; Tamkun, 1995).

The pattern of Hox gene expression is a highly dynamic and specific process: individual Hox genes can turn on and off within a cell or cell lineage as the organism develops. It seems likely that this cell-specific change in Hox gene expression must be due to genes other than the gap and pair-rule genes which appear to affect broad swaths of cells in defined regions of the body. These genes could either act by directly activating or repressing specific Hox genes, or by inactivating the maintenance system.

Many genes that regulate expression of the *C. elegans* Hox gene *mab-5* have been identified. Some of these genes have *Drosophila* homologs which also regulate Hox gene expression: *pal-1* is homologous to the gap gene *caudal* (Waring and Kenyon, 1991), *lin-22* to the pair-rule/proneural gene *hairy* (Wrischnik, 1995), and *egl-5* to the Hox gene *AbdB* (Salser *et al.*, 1993; Wang *et al.*, 1993). Other *C. elegans* mutants, however, demonstrate that genes not primarily involved in A/P polarity can also act to regulate Hox genes. For example, *lin-17*, homologous to the *Drosophila* tissue polarity gene *frizzled* (H. Sawa and R. Horvitz, pers. comm.), and *unc-40*, a potential netrin receptor with immuoglobulin and fibronectin type III domains (S. Chan, M-W Su, H. Zheng, J. Culotti and E. Hedgecock, pers. comm.), all are required to activate *mab-5* in the migrating QL neuroblast (see Chapter 2 and Appendix). The sequence of many other Hox gene regulators, such as *egl-20*, *mig-14* and *mig-1* have not yet been determined.

Rather surprisingly, these *C. elegans* mutants all appear to have extremely tissue-specific effects on the expression of the Hox gene *mab-5* (see Table 3.1). As a means of asking whether these phenotypes accurately reflected the domains of function of these genes, or whether they might also function

in other tissues, I made double mutants between different Hox gene regulators. If their functions were redundant in certain tissues, the requirement should become apparent in the double mutants. All of these genes that affect *mab-5* expression all have *mab-5*-independent effects as well. Thus analysis of these double mutants had an additional rationale: to attempt to learn more about the roles of these genes in HSN and Q descendant migration.

Materials and Methods

General Procedures, Nomenclature, and Strains

Methods for routine culturing and genetic analysis are described by Brenner (1974) and Wood et al. (1988). All experiments were performed at 25°C, except the analysis of the *lin-22 egl-20* double mutant which was performed at 20°C. The wild-type strain N2 is the parent of all strains used. Mutations are described by Hodgkin et al. (1988) or are noted below.

Mutations used:

LGI: *mig-1(e1787), dpy-5(e61), lin-17(n671), lin-17(n677), lin-17(e1456)* (Ferguson and Horvitz, 1985)

LGIII: *pal-1(e2091)*

LGIV: *egl-20(n585), unc-24(e138), lin-22(n372), unc-17(e245)*

LGV: *him-5(e1490), muIs3*(*mab-5-lacZ*+pRF4, containing the*rol-6(su1006sd)* mutation) (Cowing and Kenyon, 1992)

Constructing double mutant strains

The construction of *lin-17; egl-20* and *mig-1; egl-20* is described in Chapter 5.

lin-22 egl-20. *lin-22; him-5* males were crossed with *unc-17; egl-20* hermaphrodites, and their non-Unc F1 hermaphrodites allowed to self-fertilize. Egl non-Unc F2 progeny were picked and used to generate strains homozygous for the recombinant chromosome. The presence of ectopic postdeirids was used to confirm that the *lin-22* chromosome was present and homozygous.

mig-1 lin-17. This cross was performed at 20°C where the QL descendant migrations are almost completely wild-type in *lin-17(n671)* mutants (see Appendix), but the Bivulva (Bivul) phenotype is about 40% penetrant. *mig-1 dpy-5/+* + males were crossed to *lin-17(n671)* hermaphrodites. Hermaphrodite (F1) progeny which segregated Dpy progeny were kept. non-Dpy F2 recombinants with a Mig phenotype, but apparently wild-type gonad, vulva and tail, which segregated Bivul progeny were kept. Strains which rechecked for the Mig phenotype were made homozygous for the *mig-1 lin-17* recombinant chromosome.

I found that 3/6 Mig non-Dpy recombinants picked up the *lin-17* mutation, suggesting that the distance between *mig-1* and *lin-17* may be approximately the same as that between *lin-17* and *dpy-5*, 8.5 map units.

Checking for the presence of an *egl-20* mutation in the putative *lin-17(n671); egl-20(n585)* strain

Since the *lin-17* mutation also suppresses the *egl-20* polarity reversal phenotype (see Chapter 5), it was necessary to demonstrate that the *egl-20* mutation was actually present in this strain. To test for the presence of an *egl-20* mutation, I looked to see whether the putative double mutant failed to

compement *egl-20(n585)*. I first crossed wild-type males into the putative *lin-17; egl-20* hermaphrodites, then crossed the F1 male progeny to *unc-24(e138) egl-20(n585)* hermaphrodites and examined the positions of the QL.pa daughters in non-Unc F1 progeny grown at 20°C. At this temperature, the migrations of the QL descendants in *lin-17(n671)* mutants are essentially wild-type (see Appendix). I found that 48% of these animals had the Egl-20 QL Mig defect, as compared to only 4% of F1 Progeny from a control cross (*lin-17/+* males crossed to *unc-24 egl-20* hermaphrodites). Together, these observations suggest that the mutant animals in the complementation test had received a copy of *egl-20(n585)* from their mothers, the *lin-17; egl-20* mutants.

mig-1(e1787)* fully complements *egl-20(n585)

egl-20 gene activity is dosage sensitive (Chapter 2, Table 2.1). *egl-20* heterozygotes are also very sensitive to the dosage of *mab-5*: in *mab-5/+; egl-20/+* double heterozygotes, QL descendants migrate to positions anterior to V4.a in 48% of the animals (see Chapter 2, Materials and Methods). Since mutations in *mig-1* reduce *mab-5* expression in QL.a and QL.p 85% of the time (see Chapter 2, Table 2.2), I wondered whether being heterozygous for a *mig-1* mutation would increase the frequency of QL descendants which migrated into the anterior in *egl-20* heterozygotes. To answer this question, I made the *mig-1(e1787)/+; egl-20(n585)/+* double heterozygote and examined the position of the QL.pa daughters in this strain. I found that the frequency of QL descendants which migrated into the anterior in double heterozygotes was not significantly different from the frequency observed in *egl-20* heterozygotes alone (Table 3.2).

B-Galactosidase staining

Whole-mount staining of larvae. Staged larvae were mounted and fixed on polylysine-coated slides as follows: Washed worms resuspended in a small volume of distilled water were added to a drop (1/10 volume of worm mix) of 25% glutaraldehyde on a polylysine-coated slide. The live worms were quickly mixed with the glutaraldehyde using a pipet tip, the coverslip added and excess liquid removed. After a total fixation of 3 minutes, the slides were frozen for a minimum of 5 minutes on an aluminum block precooled on dry ice. The coverslips were pried off, the slides fixed one minute in room temperature acetone and allowed to air dry. The worms were then stained with XGal as described previously (Fire *et al.*, 1990), except with $MgCl_2$ at a final concentration of 10mM. The worms were costained with DAPI to identify nonstaining cells.

Scoring Phenotypes

Positions of migrating cells. The positions of the Q.pa daughters and HSN were scored at the end of L1, relative to the V cell daughters, as described in Chapter 2.

Rays. Ectopic sensory rays were scored in males in L4 lethargus, when the ray papillae are clearly visible in the new, thin cuticle.

Results

If two genes are functionally redundant in certain cells, then a requirement for either would be observed only if both are mutated. Similarly, a mutation which reduced but did not eliminate gene activity might still

function sufficiently well that some cells or tissues could undergo wild-type development. By reducing or eliminating the products of other genes in the same pathways, it might be possible to decrease the activity of the pathway enough to observe an effect of these mutations in other cells.

Thus, to see if I could uncover new roles for these *mab-5* regulators in other tissues, I made double mutant combinations between different mutations known to affect the pattern of *mab-5* expression: first, between mutations which affect *mab-5* expression in the neuroblast QL and its descendants and second, between mutations which affect *mab-5* expression in the ectodermal blast cells V1-6.

Although we did observe additional effects of these mutations on the migrations of HSN and the Q descendants, double mutant analysis did not reveal any novel defects in other hermaphrodite tissues. This analysis does not rule out a role for these genes in other tissues, since there might be subtle effects in specific lineages that we did not observe, or defects in the development of male-specific structures, which we did not examine.

I. Upstream of *mab-5* in the QL lineage: *egl-20, lin-17* and *mig-1*

egl-20, lin-17 and *mig-1* are all required to turn on *mab-5* within the migrating QL neuroblast. When these gene activities are reduced or eliminated, *mab-5* is not expressed and the QL daughters reverse direction, migrating towards the anterior rather than the posterior (see Chapter 2). I made all three pair-wise double mutants between *egl-20(n585), mig-1(e1787)* and *lin-17(n671)*. Analysis of each double mutant produced some unexpected results, indicating that the regulation of migration is more complex than

anticipated. I will first present the effects on the migrations of the Q descendants, then the effects on the migrations of the HSN neuron.

A. Migration of the Q descendants

mig-1(e1787) is epistatic to *lin-17(n671)*

In all three mutants, the QL descendants reverse direction and migrate towards the anterior because they fail to express *mab-5* (Chapter 2). Since neither the *lin-17(n671)* nor the *mig-1(e1787)* phenotypes are fully penetrant, I wondered whether introducing both mutations into the same strain would increase the percentage of animals with such a reversal. Since the QL descendants are found in the anterior in 84% of *mig-1* mutants and 53% of *lin-17* mutants, if the two phenotypes were additive, more than 84% should migrate into the anterior in *mig-1 lin-17* double mutants. Instead, I found that the QL daughters reversed direction in the double mutant at approximately the same frequency that they did in *mig-1* single mutants, 82% (Fig. 3.1).

egl-20(n585) is not epistatic to *mig-1(e1787)* and *lin-17(n671)*

The QL descendants in *egl-20, mig-1* and *lin-17* mutants migrate into the anterior because they fail to express *mab-5* (see Chapter 2). Mutations in *mig-1* and *lin-17* are only partially penetrant: the QL descendants remain in posterior (wild-type) positions in 16% of *mig-1* mutants and 47% of *lin-17* mutants (Fig. 3.1). Since the *egl-20(n585)* mutation blocks expression of *mab-5* in the QL lineage in all animals (100%; see Chapter 2) and causes migration reversals in most animals (98%), I expected the QL descendants in all *mig-1; egl-20* and *lin-17; egl-20* double mutants to reverse direction and migrate towards the anterior. Surprisingly, I found that the QL descendants remain in

the posterior in 12% of *mig-1; egl-20* and 11% of *lin-17;egl-20* double mutants (Fig. 3.1).

mab-5 promotes posterior migration in a _egl-20_-independent way in _mig-1_ mutants

In *mig-1* mutants, the QL descendants require *mab-5* to remain in the posterior. We wondered whether the posteriorly migrating QL descendants in *mig-1; egl-20* double mutants also required *mab-5* in order to migrate posteriorly. To test this, Naomi Robinson constructed *mig-1; mab-5(null); egl-20* triple mutants (Robinson, 1995), and showed that the QL descendants in this strain always migrate into the anterior (Fig. 3.2). This observation demonstrated that the QL descendants which migrate into the posterior in *mig-1; egl-20* mutants do so as a result of *mab-5* activity. This result was surprising, because in *egl-20* single mutants, *mab-5* is unable to direct the QL descendants to migrate towards the posterior. Thus, in *mig-1* mutants, *mab-5* is able to promote posterior migration in an *egl-20*-independent way. Since *mab-5* was able to direct some QL descendants to remain in the posterior in *mig-1* mutants, I looked to see whether *mab-5* was expressed in QL and its daughters in *mig-1; egl-20* mutants. I examined the effect of these mutations both on expression of a *mab-5*-lacZ translational fusion (Salser and Kenyon, 1991; Cowing and Kenyon, 1992) and on expression of *mab-5* directly, using polyclonal antisera to MAB-5 (Salser *et al.*, 1993). To my surprise, I found that QL.a and QL.p in *mig-1; egl-20* double mutants did not appear to express either the endogenous *mab-5* gene or the *mab-5*-lacZ fusion gene (Table 3.3).

Mutations in _egl-20_ prevent the QL descendants in _lin-17_ and _mig-1_ mutants from migrating all the way into the anterior

In addition to turning ON expression of *mab-5* in QL and its descendants, *egl-20* has a second effect on QR descendant migration (see Chapter 2). In *egl-20* mutants, the QR descendants migrate into the anterior just as they do in wild-type, but do not migrate as far. This shift is independent of *mab-5* activity and not due to a defect in motility. I found that introducing the *egl-20(n585)* mutation into a *mig-1* or *lin-17* mutant strain shifted the anterior boundary of the QR.pa daughters' positions towards the posterior (Fig. 3.3) as it does to other Mig mutants (Chapter 2, Fig. 2.7). I also observed a similar shift on the left side of the animal: the final positions of the QL.pa daughters in *mig-1; egl-20* and *lin-17; egl-20* double mutants were shifted posteriorly relative to the *mig-1* and *lin-17* single mutants (Fig. 3.1). Surprisingly, the posterior shift in final position caused by the *egl-20* mutation in *mig-1* and *lin-17* mutants was not as severe as expected. Since *mig-1* and *lin-17* mutations allow anteriorly migrating QL descendants in *mab-5* mutants to migrate to positions anterior to those that they would normally occupy (Julin Maloof and Cynthia Kenyon, unpublished data; (Way *et al.*, 1992), it may be that these mutations have a similar, although mild, effect on the final positioning of the QL descendants in *egl-20* mutants.

In animals mutant for *lin-17* or *mig-1*, QL descendants can be found in positions posterior to wild-type

Mutations in *mig-1* and *lin-17* can allow QL descendants to migrate to positions posterior to wild-type (i.e. posterior to V5.p; Fig. 3.1). This phenotype is also seen in double mutants containing either a *lin-17* or *mig-1* mutation (Fig. 3.1) or in mutants carrying the weak *egl-20* mutation, *mu39* (see Appendix). A common feature of *egl-20*, *mig-1* and *lin-17* mutants is that QL always migrates too far, placing it in a more posterior position than wild-

type (see Chapter 2, Figs 2.3 and 2.4). Thus, even if the QL.p descendants never migrated, as in wild type, the extended migration of QL could be sufficient to explain the more posterior position of the QL.pa daughters.

B. HSN migration

Mutations in *lin-17* partially suppress the *egl-20* HSN migration defect

In hermaphrodites, the two HSN (hermaphrodite-specific neuron) cells, HSNL and HSNR, migrate from their birthplace in the tail to positions over the midpoint of the gonad primordium. This short migration takes place during embryogenesis, before elongatation. Mutations in both *egl-20* and *mig-1* cause the HSN cells to stop along the migration pathway at positions posterior to wild type (Desai *et al.*, 1988; Desai and Horvitz, 1989). In my analysis of the *lin-17* single mutant phenotype, I found that mutations in *lin-17* cause the HSN cells to stop at positions anterior to wild type (Chapter 2, Fig. 2.9, and this chapter, Fig. 3.4). When I analyzed *lin-17* double mutants, I found that a mutation in *lin-17* could partially suppress the *egl-20* HSN migration defect, although I observed no significant suppression of the weaker *mig-1* defect (Fig. 3.5). However, the distribution of HSN positions appeared to be broader in the *mig-1 lin-17* double mutant than in *mig-1* mutants alone.

II. Upstream of *mab-5* in the V cells: *lin-22* and *egl-20*

Two genes, *pal-1* and *lin-22*, act upstream of *mab-5* in the V cells. *pal-1*, the *C. elegans caudal* homolog, functions to turn *mab-5* ON in V6 (Salser and Kenyon, 1996) and *lin-22*, the *C. elegans hairy* homolog, functions to turn *mab-5* OFF in the V1-V4 lineages (Wrischnik, 1995) (Table 3.1). *egl-20* can also

activate expression of *mab-5* in V6 (after neighbor ablation in *pal-1*(-) mutants; see Chapter 4) and may also be able to activate *mab-5* expression in V5 after neighbor ablation (see Chapters 4 and 5). In addition to its role in V cells, *egl-20* activates *mab-5* in the migrating neuroblast QL and its descendants. Analysis of the *pal-1; egl-20* double mutant is presented in Chapter 4, and analysis of the *lin-22 egl-20* double mutant is presented here.

Mutations in *lin-22* and *egl-20* do not suppress each other

In *egl-20* mutants, the QL descendants reverse direction and migrate into the anterior because they fail to express *mab-5* (see Chapter 2). In *lin-22* mutant males, descendants of the anterior V cells, V(1-4).pp, which normally do not activate *mab-5* and thus produce anterior-specific lineages leading to the synthesis of alae, now express *mab-5* and produce up to two rays (Fixsen, 1985; Wrischnik, 1995). In an attempt to uncover a more general role for *egl-20* in the V cells or of *pal-1* and *lin-22* in the QL lineage, I constructed a *lin-22(n372) egl-20(n585)* double mutant strain (see Materials and Methods) and examined the fates of the V and QL descendants. Since mutations in *lin-22* and *egl-20* have opposite effects on *mab-5* expression (*egl-20* mutations keep *mab-5* OFF in QL while *lin-22* mtuations turn *mab-5* ON in V1-4), I looked to see whether a mutation in *lin-22* could suppress the *egl-20* mutant phenotype be turning *mab-5* ON in the QL lineage. I found that it did not: in *lin-22 egl-20* double mutants the QL descendants migrated into the anterior in 100% of animals examined (Fig. 3.6). I then looked to see whether an *egl-20* mutation could suppress the *lin-22* mutant phenotype by keeping *mab-5* OFF in V1-4. I found that it did not: *lin-22 egl-20* double mutants produced ectopic rays at a high frequency, just as *lin-22* single mutants do (data not shown). Together,

these observations suggest that *egl-20* and *lin-22* do not function in the same cell-fate decisions.

Discussion

All the known regulators of the *C. elegans* Hox gene *mab-5* appear to be very tissue-specific. This could be the result of redundancy with another gene function in certain cells, or it could be because the mutations that have been analyzed do not eliminate gene function in all tissues. As a means of asking whether there might be a role for these genes in the specification of other cell fates, and to learn more about their function in tissues where they were known to have an effect, I constructed and analyzed double mutants between mutations in genes known to regulate *mab-5* expression. This analysis did not uncover a role for any of these genes in a previously unidentified tissue, but, it did reveal some surprising interactions between the genes which regulate Q descendant migration. Our findings suggest that the interactions between *egl-20*, *mig-1* and *lin-17* may be quite complex, both in their effect on Q descendant migration and on *mab-5* regulation.

A *mig-1* mutation can suppress the *egl-20* QL descendant migration defect

The QL daughters reverse direction in 98% of *egl-20* mutants, but only 84% of *mig-1* mutants (Fig. 3.1). Suprisingly, I found that the *mig-1; egl-20* double mutant is similar to *mig-1* mutants, with the QL descendants reversing direction in only 88% of double mutants (Fig. 3.1). As in *mig-1* mutants, the QL descendants in *mig-1; egl-20* double mutants remain in the posterior as a result of *mab-5* activity (Robinson, 1995): in *mig-1; mab-5(0); egl-20* triple mutants, the QL descendants all migrate into the anterior (Fig. 3.2).

This observation indicates that *mig-1* mutations can suppress the inability of *egl-20* mutants to turn on *mab-5* because they activate *mab-5* in another way. There are two ways that mutations in *mig-1* could bypass *egl-20*. **1.** *mig-1* mutations could activate *mab-5* in the QL lineage in an *egl-20*-independent way. This possibility seems less likely, since I was not able to detect any *mab-5* expression in the QL daughters in *mig-1; egl-20* double mutants (Table 3.3). It remains possible that levels too low to be detected are present in QL, and that *mig-1* mutations change the threshhold so that these levels are sufficient. However, in *mig-1* single mutants, the frequency of animals with QL daughters that stained with antisera to Mab-5 was higher than the frequency of animals in which the QL descendants migrated into the anterior (Chapter 2, Table 2.1). These findings suggest that QL daughters that stained only faintly with anti-MAB-5 antisera did not express enough *mab-5* to remain in the posterior (for discussion, see Chapter 2). **2.** *mig-1* mutations could allow *mab-5* to act non-autonomously, either by activating *mab-5* in another cell, or by enabling a cell in which *mab-5* was already expressed to signal the QL cell. Since the pattern of *mab-5*-expressing cells in *mig-1* and *mig-1; egl-20* mutants at this stage is indistinguishable from wild type, with the exception of QL.a and QL.p, mutations in *mig-1* do not appear to activate *mab-5* in new cells. Activation of *mab-5* within single cells indicated that expression of *mab-5* within the migrating cell itself was sufficient to direct it to migrate towards the posterior, but did not rule out the possibility that *mab-5* could also act within another cell to direct the migration of the Q descendants (Chapter 2, Fig. 2.2). Mosaic analysis of *mab-5* indicated that in a wild-type background, *mab-5* is required in the AB.p lineage to permit wild-type migration of the QL descendants. However, there are many AB.p descendants, and mutations in *mig-1* might alter where *mab-5* can act. Mosaic analysis of *mab-5* in a *mig-1*

mutant background should settle these questions by indicating whether *mab-5* can act in another cell to regulate posterior migration of the QL descendants. Together, these observations raise the possibility that mutations in *mig-1* exert their effect by allowing an existing *mab-5*-expressing cell to signal the QL descendants to migrate posteriorly. In other words, mutations in *mig-1* could alter cell-signalling pathways. Such a role for *mig-1* in Q descendant migration is consistent with its behavior in determining cell polarity (Chapter 5), in which *mig-1* may be part of a signalling pathway.

mig-14 mutants have almost identical phenotypes to *egl-20* mutants and affect the same steps in cell migration (Chapter 2). However, all QL descendants migrate into the anterior in *mig-1; mig-14* double mutants (L. Honigberg and C. Kenyon, unpublished data), suggesting that *mig-14* may actually function in a different location in this pathway.

A *lin-17* mutation suppresses many *egl-20* mutant phenotypes

Like the *mig-1(e1787)* mutation, the *lin-17(n671)* mutation partially suppress the anterior migration of the QL descendants in *egl-20* mutants (Fig. 3.1). This *lin-17* mutation also partially suppresses the the *egl-20* HSN migration defect (Fig. 3.5). *lin-17* mutations cause HSN to migrate too far in many animals (Fig. 3.4), and *egl-20* migrations cause them to stop too soon (Desai *et al.*, 1988; Desai and Horvitz, 1989; Chapter 2). The contradictory nature of these mutant phenotypes may end up positioning many HSN's in a position close to wild-type. In addition to suppressing *egl-20*'s Mig phenotypes, this *lin-17* mutation suppresses an *egl-20*-dependent polarity reversal (Chapter 5). Thus this one mutation can suppress many *egl-20* phenotypes. However, not all *egl-20* phenotypes are suppressed in *lin-17; egl-20* double mutants: the animals are still Egl (data not shown).

Since both *lin-17* and *mig-1* mutations allow the QL descendants to remain in the posterior at a low frequency in *egl-20* mutants, it will be interesting to see if they both act the same way: do these posterior cells require *mab-5*? do they express *mab-5*? It will be interesting to determine the role of *mig-1* and *lin-17* in the guidance of posterior QL descendants.

An *egl-20* mutation prevents Q descendants from migrating far into the anterior in *lin-17* and *mig-1* mutants

I demonstrated previously that *egl-20* has a *mab-5*-independent effect on Q descendent migration (for a discussion, see Chapter 2). Mutations in *egl-20* direct descendants of both QL and QR to migrate to positions shifted posteriorly to those they would otherwise seek. This posterior shift in final positions is evident in the *mig-1; egl-20* and *lin-17; egl-20* double mutants presented here as well (Figs 3.2 and 3.4). Thus, wild-type function of *egl-20* allows migrating Q descendants to migrate to more anterior positions in *lin-17* and *mig-1* mutants as well as wild-type.

Are these *mab-5*-regulators truly tissue-specific?

This analysis of double mutants between mutations in genes that regulate *mab-5* was initiated in part in order to identify functions for these genes outside the tissue in which they were known to act. None of these double mutants suggested a role for these genes outside their known tissue of function. However, in order to answer the question of tissue-specificity more completely, null alleles must be identified for each gene. If the mutations examined here only disrupt one function of the gene, leaving other functions fully wild-type, it might not be possible to detect a role for these genes in other tissues even in sensitized backgrounds. In addition, the development of

male-specific such as sensory rays, hooks and spicules should be examined in the *mig-1 lin-17, lin-17; egl-20* and *mig-1; egl-20* double mutants.

In summary, our findings do not rule out a role for these genes in regulating *mab-5* in other tissues, but are most consistent with a type of regulation that is predominantly cell-type-specific, controlled by several apparently independent pathways. Further analysis of these genes should help to explain how a position-specific gene like *mab-5* is regulated in an organism that appears to favor lineal control and local cell signals to regulate expression of the Hox genes (Cowing and Kenyon, unpublished data).

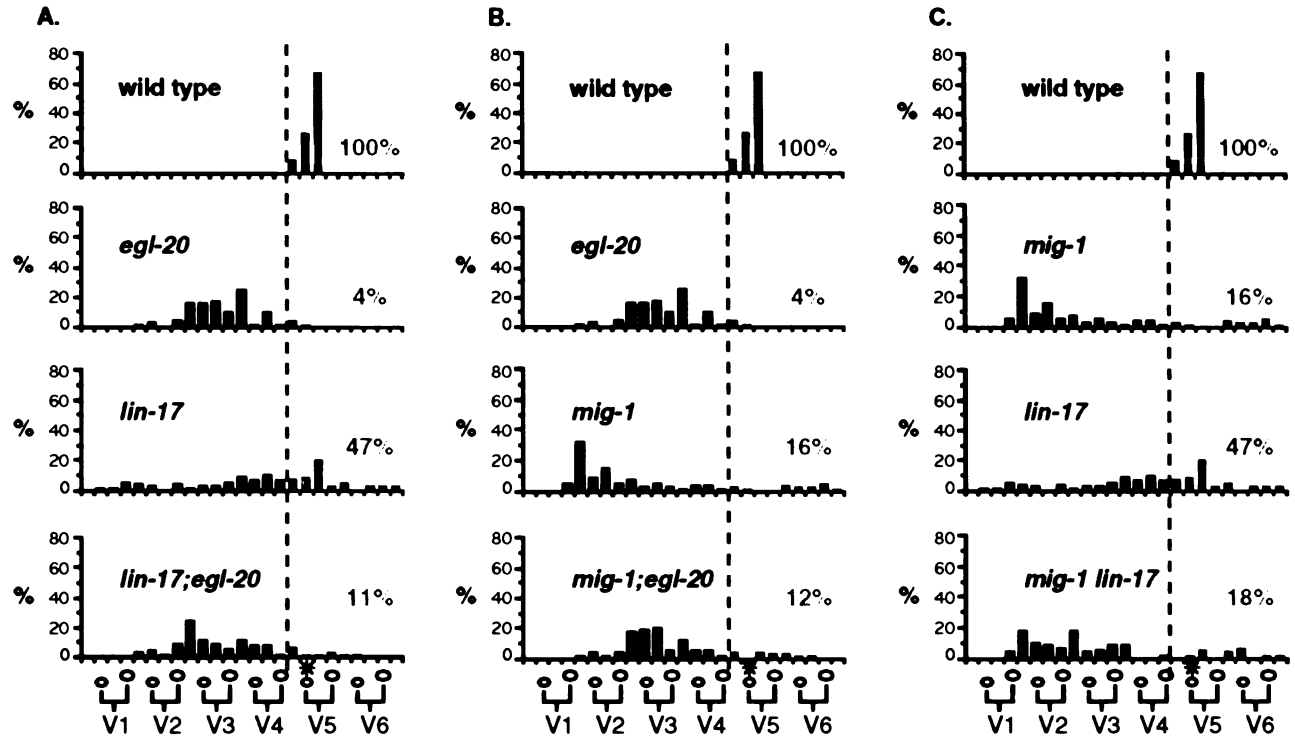

Fig. 3.1. Final positions of the QL.pa daughters in A. *lin-17(n671); egl-20(n585),* B. *mig-1(e1787); egl-20(n585)* and C. *mig-1(e1787) lin-17(n671)* double mutants relative to wild-type and the relevent single mutants.

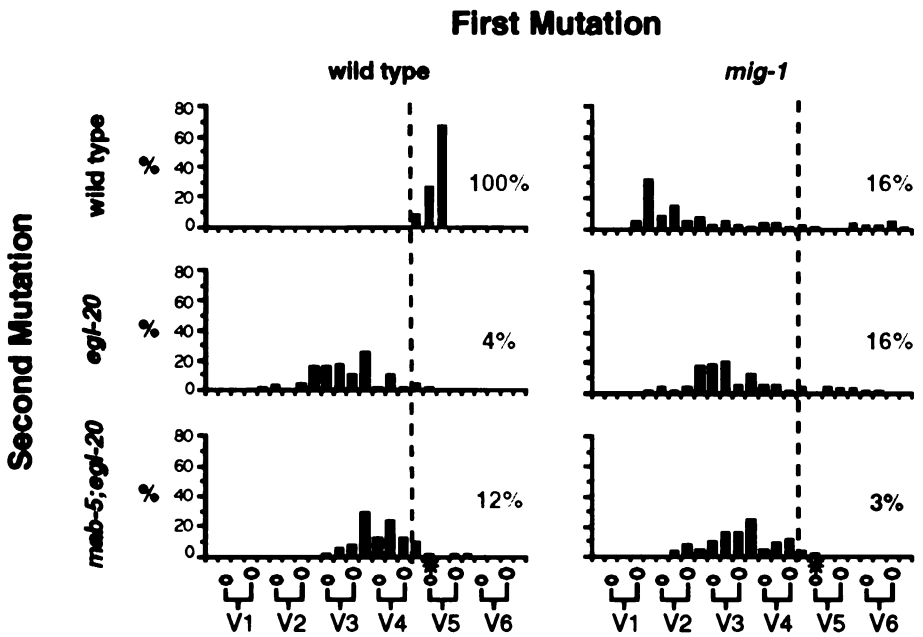

Fig. 3.2. Final positions of the QL.pa daughters in *mig-1(e1787)* single mutants and in double mutant combinations with *mab-5(e2088)*, and *egl-20(n585)*. The star above V5.a marks the birthplace of QL. n = 50 animals of each mutant genotype except: *mab-5(lf)*, n=41 and *mab-5(e2088); egl-20(n585)*, n=45. The dashed line marks the anterior boundary of QL descendant position in wild-type. The percentage of worms of each genotype with QL.pa descendants posterior to the line are noted at the right of each histogram. The data for *mig-1; mab-5; egl-20* is from Robinson (1995) and is of worms grown at 20oC. All of the other data are from worms raised at 25oC.

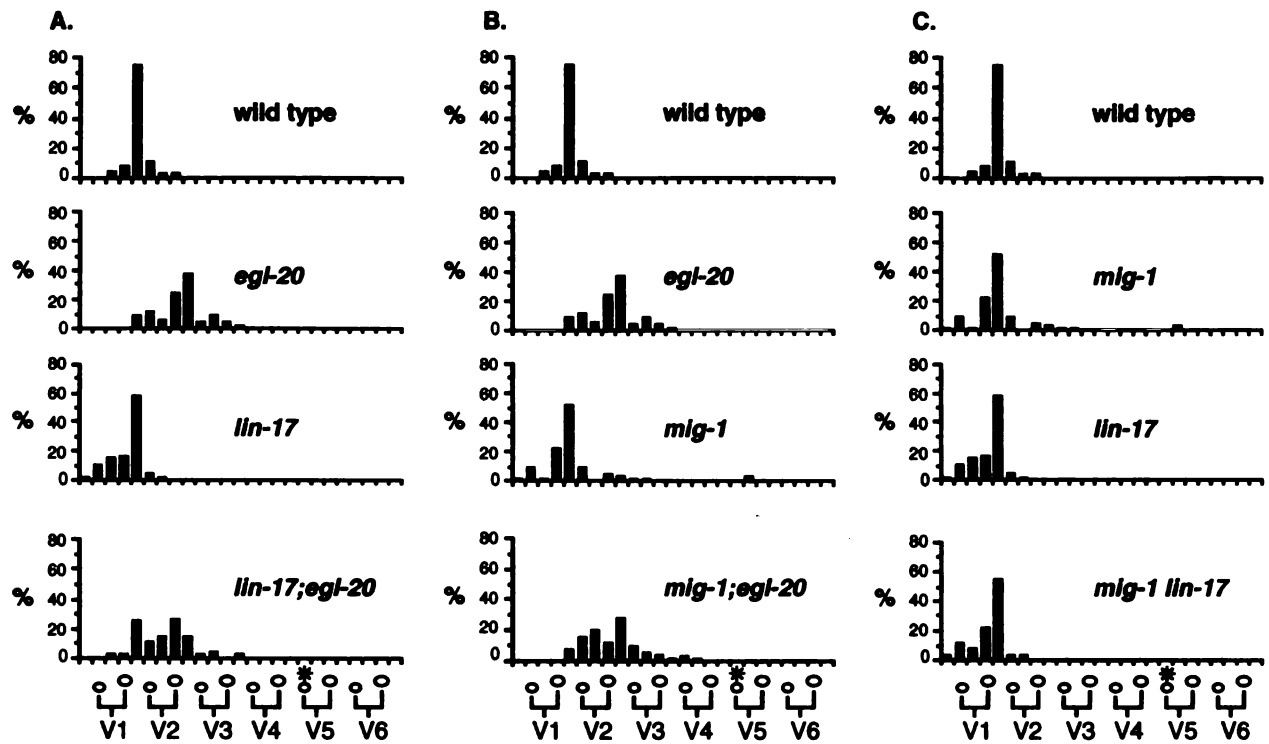

Fig. 3.3. Final positions of the QR.pa daughters in A. *lin-17(n671); egl-20(n585),* B. *mig-1(e1787); egl-20(n585)* and C. *mig-1(e1787) lin-17(n671)* double mutants relative to wild-type and the relevent single mutants. The star above V5.a marks the birthplace of QR. n > 50 animals of each mutant genotype except: *mig-1 lin-17*, n=42.

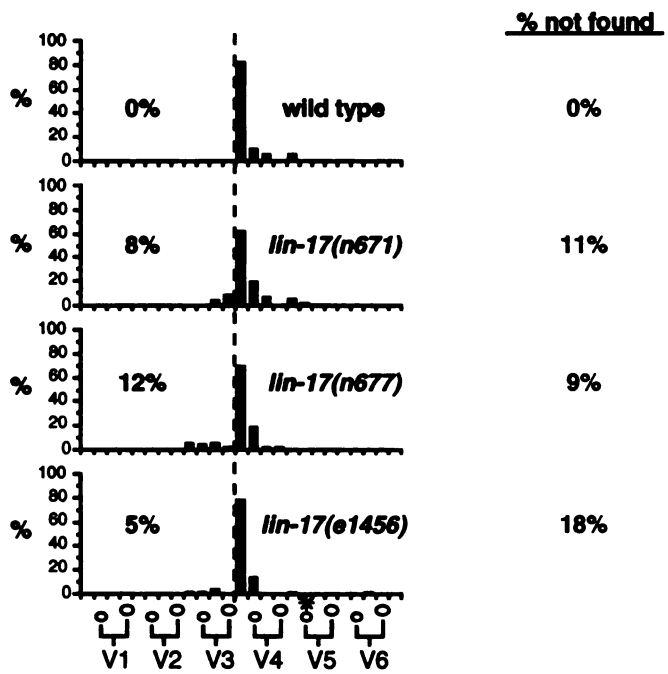

Fig. 3.4. In *lin-17* mutants, HSN can migrate farther than wild-type. The dashed line marks the anterior boundary of HSN migration in wild-type. The percentage of animals in which HSN migrated to a position anterior to the line is noted at the left of each histogram. I only became aware of the excessive HSN migration in these strains after I had begun the analysis. Thus, many of the animals in which I was unable to find HSN (see column to the right of the histograms) may have had an HSN in the anterior. However, there are also many lineage defects in these animals, so HSN may not have been born, or may have remained in the tail in some of these animals.

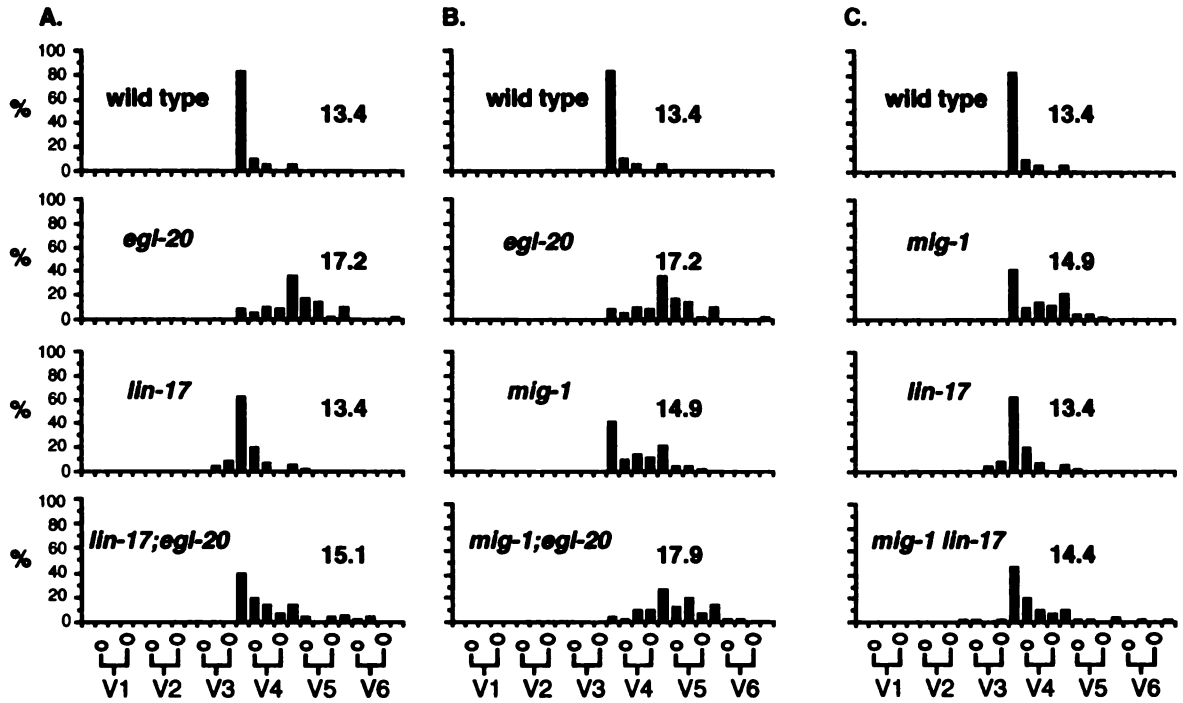

Fig. 3.5. Position of HSN in A. *lin-17(n671); egl-20(n585),* B. *mig-1(e1787); egl-20(n585)* and C. *mig-1(e1787) lin-17(n671)* double mutants relative to wild-type and the relevent single mutants. Numbers next to each histogram represent the mean HSN position for that genotype. Each tick mark on the x-axis represents one unit. The body of the worm from BDU to the anus has been subdivided into 25 units.

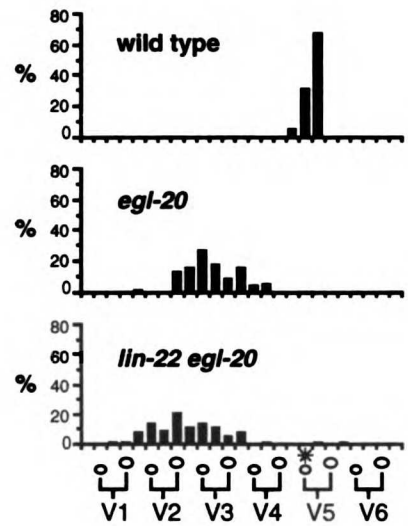

Fig. 3.6. Position of the QL.pa daughters, AVM and SDQL, in *egl-20(n585)* single mutants and *lin-22(n372) egl-20(n585)* double mutants at 20°C. The positions of the QL descendants along the A/P axis were determined relative to that of the stationary Vn.p and Vn.a epidermal cells, shown at the bottom of the figure (see Chapter 2, Materials and Methods). The asterisk above V5.a marks the birthplace of QL. *lin-22 egl-20*, n=25; wild-type= 35, *egl-20*, n=45 animals of each genotype were scored.

genotype	cells whose *mab-5* expression is affected									
	V1-V4	V5 desc.	V6	juvenile MN's (7 post.)	P7-P11	P12	muscles (post.)	QL	QR	M
wild-type	off	ON/off	ON	ON	ON	ON/off	ON	off/ON	off	ON
egl-20(n585)		off?*	off**					off		
mig-14(mu71)		off?*						off		
lin-17(n671)								off		
mig-1(e1787)								off		
lin-22(n372)	ON	ON*								
pal-1(e2091)			off							
pal-1(ct224) null										
egl-5(n945)						ON/ON				
dpy-19(								off	ON	
unc-40(e271)								off	ON	

Table 3.1. Mutations in many genes affect *mab-5* expression in a tissue-specific manner. All tissues were not examined in all mutants. Effects of mutations in the maintenance genes *pry-1* and *spy-1* are not shown here. wild-type expression of *mab-5* is from Salser and Kenyon (1993 and 1996). Effects of different mutations on *mab-5* expression are as follows: *mig-14, lin-17* and *mig-1* (Chapter 2); *egl-20* (Chapters 2, 4, and 5); *lin-22* (Wrischnik, 1995); *pal-1* (Salser and Kenyon 1996; Cowing and Kenyon, unpublished data; Hunter and

Kenyon, unpublished data); *egl-5* (Salser and Kenyon, 1993); *unc-40* (see Appendix); *dpy-19* (Honigberg and Kenyon, unpublished data).

* The pattern of *mab-5* expression in the V5 lineage is complex and very dynamic (Salser and Kenyon, 1996). None of these mutants affect *mab-5* activity or expression in all branches of the lineage. For a more complete discussion see Salser and Kenyon (1996) or this thesis, Chapters 4 and 5.

** This *egl-20* mutation prevents V6 from activating *mab-5* in response to neighbor ablation in a *pal-1(e2091)* mutant, but does not prevent of expression of *mab-5* in V6 in intact wild-type animals.

genotype	% QL.pax anterior	(n)
wild-type	0	279
egl-20/+	7%	56
mig-1/+; egl-20/+	13%	30

Table 3.2. *mig-1(e1787)* and *egl-20(n585)* do not fail to complement. *mig-1/+; egl-20/+* double heterozygotes were generated by mating *mig-1; him-5(e1490)* males to *unc-24(e138) egl-20(n585)* hermaphrodites and picking the non-Unc F1 progeny. The difference between the *egl-20* heterozygotes and the *mig-1/+; egl-20/+* double heterozygotes is not significantly different. (Fisher exact test: P= 0.38) Wild-type worms were scored at 25°C, all other worms were scored at 20°C. The percentage of QL.pa daughters which remain in the posterior in *egl-20* heterozygotes is the same at 20 and 25°C (see Chapter 2, Table 2.1).

A.

genotype	*mab-5-lacZ* expression in QL or QL.a/p stained	unstained
muIs3	11	0
mig-1; egl-20; muIs3	0	42

B.

genotype	anti-MAB-5 staining in QL.a/p bright	faint	unstained
wild type	92	2	0
mig-1; egl-20	0	0	48

Table 3.3. *mab-5* is not expressed in QL or its daughters in *mig-1(e1787); egl-20(n585)* double mutants. **A.** Expression of *mab-5-lacZ* in 3-4 hour old *mig-1; egl-20* double mutants at 20°C. *muIs3* is an integrated array containing *mab-5-lacZ* (ref). In this strain, 14% of the QL.pa daughters are posterior to V4.p (n=25) **B.** Polyclonal antisera to MAB-5 (ref) does not label QL.a or QL.p in 3-6 hour old *mig-1; egl-20* double mutants at 25°C.

Chapter 4:*egl-20* is required for signal-dependent activation of *mab-5* in V6

This work was done in collaboration with Craig Hunter in the Kenyon lab. Craig Hunter made the initial observations about the expression of *mab-5*-GFP in ablated and unablated *pal-1* mutant animals. I constructed all the *egl-20* mutant strains. Together, we performed the ablations and scored the outcomes in animals containing the *egl-20* mutation.

Chapter 4: *egl-20* activity is required for cell-signal mediated activation of *mab-5* in the V6 cell in *pal-1* mutants

Abstract

How is the *C. elegans Antennapedia* homolog, *mab-5*, turned on in the ectoblast, V6? V6 produces five *mab-5*-dependent-sensory rays; if these structures are not produced, males are unable to mate. Possibly in response to such a powerful evolutionary selection, *C. elegans* has evolved at least two ways to activate *mab-5* in V6. Usually *pal-1*, the *C. elegans caudal* homolog, activates *mab-5* in V6; if *pal-1* is inactive, V6 does not turn on *mab-5* and does not make rays. However, *mab-5* can still be activated in V6, even in the absence of *pal-1*, if the posterior neighbor of V6, T, is killed. What gene activates *mab-5* expression in V6 in response to loss of cell signals? We show here that the gene *egl-20*, which activates *mab-5* in the migrating QL neuroblast and its descendants, is also required to turn *mab-5* on in the V6 lineage in *pal-1* mutants after T ablation. We also demonstrate a role for *pal-1*, like *egl-20*, in regulating the migrations of the QL descendants. Together, these observations suggest that *egl-20* and *pal-1* may act in the same *mab-5* activation pathway in two different cell types.

Introduction

In *C. elegans*, the *Antp* homolog *mab-5*, one of the Hox genes, is expressed in many cells in the posterior body region. The epidermal blast cell V6 turns on *mab-5* shortly after it is born (Cowing and Kenyon, 1992), and *mab-5* continues to be expressed in V6 and its descendants throughout development. In the male, V6 produces sensory rays used in mating, a cell-fate that is *mab-5*-dependent. The product of the *pal-1* gene, the *C. elegans*

caudal homolog (Waring and Kenyon, 1991), is required for *mab-5* expression in V6 (Salser and Kenyon, 1996).

Like its counterpart in *Drosophila*, *pal-1* is expressed in the posterior of the early embryo where it promotes development of posterior fates (Hunter and Kenyon, unpublished results). *pal-1* null mutants die lacking a recognizable posterior (Yandell *et al.*, 1994), but animals carrying the reduction-of-function mutation, *e2091*, are viable and fertile (Hodgkin *et al.*, 1988). Like *pal-1* null mutants, *pal-1(e2091)* mutants have defects in the posterior: the V6 epidermal cell does not express *mab-5*, and thus produces no rays. At a low frequency, L1 animals are born with a bulged, and somewhat disorganized, middle.

Surprisingly, the inability of *pal-1* mutants to activate *mab-5* expression in V6 and produce rays can be suppressed by ablating the T cell. When T is ablated with a laser microbeam, V6 expresses *mab-5* (Salser, Hunter and Kenyon, unpublished data) and produces up to five rays (Waring and Kenyon, 1990). The six V cells in the body and the T cell in the tail, together with the H cells in the head, are all specialized epidermal blast cells placed end to end along the lateral midline of the worm. Together, these blast cells form a "seam" of individual cells which stretches across a large epidermal syncytium, hyp7. Signals between cells in the seam influence the development of these cells. Seam cells signal their anterior neighbors to repress *mab-5* and develop anterior fates. When posterior seam cells are ablated, anterior cells can express *mab-5* and develop posterior fates. As these seam cells divide, they go through cycles of loss-of-contact, extension and recontact (Austin and Kenyon, 1994; Podbilewicz and White, 1994). (Austin and Kenyon, 1994) have shown that signalling is correlated with cell-cell contact, suggesting that cells must be touching or very close in order to signal.

Waring and Kenyon (1991) have shown that *pal-1* acts in V6, suggesting that that T also signals its anterior neighbor in the seam, V6, to repress *mab-5* in the wild-type, but that *pal-1* activity allows V6 to express *mab-5* in spite of the cell signals. Salser and Kenyon (1996) have recently shown that *pal-1* has a second function in V6: in addition to allowing V6 to ignore signals from posterior neighbors and express *mab-5* (Salser, Hunter and Kenyon, unpublished data), it also makes V6 more responsive to the effects of *mab-5*.

What activates *mab-5* in V6 in T-ablated *pal-1* mutants? We have found that the *egl-20* gene, which is required for *mab-5* activation in the migratory neuroblast QL and its descendants, is also required to activate *mab-5* in *pal-1*-V6 cells after ablation of posterior neighbors. We show that *egl-20* mutants are unable to activate *mab-5* in V6.p after T ablation, although analysis of the ray phenotype suggests that a later descendant of V6 may be able to. Like *pal-1*, *egl-20* is required for several other aspects of anterior/posterior (A/P) patterning: *egl-20* functions to position the migrating Q descendants correctly along the A/P axis (see Chapter 2) and determines the polarity of certain epidermal cells, including V5, along the A/P axis (see Chapter 5). Our analysis of *egl-20*'s role in *mab-5* activation in *pal-1* mutants and in V5 polarity (see Chapter 5) suggests that *egl-20* may function in a seam-cell signalling pathway. We also demonstrate a previously unknown role for *pal-1* in the regulation of QL descendant migration. Together, these observations suggest that *egl-20* and *pal-1* may function in the same pathway in two different tissues to activate expression of the Hox gene *mab-5*.

Materials and Methods

General Procedures, Nomenclature, and Strains

Methods for routine culturing and genetic analysis are described by Brenner (1974) and Wood et al. (1988). All experiments were performed at 20°C, except for analysis of postdeirid formation, which was performed at 25°C. The wild-type strain N2 is the parent of all strains used. Mutations are described by Hodgkin et al. (1988) or are noted below.

Mutations used:

LGII: *muIs16(mab-5-GFP + dpy-20+)* (C. Hunter and C. Kenyon, unpublished data)

LGIII: *pal-1(e2091)*

LGIV: *egl-20(n585)*, *egl-20(mu25)* (Chapter 2), *dpy-20(e1282)*

LGV: *him-5(e1490)*

Strain construction

Since both *pal-1* and *egl-20* affect the migration of the QL descendants, other phenotypes were used to score the presence of *pal-1* and *egl-20* in these strains: the bulge and ray phenotype for *pal-1* and the HSN Mig defect for *egl-20*.

pal-1; egl-20. *pal-1; him-5(e1490)* males were mated to *egl-20(n585)* hermaphrodites. F1 *pal-1/+; egl-20/+; him-5/+* males from this cross were mated to *pal-1; dpy-20; him-5* hermaphrodites. non-Dpy hermaphrodite F1 progeny from this cross were cloned out and allowed to self-fertilize. Clones which were Him and Pal and segregated Egl's were kept. Hermaphrodites from these clones with an HSN Mig defect were cloned out. To confirm that *egl-20* was homozygous in this strain, the progeny of these animals were checked for an HSN Mig phenotype the following generation.

muIs16; pal-1; egl-20. *muIs16; dpy-20; him-5* males were mated to *pal-1; egl-20; him-5* hermaphrodites and hermaphrodite progeny cloned out. Clones which segregated Dpy progeny were kept. F2 bulged (Pal), non-Dpy progeny

from these plates were cloned out. Clones which segregated only GFP+ animals, all of which were had an HSN Mig phenotype, were kept.

Ablations of cells using a laser microbeam

Larvae were staged by collecting newly hatched animals at 30 minute intervals. In experiments to test postdeirid production, newly hatched animals were transferred to a fresh plate and allowed to develop for 30 minutes before mounting for ablation. (The staged worms were thus 1/2 to 1 hour old at the start of ablations.) In experiments to test ray production, or ray and postdeirid production, the newly hatched animals were allowed to develop for 2 hours before mounting for ablation. (The staged worms were thus 2 to 2 1/2 hours old at the start of ablations.) Worms were ablated over the course of the next 1/2 hour, so that for the ray experiments, all ablations were complete by 3 hours after hatching.

Individual cells were killed using a laser microbeam as described in Waring et al. (1992). The laser used in these experiments was a VSL 337 nitrogen-pumped dye laser with 7-amino 4-methyl coumarin dye, which produces a wavelength of 440 nm. Worms were immobilized for ablation on agarose pads containing 2-3mM Sodium Azide. The laser was focused on the nucleolus and fired continuously until the nucleolus shriveled and began to break up. Ablated worms were removed from the pad as soon as possible to minimize effects of the azide on development and viability and allowed to develop on a plate. Operated worms were then remounted either after 20-24 hours (at 25^{o}C) to confirm the absence of ablated cells and determine the fate of V5.pa (epidermal versus neural), or after 2 days (at 20^{o}C) to examine ray production. In general, the ablation procedure produced only small

developmental delays. Operated animals whose development appeared significantly retarded were discarded.

Ray Production: Rays were scored in late L4 males (in lethargus), or in young adult males immobilized on azide.

Results

What activates *mab-5* in V6 in *pal-1* mutants after T ablation? We wondered whether another known *mab-5* activator might be required to activate *mab-5* in V6 in *pal-1* mutants in response to neighbor ablation. Several genes activate *mab-5* expression in different cells (for a description, see Table 3.1, Chapter 3), but only one had been implicated in V-cell signalling: *egl-20* (see Chapter 5).

***egl-20* mutants alter the response of V5 to the loss of neural-promoting cell signals**

In *egl-20* mutants, the anterior and posterior seam cells send polarity-determining signals to V5, V6's neighbor (see Chapter 5). In the wild-type, posterior seam cells signal their anterior neighbors to repress *mab-5* activity. Might *egl-20* mutations affect the same seam-cell signalling pathways that activate *mab-5*? To answer this question, we examined a *mab-5*-sensitive fate in the V5 lineage in *egl-20* mutants.

In wild type, posterior seam cells instruct the V5.pa cell to repress *mab-5* expression and make a neuronal sensillum, the postdeirid. When posterior seam cells are ablated, V5.pa expresses *mab-5* (Salser, Hunter and Kenyon,

unpublished data) and makes epidermal cells instead (Sulston and White, 1980). In the absence of *mab-5* activity, V5.pa can continue to make a postdeirid after neighbor ablation (Austin and Kenyon, 1994). We wondered whether mutations in *egl-20* would also affect the decision of V5.pa to follow an epidermal fate after the ablation of posterior neighbors. To test this, we ablated either V6 alone or both V6 and T in *egl-20* mutants, allowed them to develop until late L2, and then examined them for the presence of the postdeirid cell group. We found that some *egl-20* mutant animals still made a postdeirid following ablation of posterior neighbors, unlike wild type (Fig. 4.1). Thus, mutations in *egl-20* allow V5.pa to develop as a neuroblast even in the absence of neighboring cells, just as mutations in *mab-5* do.

Since mutations in *mab-5* and *egl-20* both affect the neural/epidermal (N/E) fate decision of V5.pa in the same way, it is possible that they function in the same pathway. *egl-20*(+) activates *mab-5* expression in QL. Might *egl-20* act upstream of *mab-5* in V6 as well? To test this, we examined whether *egl-20* mutations would fail to activate expression of a *mab-5*-GFP reporter gene in V5 in response to neighbor ablation. Craig Hunter had shown that *mab-5*-GFP can be expressed in V5 after V6 ablation (unpublished data), mimicking the expression of the endogenous *mab-5* gene (Salser and Kenyon, unpublished data). However, we were unable to answer whether *egl-20* was required to acvtivate *mab-5* in V5 in response to V6 ablation, because the responce of the *mab-5*-GFP array altered the outcome of the experiment. In *egl-20* mutants containing *muIs16*, the integrated *mab-5*-GFP array, V5 never made a postdeirid after V6 ablation (data not shown), unlike *egl-20* single mutants, which made either a postdeirid or a N/E hybrid lineage (Waring *et al.*, 1992; Austin and Kenyon, 1994) after V6 ablation (Fig. 4.1). The results of these experiments suggest that the presence of multiple copies of the *mab-5*

promoter may inhibit *mab-5* activation in V5 in response to neighbor ablation.

In *egl-20* mutants V6 ablation no longer induces production of five V5 rays

Although we were unable to test whether *egl-20* is upstream of *mab-5* in V5 in the response of that cell to V6 ablation, a similar situation existed for the V6 cell in a *pal-1* mutant. In wild-type animals, loss of posterior V cells can also induce more anterior V cells, which would normally only produce seam cells, to produce sensory rays. *egl-20* mutations affect the response of V5.pa to loss of posterior neighbors; might they affect ray production as well? To test this, we ablated V6 in *egl-20* mutant L1 worms and examined ray production two days later. After V6 ablation in wild-type worms, V5 can produce up to five rays, two from V5.pa and three from V5.pp (Sulston and White, 1980). In *egl-20* mutants, however, V5 rarely made more than two rays, even when V5.pa failed to produce a postdeirid (Table 4.1). Our results indicate that V5 responds to V6 ablation, since it increases the number of rays it produces (from 1 to 2), however, it does not respond as vigorously as wild-type. Thus, *egl-20* activity appears to be required for V5 to produce rays after V6 ablation as well as for V5.pa to differentiate an epidermal fate.

In *egl-20* mutants T ablation no longer induces production of *five* V6 rays in *pal-1* mutants

Since our findings suggested that *egl-20* plays a role in V-cell signalling, we wondered whether *egl-20* might also affect the ability of V6 to respond to cell signals in *pal-1* mutants. To test this, we examined the ability of V6 to produce rays after T ablation in *pal-1* mutants carrying an *egl-20* mutation. We found that in *pal-1; egl-20* mutants, V6 was only rarely able to produce

five rays, in contast to *pal-1* single mutants (Table 4.2). Just as V5 in *pal-1+* animals did, V6 in *pal-1-* mutants now usually made *two* rays. In both cases, the V cell anterior to the ablated cell increases ray production but does not make the full number of possible rays. These observations suggest that ray production in V5 and V6 in *egl-20* mutants is still induced by ablation of posterior neighbors, but that the affected cells cannot respond fully. Thus, *egl-20* activity is required for full induction of V6 ray production in *pal-1* mutants.

egl-20 mutations block _mab-5_ expression in V6.p in T-ablated _pal-1_ mutants

egl-20 mutations block full ray induction of V6 by T in *pal-1* mutants; is this due to a failure to activate *mab-5* expression in V6? To test this, we examined the effect of an *egl-20* mutation on expression of a *mab-5*-GFP construct (C. Hunter and C. Kenyon, unpublished data) in *pal-1* mutants. In *pal-1* mutants, this *mab-5*-GFP construct is not expressed in V6.p unless T is ablated, paralleling expression of endogenous MAB-5 (Salser and Kenyon, unpublished data). We found that in *egl-20* mutants, *mab-5*-GFP is not expressed in V6.p in *pal-1* mutants following T ablation (Table 4.3).

Since many copies of the *mab-5* promoter are present in strains carrying the *mab-5*-GFP fusion, we wondered whether it might affect the ability of V6 to make rays following T ablation. To answer this question, we examined ray production in strains carrying the *mab-5*-GFP reporter construct and found that it was similar to that of the corresponding non-GFP strains (Table 4.4). Thus we conclude that the presence of multiple copies of the *mab-5* promoter does not affect the ability of a *pal-1*(-) V6 cell to make rays

pal-1 regulates migration of cells in the QL lineage

In addition to its V cell functions, *egl-20(+)* activates *mab-5* in the migrating QL neuroblast to direct its descendants to migrate and remain in the posterior. In the absence of *mab-5* or *egl-20* activity, the QL descendants migrate into the anterior (see Chapter 2). To my surprise, during the construction of the *pal-1; egl-20* double mutant, I noticed that *pal-1* mutants also affect QL descendant migration. I found that at a low frequency, the QL descendants migrate into the anterior in *pal-1(e2091)* mutants, just as they do in *mab-5* or *egl-20* mutants (Fig. 4.2). Interestingly, this phenotype was only observed in animals with bulges (Fig. 4.2), caused by mild to severe disorganization of the hypodermis, and possibly other tissues, in the central body region. Bulged animals look like a weaker version of the embyonic lethal phenotype; thus these animals may be those more severely affected by the *e2091* reduction-of-function mutation. In conclusion, our findings demonstrate that *pal-1* activity is required for wild-type migration of cells in the QL lineage.

Discussion

How is *mab-5* turned on in the epidermal blast cell, V6? V6 produces five *mab-5*-dependent-sensory rays; if these structures are not produced, males are unable to mate. Activation of *mab-5* in the V6 lineage is thus essential for male development. Possibly in response to such a powerful evolutionary selection, *C. elegans* has evolved at least two ways to activate *mab-5* in V6. Usually *pal-1*, the *C. elegans* caudal homolog, activates *mab-5* in V6; if *pal-1* is inactive, V6 does not turn on *mab-5* and does not make rays. However, a worm can still activate *mab-5* in V6 even in the absence of *pal-1*, if the posterior neighbor of V6, T, is killed. I have shown here that the gene *egl-20*,

which activates *mab-5* in the migrating QL neuroblast and its descendants, is required to activate *mab-5* in V6 in *pal-1* mutants after T ablation.

Do different parts of the V6 lineage require different *mab-5* activators?

egl-20 mutations block full induction of V6 ray formation in *pal-1* mutants in which T has been ablated; however, a few rays are made. This is similar to what happens in V5 after V6 ablation, where *egl-20* mutations block full induction of ray formation (Fig. 4.2). In both V5 in a wild-type background and V6 in a *pal-1* background, *egl-20* mutations reduce the number of sensory rays from five to approximately two. Rays are a *mab-5*-dependent cell fate, and yet *mab-5* is not expressed in V6.p following ablation of T in *pal-1* mutants. Somehow *mab-5* must be activated later in the V6 lineage by a gene other than *egl-20*. If *mab-5* is activated in V6 at a later time, why are only a few rays made? One possibility is that *mab-5* is turned on late but in the entire V6 lineage in T-ablated *pal-1; egl-20* mutants. Salser and Kenyon have shown that if MAB-5 is not present during L2, the V6 descendants do not proliferate; late expression of *mab-5* can only induce the formation of a few rays, since there are not enough precursor cells (Salser and Kenyon, 1996). Similarly, late ablations of V6, which presumably do not activate *mab-5* expression until late in the V5 lineage, are only capable of inducing two to three rays (Salser and Kenyon, 1996). Alternatively, *mab-5* might only be expressed only within one branch of the V6 lineage in T-ablated *pal-1; egl-20* mutants and thus might be capable of influencing the fates of only a small number of ray precursor cells. To distinguish between these two possibilities, *mab-5* expression in these animals would have to be examined after L2. Since the *mab-5*-GFP construct used for these experiments

does not express after L2, antisera to MAB-5 would need to be used to probe *mab-5* expression in V6.

How might *egl-20* affect the decision to activate *mab-5* in V6?

Cell signals block expression of *mab-5* in V6 in *pal-1* mutants. The *egl-20(n585)* mutation renders V6 insensitive to loss of these cell signals. Does *egl-20* act upstream or downstream of cell signals? There are at least two possibilities: **1.** Cell signals keep *egl-20* inactive in V6. When T is ablated, signalling is disrupted. This activates *egl-20* in the responding cell, which can now turn on *mab-5*. **2.** *egl-20* acts in neighboring cells, most likely V5, to prevent V5 from sending T-specific signals. In *egl-20* mutants, V5 now acts as a T-like signalling center, compensating for the loss of T, and helping to maintain *mab-5* repression in V6. One way to test the second model would be to isolate V6 in a *pal-1; egl-20* double mutant and see whether *mab-5* is now activated. If *egl-20* were required in epidermal cells other than seam cells, such as the hypodermal syncytium, it would be much harder to demonstrate using ablation studies. Genetic mosaic analysis should help to identify the cells in which *egl-20* acts.

The *egl-20* gene also activates *mab-5* in the neuroblast QL. For V6, *egl-20*'s role must either be to regulate or respond to intercellular signals; might *egl-20* be part of a cell-signalling pathway that activates *mab-5* in QL as well? Interestingly, the *mig-14* gene, which is also required for activation of *mab-5* in QL, also regulates the response of V5.pa to V6 ablation. In *mig-14(mu71)* mutants, as in *egl-20* and *mab-5* mutants, V5.pa continues to produce a postdeirid even after the loss of V6 (L. Honigberg and C. Kenyon, unpublished data). As the cloning of the *egl-20* gene progresses, it will be

interesting to learn where *egl-20* acts and whether it is part of a conserved cell-signalling or Hox gene activation pathway in other organisms.

pal-1 may act upstream of _mab-5_ in the QL neuroblast

I have found that, like *egl-20*, *pal-1* is required for the posterior migration of the QL descendants. *egl-20* functions to activate *mab-5* in QL and its descendants. *pal-1* is required for V6 to activate *mab-5*; might *pal-1* have a similar function in the QL lineage? The *pal-1* Mig defect resembles that of *mab-5*. Unlike *mab-5*, however, the *Pal-1* phenotype is not fully penetrant: only the more strongly affected (i.e. bulged) animals have a Mig defect (Fig. 4.2). This difference is probably due to the fact that the *e2091* mutation is not null; the migrations of the QL descendants in animals mosaic for a *pal-1* null allele might be defective 100% of the time.

In *mab-5* mutants, only the migrations of the QL descendants are affected; the posterior-directed migration of QL is unaffected (Chalfie and Sulston, 1981; Kenyon, 1986). It is not clear whether the *pal-1(e2091)* mutation affects the same step of the migration as *mab-5*, since the actual migrations of cells in the QL lineage have not been observed directly. However, there are two observations that suggest that the QL lineage migration defect in *pal-1(e2091)* mutants may be due to misregulation of *mab-5* in QL. First, *pal-1* mutants appear to reduce expression of *mab-5* in the QL lineage as determined by staining with polyclonal antisera to MAB-5 (S. Salser and C. Kenyon, unpublished data). Second, *pal-1(e2091)* fails to complement *mab-5* null mutants for the QL descendant migration defect in much the same way that the *egl-20(n585)* mutation does (S. Salser and C. Kenyon, unpublished data). Since the *pal-1(e2091)* mutation appears to be a reduction-of-function allele

(Waring and Kenyon), our findings suggest that *pal-1* may regulate *mab-5* expression in the QL lineage as well as that of V6.

egl-20 and *pal-1* regulate *mab-5* expression in two of the same tissues: the V6 lineage and the QL lineage. *pal-1* and *egl-20* may act in parallel to regulate *mab-5* expression in V6; what is their relationship in the regulation of QL? It will be interesting where and how *pal-1* and *egl-20* act to regulate QL descendant migration.

Is *egl-20* part of a cell-signalling pathway which activates *mab-5* in V5 as well?

Cell signals regulate the N/E fate decision of V5.pa. In wild type, V5.pa adopts a neural fate and makes a postdeirid. After ablation of V6, V5.pa almost always makes epidermal cells: a seam cell and a syncytial cell (Sulston and Horvitz, 1977; Sulston and White, 1980). In both *egl-20* and *mab-5* mutants, V5.pa undergoes a neural fate approximately 50% of the time (Austin and Kenyon, 1994)(Fig. 4.1), suggesting that they might both act in the same pathway. However, I was unable to test whether *egl-20* was upstream of *mab-5* in V5 as well, because the presence of the *mab-5*-GFP reporter gene appeared to alter the outcome of the experiment. The results of these experiments suggest that the presence of multiple copies of the *mab-5* promoter may titrate some factor or factors required for *mab-5* activations. Since the response of V5 to V6 ablation in the wild-type is to express *mab-5* rather weakly (C. Hunter, S. Salser, and C. Kenyon, unpublished data), perhaps the copy number of the *mab-5* promoter present in muIs16 is sufficient to titrate enough of this factor. This same reporter gene, however, was used to test *mab-5* expression in V6 in T-ablated *pal-1* mutants, yet did not affect the outcome of those experiments (i.e. ray production by V5, Fig. 4.4). It may be that *muIs16* (*mab-5*-GFP), did not affect *mab-5* activation in V6

because its response to the ablation of posterior neighbors is so robust (C. Hunter, S. Salser, and C. Kenyon, unpublished data). Alternatively, the temperature dependence of postdeirid formation may be more sensitive in *egl-20* mutants. Preliminary experiments suggested that postdeirid formation was equal in V6-ablated *egl-20* mutants at 20 and 25°C (data not shown), but perhaps cooler conditions during the *muIs16* experiment inhibited postdeirid formation more strongly.

Conclusion

In this chapter I have shown that wild-type function of the *egl-20* gene is required to activate cell-signal-induced expression of *mab-5* in the V6 epidermal cell. Curiously, our findings indicate that disruption of local cell signals must also activate other genes required to turn *mab-5* on later in the V6 lineage. Our studies demonstrate that the regulation of a single Hox gene, *mab-5*, within a single cell, V6 can be quite complex: different activators respond to different situations and can affect all or part of the lineage. If *C. elegans* has evolved to rely more on lineal regulation of Hox gene expression (Cowing and Kenyon, unpublished data) than on anterior/posterior position, perhaps this system of local control (V-cell signalling) has evolved to provide greater flexibility in case of errors of development. Further analysis of these genes should clarify the role of cell-signalling in Hox gene regulation, and perhaps identify other components of this pathway.

Acknowledgments

I would like to thank Craig Hunter for his patience in helping me with the laser and for many critical discussions of this material. Thank you for a fun collaboration, Craig.

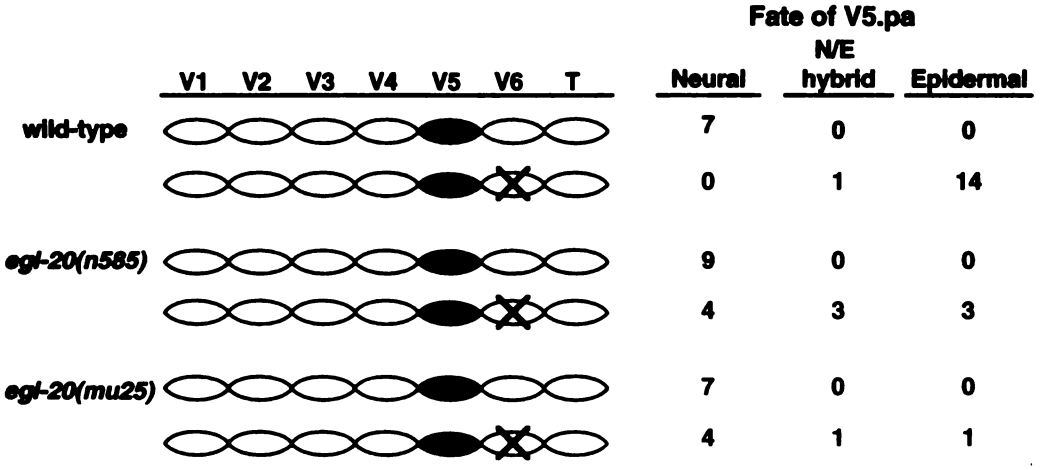

Fig. 4.1. Mutations in *egl-20* allow V5.pa to continue to produce a postdeirid, a neural fate, after V6 ablation.

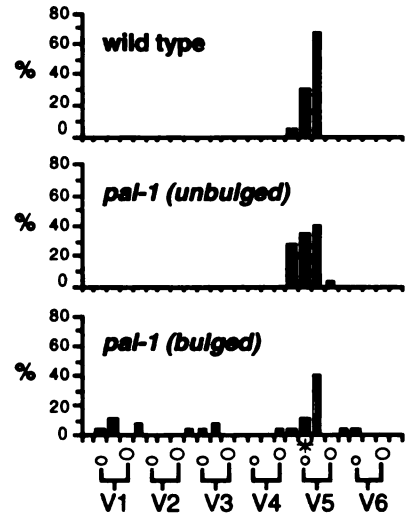

Fig. 4.2. Final positions of the QL.pa descendants in wild-type and *pal-1(e2091)* mutants at 20°C. The positions of the QL descendants along the A/P axis were determined relative to that of the stationary Vn.p and Vn.a epidermal cells, indicated at the bottom of the figure. Anterior is to the left. The asterisk above V5.a marks the birthplace of QL. More than x animals of each genotype were scored.

A. *egl-20(n585)*

	Number of V5-derived Rays						
V5.pa fate	**0**	**1**	**2**	**3**	**4**	**5**	**(n)**
no Pd		2	7	1		1	(11)
hybrid			3				(3)
Pd			4				(4)

B. wild-type

	Number of V5-derived Rays						
V5.pa fate	**0**	**1**	**2**	**3**	**4**	**5**	**(n)**
no Pd						6	(6)

Table 4.1. Production of rays by V5 after V6 ablation in *egl-20(n585)* mutants.

A. After T ablation

	Number of V-derived Rays in fan				
genotype	0	1-2	3-4	5-6	(n)
pal-1; him-5	8%	8%	17%	67%	(12)
pal-1; egl-20; him-5	50%	33%	11%	6%	(18)
egl-20; him-5	0%	0%	9%	91%	(11)

B. Control unablated sides

	Number of V-derived Rays in fan				
genotype	0	1-2	3-4	5-6	(n)
pal-1; him-5	67%	33%	0%	0%	(12)
pal-1; egl-20; him-5	89%	6%	0%	6%	(18)
egl-20; him-5	0%	0%	0%	100%	(11)

Table 4.2. An *egl-20* mutation blocks induction of V6 rays by T ablation in *pal-1* mutants.

genotype	V6.p stains	(n)
muIs16; pal-1; him-5	100%	(19)
muIs16; pal-1; egl-20; him-5	0%	(14)

Table 4.3. *mab-5-GFP* is not expressed in V6.p in *pal-1(e2091); egl-20(n585)* mutants following T ablation. *mab-5-GFP* was scored at 13-15 hours after hatching.

A. After T ablation

genotype	Number of V-derived Rays in fan 0	1-2	3-4	5-6	(n)
muIs16; pal-1; him-5	25%	0%	0%	75%	(4)
muIs16; pal-1; egl-20; him-5	100%	0%	0%	0%	(10)

B. Control unablated sides

genotype	Number of V-derived Rays in fan 0	1-2	3-4	5-6	(n)
muIs16; pal-1; him-5	100%	0%	0%	0%	(4)
muIs16; pal-1; egl-20; him-5	90%	10%	0%	0%	(10)

Table 4.4. A *mab-5*-GFP reporter construct does not alter the effect of an *egl-20* mutation on induction of V6 rays by T ablation in *pal-1* mutants.

Chapter 5: Cell signals reverse stem-cell polarity in *egl-20* mutants

This work was done in collaboration with Jennifer Whangbo in the Kenyon lab and prepared for submission to Development.

I made the initial observations of the V5 polarity reversal in *egl-20* mutants and characterized the frequency of this phenotype in all alleles. I noticed and characterized the later reversals as well. I found that neighbor ablation influenced the polarity of the V5 cell division in *egl-20* mutants, i.e. posterior ablations always rescued and anterior ablations always reversed the polarity. Jennifer Whangbo continued these experiments, finding that an isolated V5 cell would always divide with wild-type polarity in an *egl-20* mutant, and that ablating seam cell neighbors had no effect on the polarity of the V5 cell division in wild-type. In addition, Jennifer performed the MH27 staining and the temperature shift experiments. I identified two enhancers and a suppressor of the *egl-20* V5 polarity reversal phenotype, *mig-1(e1787)*, *mig-14(mu71)* and *lin-17(n671)*, respectively. Jennifer extended this work by finding that a *lin-18* mutation could also act as a suppressor, and that a stronger *mig-14* allele, k124, both enhanced the *egl-20* polarity reversal and also affected V5 polarity on its own. Jennifer then tested the ability of the *lin-17* and *mig-1* mutations to enhance or suppress the response of the V5 cell in *egl-20* mutants to neighbor ablation.

Abstract

At hatching, a single row of specialized epidermal cells, named seam cells, runs down each side of the nematode *C. elegans*. As the worm develops, the seam cells in the main body region divide according to a modified stem-cell lineage: the posterior daughter is always a stem cell, while the fates of the anterior daughters are different at different developmental stages. We have found that mutations in the gene *egl-20* can reverse the anterior/posterior polarity of one of these cells, V5. We show that this reversal is influenced by the presence of posterior neighbors: when posterior seam cells are ablated, V5 divides with wild-type polarity, and when anterior neighbors are ablated, it always divides with reverse polarity. Thus, our findings suggest that there are at least two mechanisms for determining the A/P polarity of V5 in *egl-20* mutants: one which involves signals from neighboring seam cells and one which is seam-cell independent. Surprisingly, the anterior/posterior polarity of seam cells in wild-type animals is unaffected by ablation of neighbors. Thus, the seam-cell signalling pathway may act redundantly with another polarity-determining mechanism in wild-type or may only exist in *egl-20* mutants. Candidates for genes involved in the signal/response pathway are *lin-17*, the *C. elegans* homolog of the *Drosophila* tissue polarity gene *frizzled*, *mig-1*, and *mig-14*. These four genes, *egl-20*, *mig-14*, *mig-1* and *lin-17*, all regulate the same step of cell migration, activation of the Hox gene, *mab-5*. In addition, *egl-20* and *mig-14* also act to determine the stopping points of these migrating cells along the A/P axis. Together, these observations suggest that stationary and migratory cells may share a system for determining position and orientation along the anterior/posterior axis.

Introduction

During development, cells must divide to produce progeny with different developmental fates. This process of asymmetric cell division is also used by single celled organisms such as *Caulobacter crescentus* (Marczynski and Shapiro, 1995) and *S. cerevisiae* (Way *et al.*, 1994) to produce daughter cells with different developmental potentials. In many cases, the polarity of an asymmetric division relative to its environment is predictable (e.g. *Caulobacter*, *S. cerevisiae*, the *Fucus* zygote, many cells in *C. elegans*, the cortical progenitor cells in the vertebrate brain, and neuroblasts in the *Drosophila* neuroectoderm, reviewed in (Quatrano *et al.*, 1979; Kropf *et al.*, 1988; Horvitz and Herskowitz, 1992; Way *et al.*, 1994; Marczynski and Shapiro, 1995)Quatrano *et al.*, 1979; Kropf *et al.*, 1988; Horvitz and Herskowitz, 1992; Way *et al.*, 1994; Marczynski and Shapiro, 1995; Rhyu and Knoblich, 1995; Drubin and Nelson, 1996)). Such predictability could either be due to an asymmetry within the mother cell itself, or to an asymmetry in the environment of the daughter cells. We are interested in the first case: an intrisically asymmetric mother cell dividing to give rise to two different daughter cells. What controls the polarity of such an intrinsically asymmetric cell division?

There are many examples of cell-fate determinants that become localized within a cell, and are thus unequally segregated to the two daughters during cell division (some of the better known examples are vg-1, HO, Ash-1p, *numb*, *prospero*, and Notch, reviewed in Slack, 1994; Rhyu and Knoblich, 1995; Amon, 1996), but the source of that asymmetry is rarely known. In budding yeast, a molecular mark is left at the site where earlier buds were formed. A small GTPase, Bud-1p, recognizes this mark and signals the

budding machinery to assemble at that location (Drubin and Nelson, 1996). In *Caulobacter*, the site of the previous cell division marks that pole of the cell in some unknown way, so that it becomes a site for flagellar assembly (Marczynski and Shapiro, 1995). In both of these examples, the site of an earlier division is marked and remembered, providing an internal asymmetry. External signals, both from the physical environment and from neighboring cells, can also create an asymmetry within the mother cell. The developing zygote of the brown alga, *Fucus*, is thought to be polarized by a localized Ca^{++} current, generated by a gradient of light, as the cell floats in the water (Quatrano *et al.*, 1979; Kropf *et al.*, 1988). Similarly, the dorsal/ventral polarity of the *Drosophila* oocyte, and later the embryo, is generated by a series of signals back and forth between the developing oocyte, or embryo and its neighboring somatic cells, the follicle cells (Shupbach and Roth, 1994; Gavis, 1995).

We have examined the polarity of asymmetric cell divisions in the nematode, *C. elegans*. At maturity, this small worm has just over 1000 non-germline cells. To generate enough cells of different types, 807 of these 949 cell divisions are asymmetric (reviewed in Horvitz and Herskowitz, 1992; Way *et al.*, 1994). In general, the orientation of these asymmetric divisions is the same from worm to worm. However, in only a few cases is the source of this polarity understood. In the very first cell division of the *C. elegans* zygote, an asymmetry results from segregation of cytoplasmic determinants to the posterior daughter, P1 (reviewed in Horvitz and Herskowitz, 1992; Way *et al.*, 1994). The polarity of this asymmetry may be determined by an external signal, the point of sperm entry (B. Goldstein and S. Hird, pers. comm). Much later in development, the polarity of certain asymmetric cell divisions in the tail of the worm (B, T, F, and U) are also determined by signals from

neighboring cells (Chamberlin and Sternberg, 1993). When these signals are disrupted, by ablating the signalling cell or mutating components of the signalling pathway, these tail cells divide asymmetrically, but with abnormal orientations (Herman and Horvitz, 1994; Chamberlin and Sternberg, 1995).

C. elegans is highly amenable to genetic analysis and several genes have been identified which orient the polarity of certain asymmetric cell divisions, *lin-17*, *lin-18* and *lin-44* (reviewed in (Horvitz and Herskowitz, 1992; Way *et al.*, 1994). We have shown that an additional gene, *egl-20*, is required to correctly orient certain asymmetric cell divisions along the anterior/posterior (A/P) axis. Mutations in *egl-20* reverse the A/P polarity of certain epidermal cell divisions, including that of the stem-cell V5. This stem-cell is one of six V cells placed end-to-end along the side of the worm. Together with the H cells in the head and the T cell in the tail, the V cells form a thin "seam" of individual cells which stretch from anterior to posterior, across a large epidermal syncytium (Sulston and Horvitz, 1977; Francis and Waterston, 1991). We show that the orientation of the V5 cell division in *egl-20* mutants, but not in wild type, is determined by interactions with neighboring seam cells: in mutants, posterior neighbors signal V5 to divide with a reversed polarity and anterior neighbors signal V5 to divide with a wild-type polarity. However, some other polarity-determining mechanism that orients V5 must remain functional in *egl-20* mutants, since when V5 is isolated from both its anterior and posterior neighbors by ablation in *egl-20* mutants, it always divides with a wild-type polarity. Our findings suggest a model in which the polarity of V5 can be determined either by an *egl-20*(-)seam-cell signalling pathway or by an *egl-20*-dependent pathway.

We have analyzed the *egl-20* polarity reversal phenotype and have identified both enhancers and suppressors. These genes are candidates for

components of the signal/response pathway. One suppressor, *lin-17*, is homologous to the *Drosophila* tissue polarity gene, *frizzled* (H. Sawa and R. Horvitz, pers. comm). *frizzled* is responsible for orienting asymmetric cells correctly along body axes and appears to act both autonomously and non-autonomously (Vinson and Adler, 1987; Krasnow and Adler, 1994). Similarly, *lin-17* is required for the generation and orientation of asymmetry of many cell divisions (Sternberg and Horvitz, 1988).

In addition to their role in cell polarity, *egl-20*, its suppressor *lin-17*, and its enhancers *mig-14* and *mig-1*, all regulate the same step in the migrations of certain cells: activation of the *Antennapedia* homolog *mab-5* in the descendants of the neuroblast QL. Independent of their effect on *mab-5*, *egl-20* and *mig-14* also act to determine the stopping points of migrating Q descendants along the A/P axis (see Chapter 2) Together, these observations suggest that stationary and migratory cells may share a system for determining position and orientation along the A/P axis.

Materials and Methods

General Procedures, Nomenclature, and Strains

Methods for routine culturing and genetic analysis are described by Brenner (1974) and Wood et al. (1988). All experiments were performed at 25°C, unless otherwise noted. The wild-type strain N2 is the parent of all strains used. Mutations are described by Hodgkin et al. (1988) or are noted below.

Mutations used:

LGI: *mig-1(e1787)*, *lin-17(n671)*, *lin-17(n677)*, *lin-44(n1792)*

LGII: *mig-14(mu71)*, *mig-14(k124)* (Kiyoji Nishiwaki, pers. comm.)

LGIV: *egl-20(n585)*

LGX: *lin-18(n620)*

Larvae were staged by collecting newly hatched animals at 30 minute intervals. For all ablation experiments except the time course, newly hatched animals were transferred to a fresh plate and allowed to eat for 30 minutes before mounting for ablation. (Thus the staged worms were 1/2 to 1 hour old at the start of ablations.) Worms were ablated over the course of the next 1/2 hour, so that all ablations were complete by 1 1/2 hours after hatching.

Scoring the fates of V5.a and V5.p

Intact animals: In general, cell fates were scored at the end of L1 after V5 has divided once to produce V5.p and V5.a. At this time the daughter which develops as a seam cell has a distinctive eye-shaped outline and is located laterally, directly below the alae (cuticular ridges). The daughter which joins the syncytium has already fused at this point, and no longer has a cellular outline. In addition, the nucleus of this cell is usually slightly ventral to the seam cell nucleus and, although it has the large nucleolus of an epidermal cell, the nucleoplasm has a grainier texture than that of the seam cell. In a few animals in which the division of V5 appeared to be reversed, however, the seam cell nucleus was ventral to the syncytial nucleus. Since by all other criteria the fates of V5.p and V5.a appeared to by reversed, these animals were scored as reversed.

Ablated animals: In ablated animals, the fates of V5.a and V5.p were scored later than intact animals, during L2 or early L3. At this time, the seam cell daughter of V5 (V5.p in wild type) had divided, but the syncytial daughter (V5.a in wild type) had not, although its nucleus continued to grow. Thus, the position of the seam cell daughter of V5 was inferred from the position of its

daughter cells. The syncytial daughter was identified based on the position and morphology described above (its large size was used to distinguish it from other cells which had joined the syncytium more recently). If the syncytial daughter was posterior to the midpoint of the seam cell daughters, then the V5 division was scored as reversed.

Temperature shift experiments.

Gravid hermaphrodites grown for at least two generations at either 15 or 25°C were treated with alkaline hypochlorite to release their eggs (Sulston and Hodgkin, 1988). Larvae were staged by collecting newly hatched animals at 30 minute intervals and placing them on plates preincubated at the temperature the worms were grown at. At certain times, animals were collected in M9 media preincubated to the new (shifted) temperature, pelleted briefly, and transferred to plates preincubated to the shifted temperature. Thus, the temperature shift began at the start of the transfer. V5 polarity was scored at the equivalent of 9 hours post-hatching at 25°C, after all V cells had divided once, and the P nuclei had mostly descended into the ventral nerve cord.

Immunofluorescence.

Animals were fixed and stained as described in (Salser and Kenyon, 1996) using the MH27 monoclonal antibody (provided by R. Barstead and R. Waterston.).

Ablations of cells using a laser microbeam

General procedure. Individual cells were killed using a laser microbeam as described in Waring et al. (1992). The laser used in these experiments was a

VSL 337 nitrogen-pumped dye laser with 7-amino 4-methyl coumarin dye, which produces a wavelength of 440 nm. Worms were immobilized for ablation on agarose pads containing 2-3mM Sodium Azide. The laser was focused on the nucleolus and fired continuously until the nucleolus shriveled and began to break up. Ablated worms were removed from the pad as soon as possible to minimize effects of the azide on development and viability and then allowed to develop for 10-20 hours on a plate. Operated worms were then remounted to confirm the absence of ablated cells and determine the pattern of V5 daughter nuclei. In general, the ablation procedure produced only small develpmental delays. Operated animals whose development appeared significantly retarded were discarded.

Lineage after ablation. After ablating cells as described above, operated worms were allowed to recover for x hours on a seeded plate, then remounted and continuously observed using Nomarski optics (Sulston and Horvitz, 1977) until the V5 cell had divided and the fates of the daughters unambiguously determined based on cellular and nuclear morphology and position.

Construction of double mutant strains

In general, *egl-20* double mutant strains were constructed by first allowing the non-*egl-20* mutation to become homozygous. The *egl-20* mutation was then made homozygous by chasing out an an *unc-24(e138) dpy-20(e1282)*-marked chromosome IV. (The *unc-24* and *dpy-20* genes flank *egl-20*). Wherever possible, a phenotype other than a QL descendant or HSN migration (Mig) defect was used to determine the presence of the non-*egl-20* mutation. Although *egl-20* partially fails to complement *mab-5* mutations for

the QL descendant Mig defect, *egl-20* does not have a transheterozygous interaction with *lin-17* or *mig-1* mutations at 20°C (data not shown).

***lin-18; egl-20* and *lin-44; egl-20*.** To make these strains, we determined the presence of the *egl-20* mutation by scoring the Mig defect of the QL descendants. *lin-44(n1792)* and *lin-18(n620)* do not affect QL descendant migrations (data not shown). The phasmid neurons in *lin-44* mutants, but not *egl-20* mutants (data not shown), do not stain with the fluorescent dye, DiI (1,1'-dioadecyl-3,3,3',3'-tetramethylindocarbocyanine, perchlorate) (Herman and Horvitz, 1994). This dye-filling phenotype was used to determine the presence of the *lin-44* mutation in the double mutant strain. The *lin-18* mutation was determined by the presence of a Bivulva phenotype (Ferguson and Horvitz, 1985).

***lin-17; egl-20*.** Since the *lin-17(n671)* mutation suppressed the *egl-20* polarity reversal phenotype (Table 5.2) and partially suppressed the HSN migration defect and QL descendant Mig defect (data not shown), we performed a complementation test to demonstrate the presence of an *egl-20* mutation in this strain (data not shown).

Results

egl-20 is required for V5 to adopt a wild-type polarity

In wild-type animals the posterior daughters of the six epidermal V cells (Vn.p cells) always develop as lateral seam cells, like their mothers, whereas the anterior daughters (Vn.a cells) fuse with the hypodermal syncytium (Sulston and Horvitz, 1977). These two cell types can be distinguished by differences in the morphology and placement of their nuclei and by the distinctive eye-shaped outline of the Vn.p cells (see Materials and Methods).

Thus, in wild-type animals there is an alternating pattern of seam cells and syncytial nuclei along the body of the worm (see Fig. 5.1). We noticed that in *egl-20(n585)* mutants this repeating pattern was sometimes interrupted. In all cases, the cell at the position of V5.p had the morphology and placement of a syncytial nucleus and the cell at the position V5.a had the morphology and placement of a seam cell (Fig. 5.1 and Table 5.1). In wild-type animals only the seam cell (posterior) daughter divides again: the anterior daughter fuses with the hyp7 syncytium and is incapable of division. In several *egl-20* mutants, we observed an anterior, "seam-cell"-like daughter divide (Fig 5.1C,F), indicating that in addition to having the morphology of a seam cell, these anterior daughters had the developmental potential of a seam cell.

To ask whether this apparent reversal of cell fates was due to the *egl-20(n585)* mutation, we examined animals homozygous for other *egl-20* alleles. We found that all four strong *egl-20* alleles caused such an apparent fate reversal (Table 5.1), suggesting that this defect was due to a mutation in the *egl-20* gene. We chose to analyze this phenotype primarily in *egl-20(n585)* mutants at 25°C for two reasons: the frequency of reversals is quite high under these conditions (50%) and the *n585* allele has been shown to be a strong reduction-of-function allele by genetic criteria (Chapter 2; and this Chapter, Table 5.1). Unless otherwise indicated, all further analysis is of *egl-20(n585)* mutants at 25°C.

How is the pattern of alternating V cell fates disrupted in *egl-20* mutants? Are the fates of V5.p and V5.a actually changed, or do correctly specified cells move past each other to switch positions, as the daughters of the head seam cell H1 do (Sulston and Horvitz, 1977)? To distinguish between these two possibilities, we observed the division of the V5 cell in 14 *egl-20* mutants until the fates of the two daughter cells could be determined unambiguously.

We found that in all cases, V5 divided to give an anterior and a posterior daughter that both remained stationary. In 6 of these animals the fates of V5.a and V5.p were reversed, and in 8 animals they were wild-type. This observation indicates that the fates of V5.p and V5.a are actually reversed in *egl-20* mutants.

Since the fates of V5.p and V5.a are reversed in *egl-20* mutants, we wondered whether the polarity of the V5 cell itself was reversed. To examine this possibility, we used the monoclonal antibody MH27 which recognizes septate junctions (Francis and Waterston, 1991). In wild-type animals, the V cells all have an anterior foot, which extends to the ventral midline (Austin and Kenyon, 1994) (Fig. 5.2). We found that MH27 staining of V5 in *egl-20* mutants was indistinguishable from wild-type (Fig. 5.2), indicating that this aspect of V5 polarity was wild-type. Since MH27 stains the junctions between cells, it can also be used to assay the cell fusion decision. When a cell fuses with the syncytium, its cell-cell junctions, and thus MH27 staining, disappear. When we examined MH27 staining in animals in which V5 had divided, we observed a reversal in the fates of V5.p and V5.a in approximately 50% of *egl-20* mutants (Fig. 5.2), consistent with our earlier observation based on cell morphology and position. Together these findings indicate that *egl-20* is required for the seam cell fate to be confined to V5.p and the syncytial fate to V5.a, but not for the correct morphological polarity of their parent, V5.

Mutations in *egl-20* also reverse later divisions in the V cell lineages.

Since *egl-20* is required for correct polarity of the V5 cell division, we asked whether it was required for the polarity of other cell divisions in the V5 lineage. We examined the positions and morphology of the V cell descendants in L3 larvae, and found additional polarity reversals later in the

V5 lineage (Fig. 5.3). We also noticed reversals later in the V2-4 and V6 cell lineages in *egl-20* mutants (Fig. 5.3). This was unexpected, since the first division of these V cells is almost always wild-type in *egl-20* mutants (data not shown). Since the frequency of polarity reversals in later cell divisions is much lower than that of V5, we will focus the rest of this paper on the V5 cell division.

The temperature-sensitive period for *egl-20(n585)* is during the V5 division

When is *egl-20* required for V5.p and V5.a to adopt the correct fates? To address this question, we determined the temperature-sensitive period (TSP) of the temperature-sensitive allele *n585*. We found that the *egl-20* TSP was before the V5 cell division (Fig. 5.4). Before V5 had divided, shifting *n585* mutants to the permissive temperature rescued the polarity reversal, and shifting to the restrictive temperature reversed the fates of V5.p and V5.a. After V5 had divided, shifting *n585* mutants to the permissive temperature no longer rescued, and shifting to the restrictive temperature no longer reversed the fates of the V5 daughters. These results are consistent with a role for *egl-20* before or during V5 division, but also with a later role. For example, shifting to the restrictive temperature might block production of the *egl-20* gene product, which might not actually function until much later. In this case, *egl-20* would be required early for a much later function.

Ablation of posterior neighbors rescues the reversal of the V5 cell division in *egl-20* mutants.

Previous studies have shown that signalling between V cells can influence the fate of cells in the V5 lineage in wild-type animals (Sulston and White, 1980; Waring *et al.*, 1992). We wondered whether signals from

neighboring cells might affect the polarity of the V5 cell division in *egl-20* mutants. To test this, we used a laser microbeam to ablate the seam cells posterior to V5. We found that if we ablated both V6 and T in an *egl-20* mutant, the polarity of the V5 cell division was always wild-type (Fig. 5.5). To examine whether loss of both V6 and T was necessary to rescue the V5 polarity reversal in *egl-20* mutants, we ablated either V6 or T in *egl-20* mutants and then examined the polarity of the V5 cell division. We found that ablating V6, the cell just posterior to V5, restored the wild-type polarity of the V5 cell division in 90% of animals examined, but did not fully rescue (Fig. 5.5). Ablating T in an *egl-20* mutant, however, had no effect on the polarity of the V5 division (Fig. 5.5). Together, these results suggest that direct contact between V5 and its posterior neighbors may be important for signalling.

Ablation of posterior neighbors in an *egl-20* mutant might allow V5 to divide with a wild-type polarity. Alternatively, V5 might still divide with a reversed polarity 50% of the time, as in intact mutants, but its daughters switch positions. Austin and Kenyon (1994) have demonstrated that seam cells stretch to cover gaps caused by ablation of neighboring seam cells. If V5 divided with reversed polarity in an ablated *egl-20* mutant, its posterior daughter would fuse with the syncytium and remain in that position, but its anterior daughter, a seam cell, might slide past the syncytial daughter into the place previously occupied by V6 and T. Thus, the final positions of the nuclei (seam cell posterior and syncytial nucleus anterior) would misleadingly indicate that no reversal had taken place. To distinguish between these two possibilities, we observed the division of V5 in 6 *egl-20* mutants in which V6 and T had been ablated and watched the daughter cells until their fates could be determined unambiguously . We found that in all cases V5 divided to produce a posterior daughter which developed as a seam cell and an anterior

daughter which appeared to develop as a syncytial cell. In all animals examined, the nucleus of both V5.p and V5.a remained stationary. This result indicates that loss of posterior neighbors allows V5 to divide with a wild-type polarity in *egl-20* mutants, suggesting that cell-cell signalling may be involved in determining the A/P polarity of V5 in these mutants.

Interestingly, we found that after 1.5 hours, ablations no longer uniformly rescued the V5 polarity reversal, suggesting that signalling can occur before 2 hours post-hatching, well before most V5 cells have begun to divide (data not shown). This observation is consistent with V6 signalling the V5 cell itself, although it does not rule out the possibility that V6 signals the daughters of V5 as well.

Ablation of anterior neighbors enhances the reversal of the V5 cell division in *egl-20* mutants.

If signals from posterior cells help determine the polarity of the V5 cell division in *egl-20* mutants; do anterior cells signal as well? To test this, we ablated seam cells anterior to V5. We found that when we ablated V2-V4, the polarity of the fates of V5.a and V5.p were always reversed (Fig. 5.5). If we only ablated V3 and V4, however, V5 was still able to divide with a wild-type polarity (Fig. 5.5). Since V2 and V5 can form connections, albeit delayed, while V1 and V5 cannot (Austin and Kenyon, 1994), our findings suggests that close, and possibly even direct, contact may be required for the anterior seam cells to transmit polarity-determining information to V5.

We wondered whether anterior ablations would cause other V cells to divide with a reversed polarity in *egl-20* mutants. To test this, we ablated V1-V3 in *egl-20* mutants and examined the polarity of the V4 cell division. We found that V4 divided with a wild-type polarity in all 10 animals examined,

suggesting that the V5 cell division in *egl-20* mutants is uniquely sensitive to loss of anterior neighbors. As a control, we also ablated cells posterior to V4 and found that this treatment also had no effect on the polarity of the V4 cell division.

Isolated V5 cells divide with a wild-type polarity in *egl-20* mutants.

Since anterior ablations enhance and posterior ablations suppress the reversal of the V5 cell division in *egl-20* mutants, we wondered what the polarity of the V5 cell division would be if we ablated both anterior and posterior neighbors. We found that when we isolated the V5 cell in *egl-20* mutants by ablating both V1-4 and V6 and T, V5 always divided with wild-type polarity (Fig. 5.5A). Thus it appears that V5 has the potential to divide with correct polarity in *egl-20* mutants when it is isolated from the influence of neighboring seam cells: anterior neighbors enhance the ability of V5 to divide correctly and posterior neighbors prevent it.

The polarity of the V5 cell division is unaffected by neighbor ablation in wild-type animals.

The effects of neighbor ablation on the polarity of the V5 cell division in *egl-20* mutant animals suggest a role for cell signals in determining A/P polarity in these mutants. We wondered whether neighboring cells played a role in determining the A/P polarity of the V5 cell division in wild-type animals. To test this, we ablated posterior cells (V6 and T) or anterior cells (V1-V4) in wild-type animals and examined the polarity of the V5 cell division. We found that V5 divided with wild-type polarity after either posterior or anterior ablation, or when isolated (Fig. 5.5B). Thus, there must

be a mechanism for determining V5 polarity in wild-type that does not depend on signalling between seam cells.

Mutations that suppress or enhance the reversal of the V5 cell division in *egl-20* mutants

In the course of analyzing the *egl-20* mutant phenotype, we identified both a suppressor and an enhancer of the V5 polarity reversal. We found that the *lin-17(n671)* mutation is a strong suppressor of V5 reversal, and the *mig-1(e1787)* mutation a moderate enhancer (see Table 5.2). Neither the *lin-17* nor the *mig-1* mutation affect V5 polarity in the absence of the *egl-20* mutation (Table 5.2), although *lin-17* mutations are known to affect the asymmetry of many post-embryonic cell divisions (Sternberg and Horvitz, 1988).

Since a *lin-17* mutation can affect V5 polarity in an *egl-20* mutant, we wondered whether mutations in other genes known to affect cell polarity would also alter the polarity of V5 in an *egl-20* mutant. Both *lin-18* and *lin-44* mutants reverse the polarity of certain cell divisions (Ferguson and Horvitz, 1985; Herman and Horvitz, 1994). To determine whether mutations in these genes had any effect on the polarity of V5 on their own, we examined the morphology of V5.a and V5.p (see Materials and Methods) in 100 *lin-44(n1792)* and 100 *lin-18(n620)* mutants. We found that V5 divided with wild-type polarity in all animals examined. The polarity of the V5 cell division had previously been examined in five *lin-44* mutants, all of which were wild-type (Herman and Horvitz, 1994). We then examined the effect that *lin-18(n620)* and *lin-44(n1792)* had on the polarity of the V5 cell division in an *egl-20* mutant. We found that the *lin-44* mutation had no effect on V5 polarity reversals in *egl-20* mutants, but that the *lin-18* mutation suppressed the frequency of V5 reversals (from 51% to 30%; Table 5.2).

Mutations in *lin-17*, *mig-1* and *egl-20* all affect the same step in the migration of the QL neuroblast and its descendants (see Chapter 2). Since mutations in all three of these genes also affect the polarity of the V5 cell division, we wondered whether mutations in *mig-14*, which also affect this step of QL descendant migration, might affect the polarity of V5. To answer this question, we examined the polarity of the V5 cell division in *mig-14(mu71)* and *mig-14(k124)* mutants. We found that the fates of V5.p and V5.a were always wild-type in *mu71* mutants, but were reversed in 7% of *k124* mutants examined (Table 5.2). Both *mig-14(mu71)* and *k124* appear to be loss-of-function alleles, but the *k124* phenotype is more severe (Kiyoji Nishiwaki, personal comm.; Honigberg and Kenyon, unpublished data). To see whether *mig-14* mutations increased the V5 reversal in *egl-20* mutants, we constructed the *mig-14(mu71); egl-20(n585)* and *mig-14(k124); egl-20(n585)*. We found that both *mig-14* mutations increased the frequency of V5 polarity reversals in *egl-20* mutants a significant amount (from 51% to 64% for *mig-14(k124)* and to 68% for *mig-14(mu71)*; Table 5.2).

Mutations in *lin-17* and *mig-1* affect the response of V5 to neighbor ablation in an *egl-20* mutant.

Since a *lin-17* mutation can suppress the reversal of the V5 cell division in *egl-20* mutants, we wondered whether it would also suppress the ability of anterior seam-cell ablations to completely reverse the polarity of the V5 cell division. To answer this question, we ablated V1-V4 in *lin-17(n671); egl-20(n585)* double mutants. We found that anterior ablations were no longer able to reverse the V5 division in all animals, however, they did increase the frequency of reversals (Fig. 5.6). This result indicates that V5 is still responsive

to anterior ablations in *lin-17; egl-20* double mutants, but that its sensitivity to anterior ablations is decreased relative to that of the *egl-20* strain alone.

If a *lin-17* mutation can reduce the response of the V5 cell in an *egl-20* mutant to ablation of anterior neighbors, can a *mig-1* mutation reduce V5's response to the ablation of posterior neighbors? To test this, we ablated V6 and T in *mig-1(e1787); egl-20(n585)* double mutants. We found that posterior ablations were no longer able to rescue the the reversal of the V5 cell division in all animals, however, ablation did decrease the frequency of reversals seen in this strain (Fig. 5.6). This result indicates that V5 is still responsive to posterior ablations in *mig-1; egl-20* double mutants, but that its sensitivity to posterior ablations is decreased relative to that of the *egl-20* strain alone.

The *lin-17* and *mig-1* mutations might alter the response of V5 to neighbor ablation in an *egl-20* mutant by either affecting the seam-cell-independent polarity of V5 or by altering the *egl-20*-independent signal/response pathway. To distinguish between these two possibilities, we isolated V5 in *lin-17* and *mig-1* mutants by ablating V1-V4, V6 and T, and then looked to see whether the polarity of the V5 cell division was reversed or wild-type. We found that isolated V5 cells in both *lin-17* and *mig-1* mutants still divided with wild-type polarity (Fig. 5.6), suggesting that both *lin-17* and *mig-1* are candidates for genes involved in the signal/response pathway that determines V5 polarity in *egl-20* mutants.

Discussion

Signals from neighboring cells determine V5 polarity in *egl-20* mutants

The V cells of the *C. elegans* epidermis are stem cells that divide with a characteristic A/P polarity: the posterior daughter is a stem cell, like its mother, and the anterior daughter fuses with a large syncytium (Sulston and Horvitz, 1977). In *egl-20* mutants, however, these fates can be reversed: the anterior daughter can develop as a stem cell and the posterior daughter can fuse with the syncytium (Fig. 5.1 and Table 5.1). Thus, *egl-20*(+) activity is required for certain epidermal stem cells to divide with wild-type polarity.

The V cells are lined up end to end along the A/P axis of the worm. Together, they form a thin seam of epidermal cells that stretches across a large epidermal syncytium that covers most of the worm (Sulston and Horvitz, 1977; Francis and Waterston, 1991). We have shown that the reversal of the V5 cell division is caused by signals from its posterior neighbors in the seam, V6 and T. If V6 and T are ablated with a laser microbeam prior to the division of V5, wild-type polarity is restored (Fig. 5.5A). In contrast, if V5's anterior neighbors in the seam, V2-V4, are ablated, then V5 always divides with a reversed polarity (Fig. 5.5A). Thus, in *egl-20* mutants, signals from anterior and posterior neighbors have opposite effects on the polarity of the V5 cell division: posterior neighbors signal V5 to divide with reversed polarity, whereas anterior neighbors signal it to divide with wild-type polarity.

Mutations in *egl-20* reverse divisions in the other V-cell lineages, but only after L1. The polarity of the V5 division, however, is reversed in 50% of *egl-20(n585)* mutants in the L1. What is special about V5? Although we don't know why V5 is the only V cell affected, there are three aspects of the V5 lineage that make it stand out. First, the anterior boundary of *mab-5* expression passes through the V5 lineage. Thus, V5 is the only V cell in which some descendants adopt anterior and others posterior fates (Kenyon, 1986; Francis and Waterston, 1991). Second, V5 is the only V cell to produce a

neuronal sensillum, the postdeirid, in the L2. Finally, V5 is the sister of the Q neuroblast, whose migrations are affected in *egl-20* mutants. In fact, the six blast cells born in the early embryo are V1-V4, Q/V5, and V6. Q/V5 divides shortly before hatching to produce the neuroblast, Q and the epidermal cell, V5. Thus, the first division of V5 is actually the second division of the blast cell (Sulston *et al.*, 1983).

Mutations in the gene*lin-22* allow the anterior seam cells, V1-V4, to produce a postdeirid, like V5. However, in *lin-22 egl-20* double mutants, V1-V4 still divide with wild-type polarity: the posterior daughter develops as a seam cell and the anterior daughter fuses with the syncytium (data not shown). Thus, mutations in *lin-22* do not transform the anterior V cells into a perfect copy of V5. Alternatively, since mutations in *lin-22* cannot alter the position of the anterior V cells in the embryo or their ancestry, perhaps these aspects of V5 cell fate are the ones that make V5 sensitive to mutations in *egl-20*.

What is the role of *egl-20*(+) in determining the polarity of the V5 division in wild-type?

We have shown that cell signals determine the A/P polarity of the V5 cell division in *egl-20* mutants. However, the polarity of the V5 cell division is wild-type in *egl-20* mutants in which both anterior and posterior cells have been ablated (Fig. 5.5A). Together, these data suggest that V5 polarity can be determined either by a seam-cell-signalling pathway, or by an underlying polarity-determining pathway. Mutations in *egl-20* affect only the seam-cell-signalling pathway, leaving the alternate pathway intact. Thus, when V5 cells in *egl-20* mutants are removed from the influence of their seam cell

neighbors, the underlying pathway can function to orient the polarity of V5 correctly.

Seam cells can send polarizing signals to V5 or its daughters in *egl-20* mutants. However, neighbor ablation has no effect on the polarity of V5 in wild-type animals (Fig. 5.5B): do seam cells transmit polarizing signals to V5 in wild-type? One possibility is that *egl-20*(+) could block the signalling pathway either at the start, by preventing production or release of cell signals (Fig. 5.7A), or at the end, by blocking the response of V5 to polarizing signals (Fig. 5.7B). Alternatively, *egl-20* could act extrinsically to create or strengthen other signals that override seam-cell signals (Fig. 5.7C). Further analysis of *egl-20* should distinguish between these possibilities.

Interestingly, the polarity reversal phenotype of all *egl-20* alleles appear to be temperature-sensitive to some degree (Table 5.1), suggesting that the wild-type function of *egl-20* may be to stabilize a polarity-determining mechanism. At low temperatures, the polarity-determining process would be able to function reasonably well in the absence of *egl-20* activity, but at high temperatures, *egl-20* activity would be required to maintain the ability of this process to determine V5 polarity.

Who is signalled - V5 or its daughters?

In *egl-20* mutants, V5.a and V5.p can adopt each others' fate. Since the V5 daughters almost never adopt the same fate, their choice must be coordinated in some way. Either the fates of V5.a and V5.p are coordinated at the level of the mother cell, through segregation of determinants, or at the level of the daughter cells, through lateral signalling. Our data are most consistent with the first possibility, that mutations in *egl-20* affect the polarity of the V5 cell itself. In *egl-20* mutants, V5 becomes insensitive to the loss of posterior

neighbors shortly before it divides: posterior ablations later than 1.5 hours post-hatching no longer consistently rescue the polarity of the V5 cell division. In addition, the *egl-20* TSP is before or during V5 division (Fig. 5.4). Of course, V6 might continue to signal after ablation, either because the cell takes several hours to die, or because the signal remains active for several hours in the extracellular environment. A second caveat is that the *n585* mutation might block production, rather than function, of EGL-20 at high temperatures. Alternatively, since the polarity reversal phenotype caused by the four strong alleles of *egl-20* is always temperature-sensitive, it is possible that we are detecting the temperature-sensitivity of an underlying process, rather than that of the EGL-20 protein itself. In either case, *egl-20* might be made before or during V5 division but act later.

Although our findings our most consistent with a model in which neighboring cells signal V5 , it is also possible that V6 might actually signal the V5 daughters themselves. However, additional experiments suggest that signals between the two daughters do not appear to establish their fates, since ablation of one daughter minutes after birth does not determine the fate of the other (data not shown). Thus, it appears likely that in *egl-20* mutants, the seam cells signal V5 itself.

What is the nature of the seam-cell signal?

Signals between cells in the seam influence the development of these cells. Seam cells signal their anterior neighbors to repress the Hox gene *mab-5* and develop anterior fates. When posterior seam cells are ablated, neighboring anterior cells can develop posterior fates (Sulston and Horvitz, 1977; Sulston and White, 1980). Although it is not known whether *mab-5* is expressed in V4 after ablation, V5 has been shown to activate *mab-5* in

response to ablation (Salser and Kenyon, unpublished data). As these seam cells divide, they go through cycles of loss-of-contact, extension and reconnection (Austin and Kenyon, 1994; Podbilewicz and White, 1994). The time of seam-cell signalling is highly correlated with the time of cell-cell contact, suggesting that cells must be touching or very close in order to signal (Waring *et al.*, 1992; Austin and Kenyon, 1994).

In contrast, our findings suggest that polarity-determining signals in *egl-20* mutants may be transmitted in the absence of cell contact. Ablations of V3-V4 create a large gap which V2 and V5 must span in order to restore cell contact. However, V2 is still able to influence the polarity of V5 (Fig. 5.5). Since V3-V4 are ablated just 1-3 hours before V5 rounds up and divides, there is not much time to restore seam-cell connection. Although the ability of V2 and V5 to reconnect still remains to be tested, it seems most likely that V2 can signal V5 in the absence of cell contact. This polarity-determining signal, however, must be effective only over a short range, since the larger gap created by ablating V2-V4 entirely eliminates signalling. Alternatively, V1 may not be competent to determine the polarity of V5.

Signals from anterior and posterior seam cells appear to have opposite effects on the polarity of V5. Similarly, Waring et al (1992) have shown that signals from anterior and posterior seam cells have quantitatively different effects on the ability of V5.pa to adopt a neural, rather than epidermal, fate. Austin and Kenyon (1994) have proposed that this difference may be due to the fact that the posterior process of V5 is now located in a more posterior part of the body, and thus more sensitive to the influence of the Hox gene, *mab-5*, which regulates postdeirid formation. An alternative possibility is that signals from anterior cells and posterior cells are different. This is an attractive model because it suggests a way in which V cells could determine their A/P polarity.

By sensing the difference between these two signals, V5 could distinguish between anterior and posterior and segregate determinants into daughter cells appropriately. Signals from anterior and posterior seam cells could thus differentially regulate two aspects of cell fate in the V5 lineage: A/P polarity of V5 and formation of a neural sensillum by V5.pa.

Why two polarity-determining pathways?

The existence of both the seam-cell signalling and the underlying polarity-determining pathway was unexpected. Why evolve two different pathways to determine the A/P polarity of V5? Seam-cell signals can reverse the polarity of V5, but the seam-cell independent system does not. Our findings suggests that the wild-type function of the *egl-20* gene may be to inactivate the seam-cell signalling system. Why have a system whose only role is to interfer with normal polarity? One possibility may be that in some circumstances it is beneficial to reverse seam cell polarity, although this situation has never been observed in wild-type development. Alternatively, these two V5-polarity-determining pathways may not actually be independent. Rather, the seam-cell signalling pathway and the underlying polarity-determining pathway may simply be different aspects of one system that determines both cell polarity and other aspects of cell fate. This system is reminiscent of that of the segment polarity genes in *Drosophila* (discussed below) which regulate fine-scale A/P patterning by governing both cell fate and cell polarity.

The signalling pathway

Classic studies by Peter Lawrence revealed pattern reversals in insect epidermis following wounding. The gradient model that he proposed to

explain tissue polarity has, until recently, been the most widely accepted (reviewed in (Lawrence, 1992). More detailed analysis of tissue polarity in the fly eye now suggest that local cell-cell signalling may determine the orientation of cell polarity in that tissue (Ma and Moses, 1995; Wehrli and Tomlinson, 1995; Zheng *et al.*, 1995). Further support for this model comes from the observation that *wnt* family members, *wingless* in *Drosophila* and *lin-44* in *C. elegans*, play a role in determining the orientation of polarized cells along the body (Herman and Horvitz, 1994; Theisen *et al.*, 1994; Herman *et al.*, 1995). Members of the *wnt* family are signalling molecules that act locally, perhaps only on adjacent cells, via components of cell junctions such as *armadillo*, the *Drosophila plakyglobin* homolog (Burrus, 1994; Klingensmith and Nusse, 1994; Klymkowsky and Parr, 1995). Considering the correlation between cell contact and signalling for polarity determinination in *egl-20* mutants, it is notable that a *lin-44* mutation had no effect on the *egl-20* mutant phenotype. However, *lin-44* appears only to function at the posterior tip of the tail, many cell diameters removed from the V5 cell, located in the body of the worm. There are at least two other *wnt* family members in *C. elegans* (S. Shivakumar, G. Jongeward, H. Varmus and C. Kenyon, unpublished data). It is possible that these genes play a role in signalling between V cells, but this has not been tested, since all known mutations are lethal.

Genetic analysis of the *egl-20* polarity reversal phenotype has identified several genes that are candidates for genes involved in the signal-response pathway: *lin-17*, *mig-1*, *lin-18* and *mig-14*. These genes fall into two classes: tissue polarity genes, *lin-17* and *lin-18* (Ferguson and Horvitz, 1985; Sternberg and Horvitz, 1988), and cell migration genes, *lin-17*, *mig-1* and *mig-14* (see Chapter 2). *lin-17* has an additional function: generation of cellular

asymmetry (Sternberg and Horvitz, 1988). How might these enhancers and suppressors the *egl-20* polarity reversal phenotype function in a signal-response pathway? Mutations in *lin-17* and *lin-18* mimic the ablation of posterior neighbors in their effect on V5 polarity. Thus, the wild-type functions of *lin-17* and *lin-18* must be to promote signalling from posterior neighbors or to prevent signalling from anterior neighbors. In contrast, a *mig-1* mutation mimics ablation of anterior neighbors. Thus, the wild-type function of *mig-1* must be to promote signalling of anterior neighbors or block signalling from posterior neighbors. *mig-14* and *egl-20* act at the same steps in regulation of cell migration (see Chapter 2) and have similar effects on the polarity of V5. Thus, it seems most likely that *mig-14*, like *egl-20*, functions to inactivate the seam-cell signalling pathway, although a role for *mig-14* in the underlying polarity-determining pathway cannot be ruled out.

The effect of mutations in these genes on the *egl-20* polarity reversal phenotype was specific: mutations in the cell polarity gene *lin-44* and other cell migration genes did not affect the *egl-20* polarity reversal (data not shown). Similarly, mutations in several genes that are not known to play a role in cell polarity or cell migration, such as *unc-71* and *unc-24*, did not affect the reversal phenotype (data not shown).

It was surprising to find that cell migration genes act in conjunction with tissue polarity genes to determine cell polarity. Both *lin-17* and *lin-18* act together to determine the polarity of vulval tissue, so their role in another cell polarity decision was not unexpected, although the fact that they suppress the V5 reversal in *egl-20* mutants was contrary to what one might predict. However, the observation that genes that were not known to have effects outside of cell migration could enhance this reversal phenotype was even more surprising. What unifies these genes, is that four of them, *egl-20*, *mig-*

14, *mig-1* and *lin-17*, all act at the same step of cell migration: activation of the Hox gene, *mab-5*, in descendants of the migrating neuroblast QL (Chapter 2). *mab-5*, like other Hox genes, acts to pattern the body along the A/P axis. *mab-5* expression in these cells determines their direction of migration (Salser and Kenyon, 1991). In addition to their effect on *mab-5* activation, *egl-20* and *mig-14* also act in a *mab-5*-independant way to determine the stopping points of migrating cells along the A/P axis. Thus, genes involved in regulating neuronal cell migration also function to determine the A/P polarity of the V5 epidermal cell. These observations suggest that the system used for positioning migrating cells along the A/P axis may also function to orient A/P-polarized stationary cells.

Conclusion

How might *egl-20*, *mig-14*, *mig-1* and *lin-17* regulate both the stopping points of migrating cells and the orientation of cell division? The molecular nature of most of these genes is unknown, but *lin-17* appears to encode the *C. elegans* homolog of the *Drosophila* tissue polarity gene, *frizzled* (S. Hawa and R. Horvitz, pers. comm.), a seven transmembrane domain protein (Park *et al.*, 1994) required to propagate polarizing signals throughout epithelia in wing, leg and eye (Vinson and Adler, 1987; Zheng *et al.*, 1995). In *Drosophila*, *frizzled* has been proposed to act both as receptor and signal (Vinson and Adler, 1987; Krasnow and Adler, 1994). Cell signals have been shown to orient the polarity both of vulval cell lineages (Katz and Sternberg, unpublished data) and of the epidermal cell, V5. Perhaps *lin-17* receives and transmits these polarizing signals in *C. elegans* epithelia, much as *frizzled* does in *Drosophila*. Ablation studies suggest that *lin-17* is unlikely to act in anterior seam cells, since it continues to suppress the polarity reversal of V5 even in

the absence of anterior seam cells (Fig. 5.6). It will be interesting to learn whether *lin-17* acts in V5, V6 or both. Further analysis of these genes should provide an entry point into understanding how axial cell polarity is determined in an epithelium and the role of local cell signals.

Acknowledgments

We thank members of our lab, in particular Craig Hunter, for discussions and comments on the manuscript. We thank Kiyoji Nishiwaki for sharing unpublished data and *mig-14(k124)* and and Robert Waterston and Robert Barstead for providing the MH27 monoclonal antibody. Thanks to Lee Honigberg for examining polarity reversals in *mig-14(mu71)* and to Judith Austin for many helpful suggestions on the ablation experiments. Some *C. elegans* strains were provided by the *Caenorhabditis* Genetics Center which is funded by the NIH National Center for Research Resources (NCRR). This work was supported by NIH grant GM37053 and a grant from the Packard Foundation to C.K.

Fig. 5.1. *egl-20* mutations reverse the A/P polarity of the V5 cell division. D-F, photographs using Nomarski (DIC) optics. A-C, tracings of the photographs in D-F. The positions of the daughters of V4-V6 in wild-type (A and D) and *egl-20(n585)* mutants (B and E) at the end of L1. The other daughters, the Vn.a cells in wild-type, have already fused with the hyp7 syncytium and only the nuclear outline is visible. C and F depict an *egl-20(n585)* mutant at the begining of L2. In this worm, the anterior daughter of V5, which has the position and morphology of a seam cell, is dividing and the metaphase plate visible. The posterior daughter of V5 in this animal has the appearance of a syncytial nucleus.

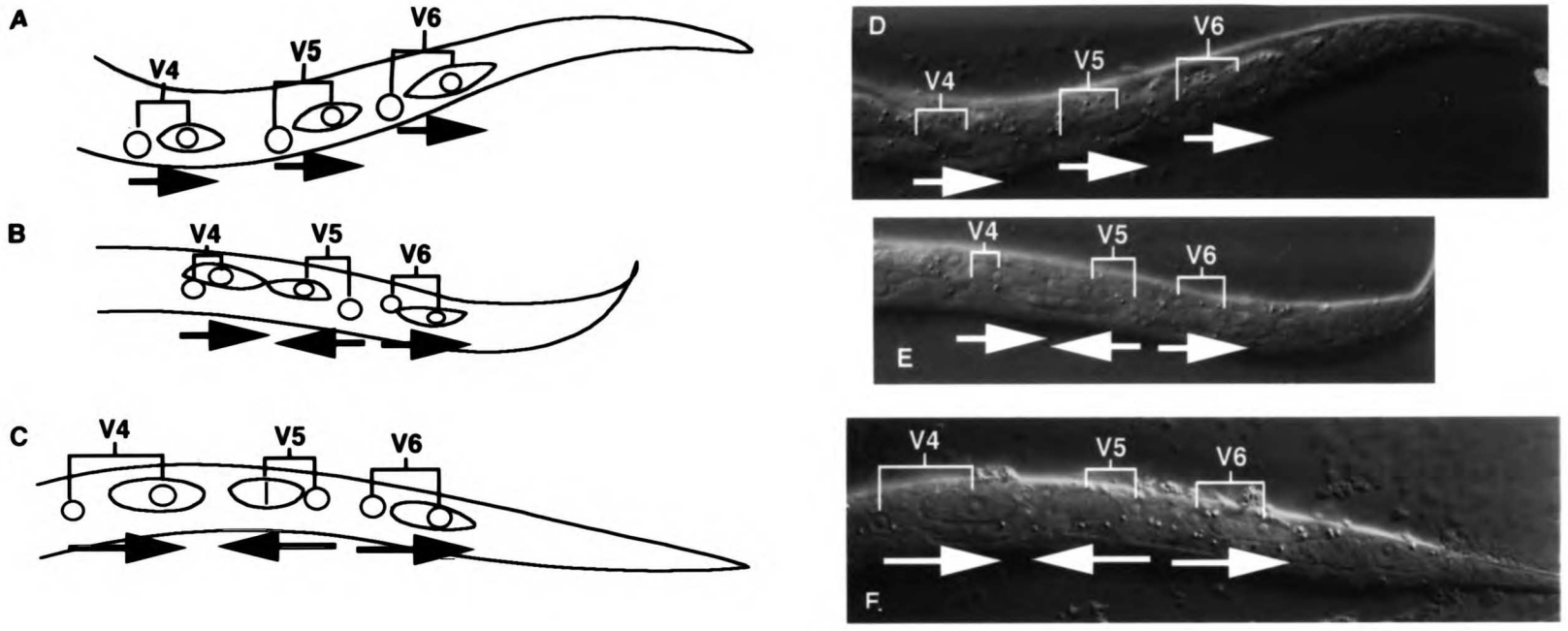

Fig. 5.1

A. wild-type

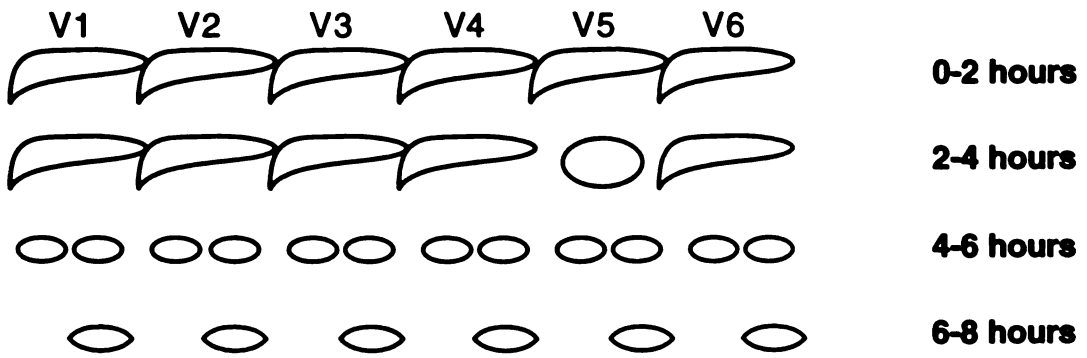

B. *egl-20(n585)*

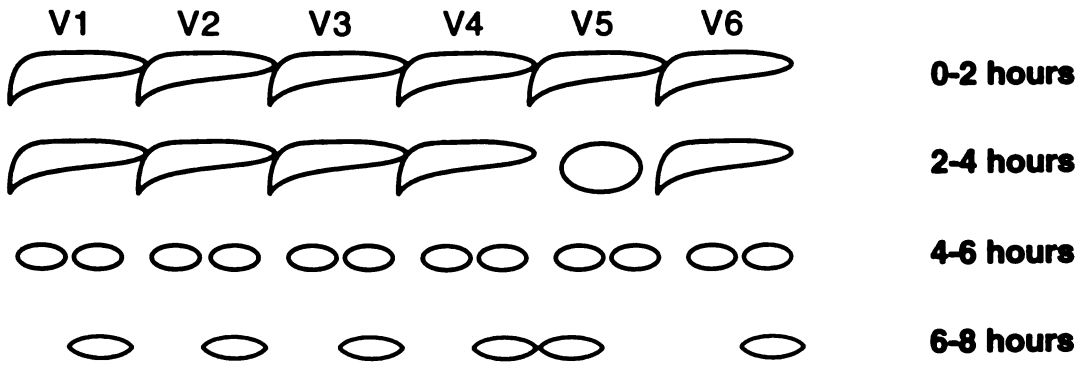

Fig. 5.2. Labelling of apical cell junctions of epidermal cells with the MH27 monoclonal antibody (Francis and Waterston, 1991) in wild-type and *egl-20(n585)* mutant worms. By 6 hours most of the V cells have divided. By 8 hours, the syncytial daughters (Vn.a in wild-type) have fused. The reversal in A/P polarity is not observed until the V daughters fuse with the syncytium. This is a sketch of data by Jennifer Whangbo.

A.

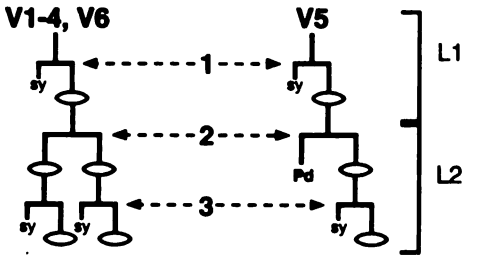

B.

	division	% Reversals V1	V2	V3	V4	V5	V6
L1	1	0	0	0	0	52	0
L2	2	sym	sym	sym	sym	20	sym
	3	0 0	0 0	4 4	0 0	24	16* 0

Fig. 5.3. *egl-20(n585)* mutations reverse the polarity of later divisions in the V cell lineages. Reversals were inferred based on the positions of the V-cell descendants in late L2. The second division of all V cells except V5 is symmetric and thus cannot be scored for polarity reversals. Reversals were also observed in the third division of the V(2-4) and V6 lineages in the control sides of ablated worms (data not shown). These control sides had a higher frequency of polarity reversals late in the V cell lineages than worms not exposed to azide or the laser. There is a weak A/P bias in the lineages affected: V6 is affected most frequently, while V1 was wild-type in all mutants examined. However, the most posterior branch of the V6 lineage was rarely affected: virtually all polarity reversals were observed in the seam cell adjacent to V5, V6.pa.

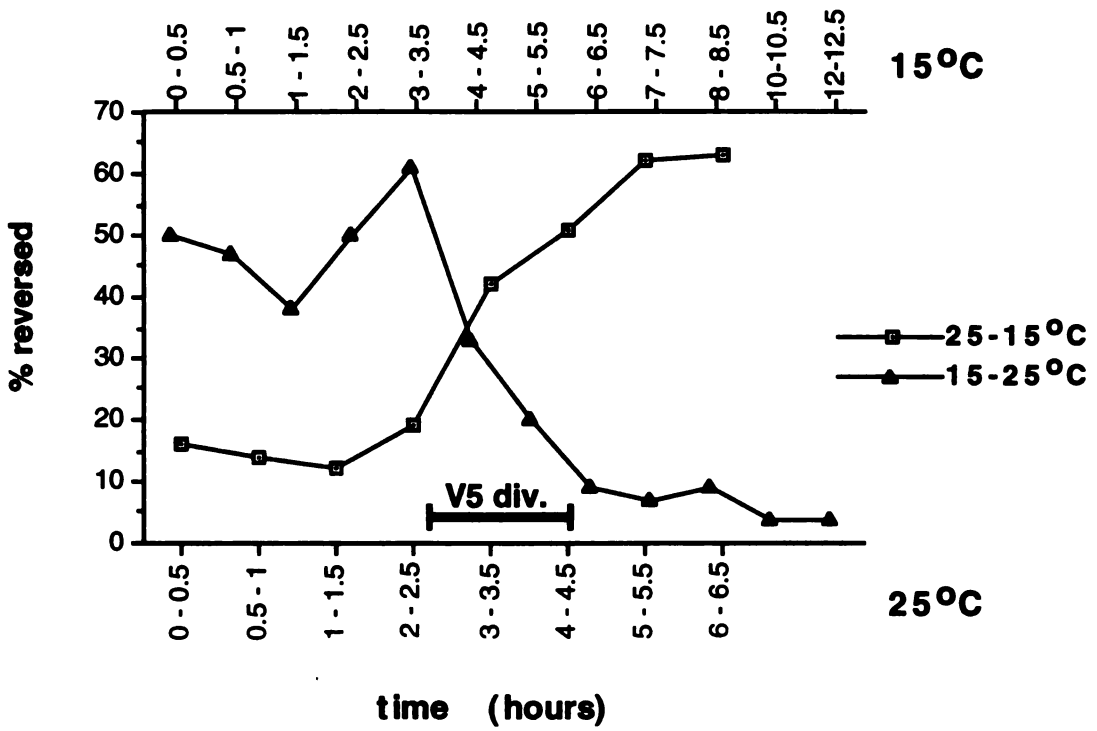

Fig. 5.4. The temperature sensitive period of *egl-20(n585)* is before or during V5 division. The x-axis marks the time at which animals were shifted to a different temperature. The lower tickmarks correspond to time at 25°C and the upper tick marks to time at 15°C. The time of V5 division is noted on the graph.This graph is a compilation of two experiments conducted on different days. More than 60 animals were examined for each data point.

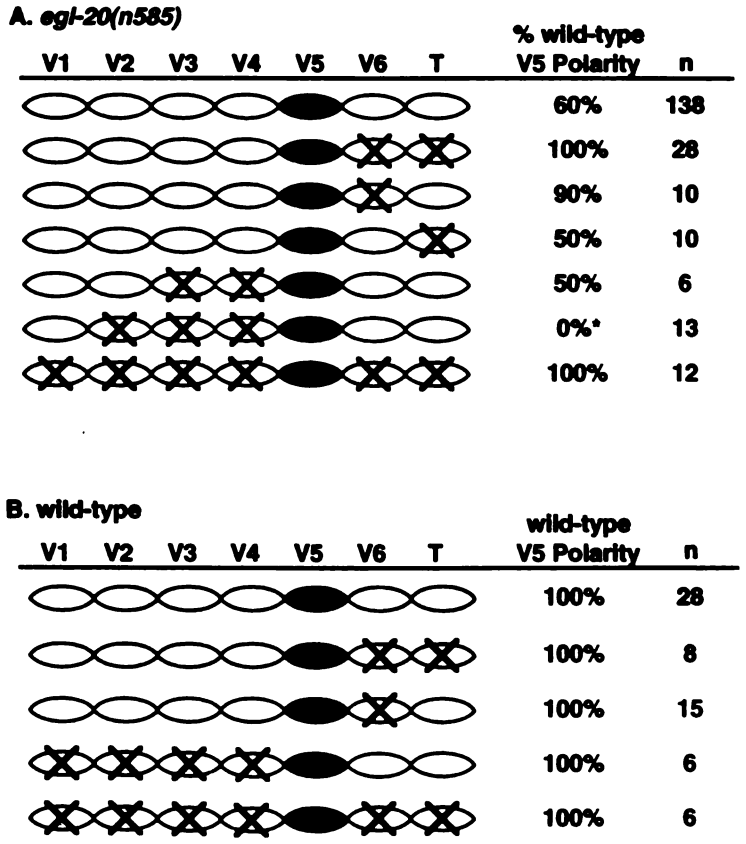

Fig. 5.5. Ablation of neighboring seam cells can influence the polarity of the V5 cell division in *egl-20* mutants but not wild type. Ablations are indicated by an X over the cell ablated. The V5 cell is indicated with grey. The unablated sides of ablated worms were used as controls (top row in parts A and B). A. Ablations in *egl-20* mutants. B. Ablations in wild-type. * One animal in which V2-4 were ablated divided with a wild-type polarity. However, V6 in this animal produced no seam cell progeny, just two syncytial daughters. Thus, the environment of V5 in this animal was more similar to that of an isolated V5 cell, and thus was not counted with the anterior ablations.

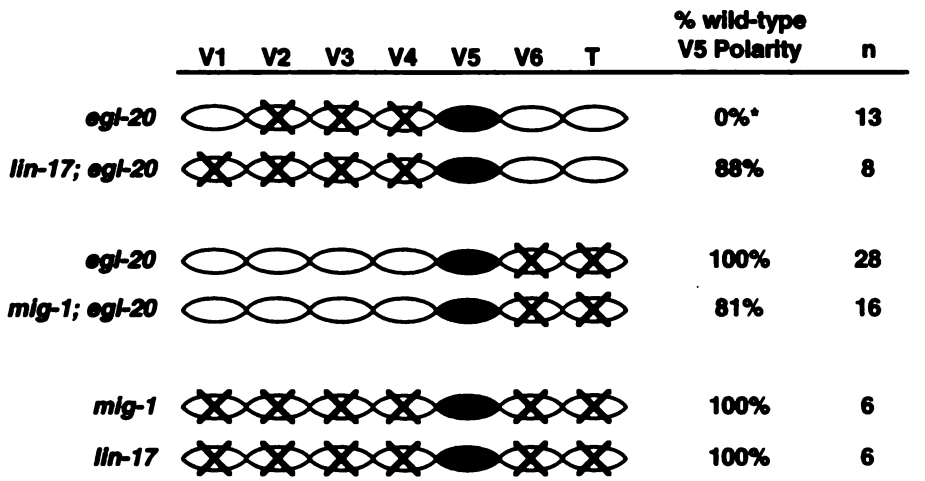

Fig. 5.6. *mig-1(e1787)* and *lin-17(n671)* mutations enhance or suppress the frequency of V5 polarity reversals in response to neighbor ablation in an *egl-20* mutant. *One animal in which V(2-4) were ablated divided with a wild-type polarity. However, V6 in this animal produced no seam cell progeny, just two syncytial daughters. Thus, the environment of V5 in this animal was more similar to that of an isolated V5 cell, and thus was not counted with the anterior ablations.

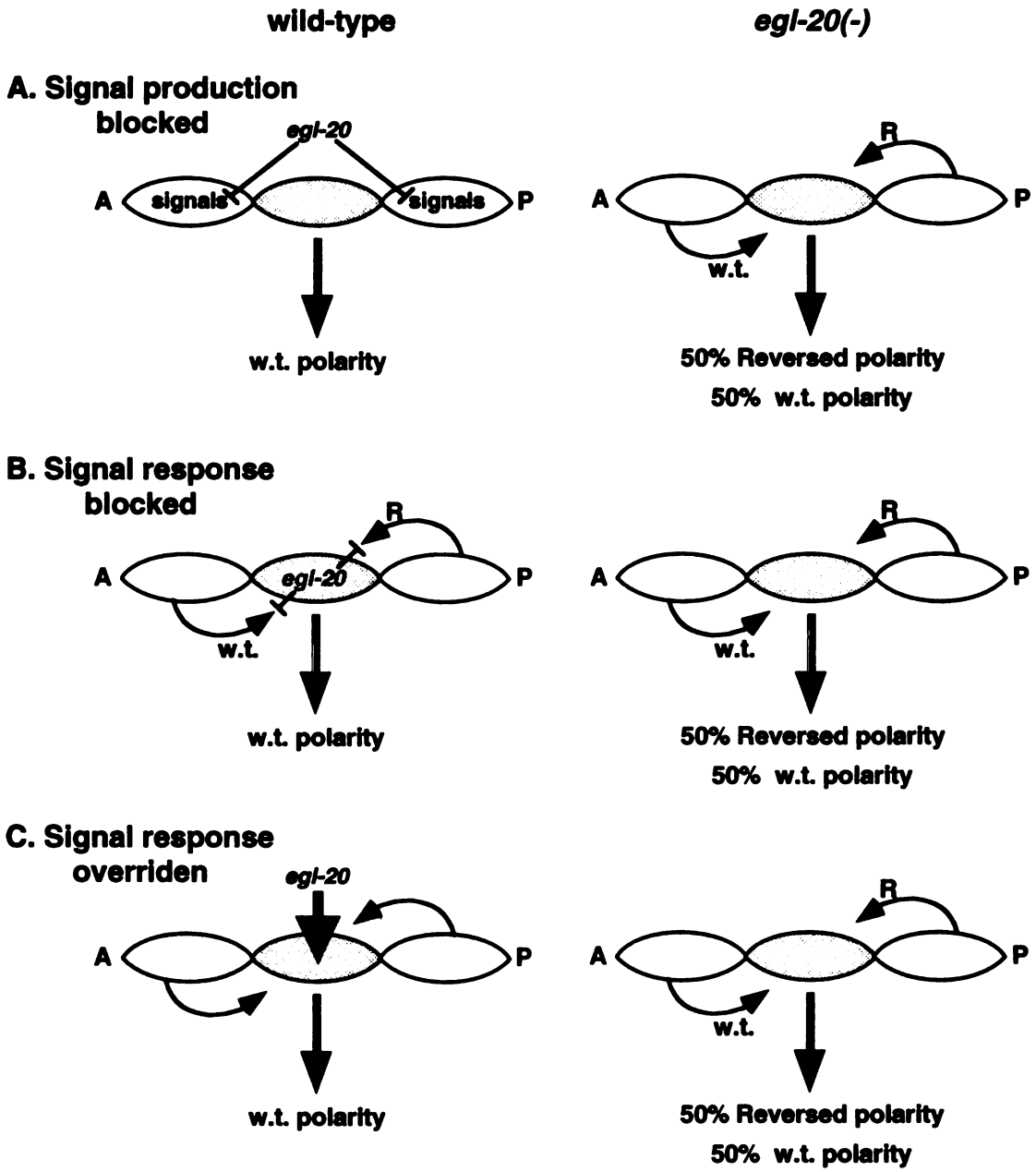

Fig. 5.7. Possible models to explain the function of *egl-20* in determining V5 A/P polarity. V5 is represented by a grey cell and its anterior and posterior neighbors in the seam are white. Signals from the posterior (labelled "R") reverse V5 polarity. Signals from the anterior (labelled "w.t.") promote wild-type V5 polarity.

	% Reversed (n)		
genotype	**15°**	**20°**	**25 °**
N2	**0%** (50)	**0%** (50)	**0%** (100)
egl-20	**6%** (49)	**39%** (88)	**50%** (100)
(n585)			
(n1437)	**10%** (51)	**4%** (51)	**52%** (61)
(mu25)	**8** (50)	**12%** (52)	**41%** (69)
(mu27)	**0%** (50)	**22%** (50)	**22%** (50)
(mu39)	**0%** (37)	**0%** (100)	**0%** (25)
n585/eDf19		**40%** (50)	
mu39/n585			**0%** (46)
mu39/eDf19		**0%** (61)	**7%** (42)
+/eDf19		**0%** (100)	**0%** (50)

Table 5.1. The Polarity of the V5 cell division is reversed in *egl-20* mutants.

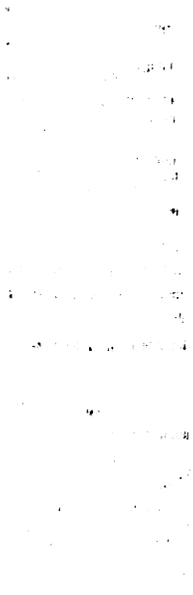

A. Double Mutants			B. Single Mutants		
genotype	**% Rev.**	**(n)**	**genotype**	**% Rev.**	**(n)**
egl-20	**51%**	(100)	wild-type	**0%**	(100)
mig-14(mu71); egl-20	**68%**	(102)	*mig-14(mu71)*	**0%**	(41)
mig-14(k124); egl-20	**64%**	(90)	*mig-14(k124)*	**7%**	(81)
mig-1(e1787); egl-20	**72%**	(100)	*mig-1(e1787)*	**0%**	(100)
lin-17(n671); egl-20	**2%**	(100)	*lin-17(n671)*	**0%**	(100)
egl-20; lin-18(n620)	**30%**	(99)	*lin-18(n620)*	**0%**	(80)

Table 5.2. Mutations which enhance and suppress the V5 polarity reversal in *egl-20(n585)* mutants.

Chapter 6: Progress towards the cloning of the *egl-20* gene

Abstract

The *egl-20* gene is required for such diverse events as establishment of cell polarity, regulation of a Hox gene, positioning of migratory cells along the anterior/posterior (A/P) body axis and the response to cell signals. In order to understand more about where and how *egl-20* acts, I initiated the cloning of the *egl-20* gene. To identify the physical location of the gene, I used three parallel approaches: mapping, using both genetic and physical markers, identification of physical changes in the DNA associated with specific alleles, and transformation rescue of *egl-20* mutants using DNA from the general region of the *egl-20* locus. I identified a small region on the physical map cloned into a YAC and two cosmids which most probably contains the *egl-20* locus. However, I was unable to either identify allele-specific DNA changes or obtain transformation rescue, which are necessary to prove the presence of the *egl-20* gene on this DNA. A screen to identify mutants with deletions of the *egl-20* locus and further transformation experiments are being continued by Gregg Jongeward. These approaches should lead to the identification of the *egl-20* sequence.

Introduction

The *egl-20* gene has many different functions: it activates the Hox gene *mab-5* (see Chapters 2 and 4), positions migrating cells (see Chapter 2) and orients stationary cells along the A/P axis (see Chapter 5). However, the effect of *egl-20* mutations is limited; they do not affect the activation of *mab-5* in all cells which would normally express it, nor do they affect all cell migrations or the polarity of all epidermal cells. The pleiotropic, yet specific, nature of mutations in *egl-20* raise several questions. How does a single gene affect such

apparently dissimilar processes as Hox gene regulation, cell polarity, and positioning of migratory cells? Why do *egl-20* mutations specifically effect such a small subset of epidermal, migratory and *mab-5*-expressing cells? Cloning the *egl-20* gene would allow us to address these questions directly. Using in situ hybridization or antibody staining we could identify which cells express *egl-20* RNA and protein and determine when they express it. An extrachromosomal array containing the cloned gene could be used to do mosaic analysis, a technique which can determine where *egl-20* is required for specific developmental events. If *egl-20* is only expressed in a subset of cells, the cloned gene would allow us to misexpress *egl-20* under the control of a heterologous promotor. For example, expression of *egl-20* in QR might cause its descendants to migrate towards the posterior, rather than the anterior. Finally, and perhaps most importantly, the sequence of *egl-20* might provide some clues as to its function. Homologies or motifs might suggest other processes *egl-20* could be involved in or other proteins it might interact with. The location and nature of the mutations should determine whether any of the alleles are null and might provide some insight into the mechanism of *egl-20* activity. Such sequence information could direct future experiments and suggest more mechanistic models for *egl-20* function.

To clone the *egl-20* gene, I tried to identify its physical location on the chromosome using three simultaneous approaches. First I mapped the *egl-20* locus using genetic markers, chromosomal deficiencies, and restriction fragment length polymorphisms (RFLP's). Second, I attempted to identify allele-specific polymorphisms. Third, I attempted to rescue the *egl-20* mutant phenotype by transforming worms with cosmids and YAC's containing DNA from the *egl-20* region of the chromosome. I identified an interval bounded by two RFLP's which includes two cosmids and a YAC, which is likely to

contain the *egl-20* gene. I was unable to identify polymorphisms associated with any of the five *egl-20* alleles or to obtain transformation rescue. I have designed a complementation screen using trimethylpsoralen which should allow us to isolate *egl-20* mutations caused by large deletions. This screen was begun by Wendy Gilbert as a rotation student and is being continued by Gregg Jongeward, who is continuing the cloning of *egl-20*. A continuation of these three approaches should lead us to the *egl-20* gene. Together, these three approaches should lead to the cloning of the *egl-20* gene.

Materials and Methods

Methods for routine culturing and genetic analysis are described by Brenner (1974) and Wood et al. (1988). The wild-type strain N2 is the parent of all strains used with the exception of *egl-20(n1437)*, which is MT2878 (G. Garriga, pers. comm.). Mutations not described in this paper are described by Hodgkin et al. (1988) or are noted below. *egl-20* mutations are described in Chapter 2. Linkage Group (LG) is the genetic term for a chromosome. Thus, "LGIV" is used when referring to genetic data and "chromosome IV" when referring to physical data.

Mutations used:

LGIV: *egl-20(n585), egl-20(n1437), egl-20(mu25), egl-20(mu27), egl-20(mu39), unc-24(e138), dpy-20(e1282), mec-3(e1338), fem-3(q20gf), fem-3(e1996), dpy-13(e184), daf-14(m77), mec-3(e1338)*

LGX: *dpy-6(e14)*

Rearrangements: *eDf18, eDf19, mDf7/nT1[let(m435)]; nT1/+*

Deficiency Mapping

eDf19.

The deficiency *eDf19* failed to complement *egl-20(n585)*. The complementation test was done in two ways. **1.** Males of genotype *unc-24(e138) egl-20(n585)/ + +; him-5(e1490)/ +* were mated to non-Unc progeny of *eDf19/ unc-24(e138) dpy-20(e1282)* hermaphrodites. Only 1/4 of the non-Unc F1 animals were of the genotype *eDf19/unc-24(e138) egl-20(n585).* **2.** Spontaneous males of genotype *eDf19/unc-24(e138) dpy-20(e1282)* were crossed with *unc-24(e138) egl-20(n585)* hermaphrodites. All non-Unc progeny were of the genotype *eDf19/unc-24(e138) egl-20(n585).* The position of the QL.pa daughters was scored in the non-Unc progeny of these crosses. The *eDf19/unc-24(e138) egl-20(n585)* strain was maintained by keeping non-Unc hermaphrodites which segregated 1/4 dead eggs and 1/4 Unc Egl animals.

mDf7.

The deficiency *mDf7* partially complemented *egl-20(n585).* Since *mDf7* fails to complement *mec-3* (Hodgkin *et al.*, 1988), *unc-24(e138) egl-20(n585) mec-3(e1338)/+* males were mated to *dpy-13(e184) mDf7/nT1[let (m435)]; nT1/+* hermaphrodites and their Mec non-Unc F1 progeny kept. (The *dpy-13* mutation linked to *mDf7* is semi-dominant and was used in subsequent generations to help identify *mDf7* heterozygotes.) These F1 hermaphrodites segregated 1/4 dead eggs, 1/4 Unc Egl Mec's and 1/2 Mec semi-Dpy non-Unc's. *mDf7* also deletes the unc-22 locus resulting in a dominant Twitching phenotype visible in the presence of nicotine under low magnification or in the absence of drug under high magnification. Since the Mec phenotype is difficult to score in L1 and L2 animals, when the positions of the QL.pa daughters are easiest to score, the Twitching phenotype was used to mark the presence of the *mDf7* chromosome. We found that the QL.pa daughters were in mutant positions in 9/50 (18%) of Twitchers.

eDf18.

Males of genotype *eDf18/unc-24(e138) dpy-20(e1282)* were crossed to *unc-24(e138) egl-20(n585)* hermaphrodites. The positions of the QL.pa daughters were determined in the non-Unc progeny of this cross. I found that the positions of these cells were wild-type in 7/7 *eDf18/unc-24(e138) egl-20(n585)* F1 progeny.

Three-factor Crosses

Many mutations can cause a low penetrance Egl phenotype; in all except the third *fem-3* cross, the *egl-20* mutants were identified on the basis of their QL.(d) migration (Mig) defect rather than their Egl defect.

Mapping relative to *fem-3*.

1. The first cross used a *fem-3* gain-of-function mutation which at 25° C causes a masculinization of the germline phenotype (Mog). From heterozygotes of genotype *unc-24(e138) fem-3(q20gf)* +/ + + *egl-20(n585)*, 10/10 Unc non-Mog recombinants segregated Mig progeny. **2.** The second and third crosses used a *fem-3* loss-of-function mutation which feminizes (Fem). From heterozygotes of genotype *fem-3(e1996)* + *dpy-20(e1282)*/ + *egl-20(n585)* +, 5/8 Dpy non-Fem recombinants segregated Mig progeny. **3.** From heterozygotes of genotype *unc-24(e138) egl-20(n585)*/ *fem-3(e1996)*, 4/9 Egl non-Unc recombinants and 2/5 Unc non-Egl recombinants segregated Fem progeny.

Mapping relative to *mec-3*.

From heterozygotes of genotype *unc-24(e138) egl-20(n585)* + *dpy-20(e1282)*/+ + *mec-3(e1338)* +, 5/18 Unc Egl non-Dpy recombinants and 17/17 Unc non-Egl non-Dpy recombinants segregated Mec progeny, indicating that *egl-20* is to the left of *mec-3*. (An additional 10 Unc non-Egl non-Dpy recombinants were not scored for the Mec phenotype.)

Mapping relative to *daf-14*.

From heterozygotes of genotype *unc-24(e138) egl-20(n585) + mec-3(e1338)/+ + daf-14(m77) +*, 34/34 Unc non-Egl non-Mec recombinants, 2/5 Unc Egl non-Mec recombinants and 0/4 Mec Egl non-Unc recombinants segregated Daf-c progeny, indicating that *egl-20* is to the left of *daf-14*.

RFLP mapping

In order to map RFLP's relative to *egl-20*, I used markers in the region to generate worms with recombination events between N2 and RW7000 in the *egl-20* region. N2/RW7000 recombinants were generated in two ways. **1.** Males heterozygous for *unc-24(e138) egl-20(n585) dpy-20(e1282)* were crossed with RW7000 hermaphrodites. F1 hermaphrodite progeny which segregated 1/4 Unc Dpy's were kept and their progeny examined for Unc non-Dpy and Dpy non-Unc recombinants. In this way we identified 26 recombinants in the *unc-24-dpy-20* interval. **2.** Males heterozygous for *unc-24(e138) egl-20(n585) mec-3(e1338)* were crossed with RW7000 hermaphrodites. F1 hermaphrodite progeny which segregated 1/4 Unc Mec's were kept and their progeny examined for Unc non-Mec and Mec non-Unc recombinants. In this way we identified 45 recombinants in the *unc-24-mec-3* interval. Of these recombinants, 13 were between *egl-20* and *mec-3*, a 0.2 map unit interval. In both crosses only one recombinant F2 from each F1 was kept. Digested DNA from strains homozygous for the recombinant chromosome was probed with labelled cosmids to identify the RFLP. Two of the nine RFLP's, the F13C8 and T01G2 polymorphisms, did not show linkage to LG IV.

Southern Blots

Radioactive: as described in (Wrischnik, 1995).

Nonradioactive: Plasmid probes were prepared and detected using the Polarplex kit by Millipore and cosmid probes were prepared and detected using the Genius Kit by Boehringer Mannheim. Cosmid probes labelled with the Genius kit were not linearized.

Identifying and mapping Tc elements in the MT3973 strain

Plasmid probes for Tc1, Tc3, Tc5 and Tc6 (pTc1, pTR10, pTW23, and pCE1061, respectively), were used to probe Southern blots containing MT3973 genomic DNA. Three extra Tc1 and two extra Tc3 elements in the MT3973 strain were mapped relative to *unc-24, dpy-20* and the MT3973 *egl-20* allele *(n1437)*. Briefly, MT3973 hermaphrodites were crossed with *unc-24(e138) dpy-20(e1282)*/+ males. F1 hermaphrodites which segregated 1/4 Unc Dpy progeny were kept, and their progeny examined for Unc non-Dpy and Dpy non-Unc recombinants. Genomic DNA from worms homozygous for the recombinant chromosomes was probed with plasmids containing Tc1 or Tc3. In all, 38 recombinants in the *unc-24-dpy-20* interval were identifed and analyzed.

Searching for allele-specific polymorphisms

Cosmids used to probe *n1437*: R04E11, F13C8, F56H11, C33A12, T05A1, T01G2, C28D4 and W02D1.

Cosmids used to probe *mu25, mu27* and *mu39*: F56H11, C33A12 and T05A1.

Cosmids used to probe *n585*: C33A12 and T05A1.

Screen

N2 males were soaked in trimethylpsoralen and exposed to UV light as described in Edgar, 1994. The mutagenized males were then mated to *unc-*

24(e138) egl-20(n585) mec-3(e1338); dpy-6(e14)hermaphrodites. F1 non-Unc hermaphrodites were grown to adulthood and screened for the Egl phenotype. These candidates were then screened for a QL.(d) migration (Mig) defect. The X-linked *dpy-6* mutation was used to prevent F1 males from mating with F1 hermaphrodites. This strategy is likely to be successful in identifying new *egl-20* mutations, since a similar complementation screen for EMS-induced alleles (see Chap. 2) produced the *egl-20(mu27)* allele.

Results

Genetic Mapping

The *egl-20* gene had previously been mapped to a region on LG IV (Trent *et al.*, 1983) between the genes *unc-24* and *dpy-20* (see Methods, Chapter 2). To define the map position of *egl-20* more precisely, I used complementation tests to map it relative to the deficiencies *eDf19* (see Chap. 2), *eDf18* and *mDf7*. I found that only *eDf19* clearly failed to complement *egl-20*, and only *eDf19/+* had a QL.(d) migration defect (see Chapter 2, Table 2.2). *mDf7* appeared to partially complement an *egl-20* mutation (see Table 6.1). However, animals heterozygous for a mutation in *egl-20* have a low frequency QL.(d) Mig defect on their own (seeTable 6.1; also Chapter 2, Table 2.2), but animals heterozygous for *mDf7* do not (Table 6.1). The *egl-20* gene is dose-sensitive; lowering the level of *mab-5* activity can enhance the QL.(d) Mig phenotype of *egl-20* heterozygotes. These observations suggest that either *mDf7* deletes only part of the *egl-20* gene, leaving some residual activity, or else that it deletes some gene or genes which interact with the *egl-20* pathway in much the way that *mab-5* does. The results of these complementation tests suggest that *egl-20* maps to the small interval between the right endpoint of *eDf18* and the left endpoint of *mDf7* (see Fig. 6.1). However, this interpretation directly

contradicts complementation data for the gene *gon-1* (S. Santa-Ana and J. Hodgkins, pers. comm.), which suggest that *eDf18* and *mDf7* overlap. The conflicting complementation data for *gon-1* and *egl-20* suggested that these deficiencies might not be simple rearrangements. If this were so, then molecular analysis of these deficiencies could be quite misleading.

To define the map position of *egl-20* more unambiguously, I used three-factor mapping to determine the position of *egl-20* relative to the cloned genes *fem-3* and *mec-3* and the putatively cloned gene *daf-14* [see Materials and Methods]. Together, these data unambiguously place the *egl-20* locus in a 0.48 map unit interval between *fem-3* and *daf-14* (see Fig. 6.1).

Physical Mapping

The cloned genes *fem-3* and *mec-3*, which flank the *egl-20* locus, defined left and right endpoints for the location of the *egl-20* gene on the physical map. The *C. elegans* Genome Project had at that time cloned more than 85% of the worm genome into cosmid and YAC vectors and had built an overlapping map of clones covering most of the chromosomes (Sulston *et al.*, 1992). Since the cosmids which contained the *fem-3* and *mec-3* genes had already been identified (Rosenquist and Kimble, 1988; Way and Chalfie, 1988), I was able to use the cosmids between these genes for more fine-scale mapping.

To identify physical markers to use in mapping *egl-20*, I took advantage of two independent wild-type isolates of *C. elegans*, N2 and RW7000, known to be polymorphic at the DNA level (Emmons, 1988). To identify such restriction fragment length polymorphisms (RFLP's), I probed Southern blots containing digested genomic DNA from N2 and RW7000 worms with labelled cosmid DNA from the *fem-3*-*mec-3* region. I identified nine cosmids

which gave polymorphic hybridization patterns between the two wild-type strains (see Materials and Methods), and used recombinants to map the *egl-20* gene between two of them, C28D4 and W02D1 (Fig. 6.2).

Transposon Tagging

In parallel with the mapping approach described in the previous section, I hoped to identify the *egl-20* gene by "tagging" it with a known DNA sequence that would then act as handle, allowing me to fish it out of the approximately 10^8 kb of *C. elegans* genomic DNA (Emmons, 1988). Gian Garriga had isolated an *egl-20* allele, *n1437*, in the mutagenic strain MT2878 (pers. comm.); this *egl-20* mutant strain is called MT3973. MT2878 contains *mut-2*, which activates transposition of five known *C. elegans* transposons, Tc1, Tc3, Tc4, Tc5 and Tc6, allowing them to insert in new genomic locations (Collins *et al.*, 1987). If the *egl-20* mutation in the MT3973 strain was caused by an insertion of a transposon of known sequence into the *egl-20* gene, then I could use probes to this sequence to isolate a clone containing *egl-20* sequence. However, if the mutation were caused by an imprecise excision event or by insertion of an unknown transposon, then I would not be able to identify the *egl-20* gene using this approach.

The MT2878 starting strain contains more Tc1 transposons than N2 and may carry extra copies of other transposons as well (M. Finney and R. Horvitz, pers. comm.). To eliminate the background from extra transposons not in the *egl-20* region of the genome, Gian Garriga first crossed *egl-20(n1437)* back to N2 (wild type) eleven times (pers. comm). These backcrosses would ideally generate a strain in which all the chromosomes were isogenic with N2 except for the cluster (central region) of chromosome IV. I then probed Southern blots containing genomic DNA from N2 and MT3973 worms with Tc1, Tc3,

Tc5 and Tc6 DNA. I identified three extra Tc1 containing bands and 2 extra Tc3 containing bands in MT3973 DNA. To determine whether any of these extra transposons were tightly linked to the *egl-20* locus, and thus might be responsible for the *n1437* mutation, I looked to see whether recombination could separate the extra Tc elements from the *egl-20* mutation [see Materials and Methods]. I found that the extra transposons all showed linkage to the LG IV gene cluster but were all separable from the *egl-20* locus (data not shown), suggesting that none of them was responsible for the *egl-20(n1437)* mutation.

Allele-specific DNA polymorphisms

In another approach to determine the physical location of the *egl-20* gene, I used DNA from the *fem-3-mec-3* region of the genome to probe for differences between the DNA of *egl-20* mutants and wild type. In this way, I hoped to identify the physical locations of the *egl-20* mutations in these strains. Four of the five *egl-20* alleles are EMS-induced and one may be transposon-induced. EMS usually induces point mutations but occasionally produces deletions large enough to be detected with Southern blot analysis (Anderson and Brenner, 1984; Dibb *et al.*, 1985). If the *egl-20(n1437)* mutation were caused by insertion of a transposon, then this approach would identify its location, even if the transposon were of a new class. Similarly, if *n1437* were caused by imprecise excision of a transposon, then probing with wild-type cosmid DNA could identify the deletion, if it were large enough or if it removed a restriction site. I used several cosmids from the *fem-3-mec-3* region to probe DNA from all five *egl-20* mutant strains (Materials and Methods). As RFLP mapping narrowed down the *egl-20* region, I focused on cosmids in the new interval. I did not find any confirmed allele-specific polymorphisms with any of the cosmids I used (see Materials and Methods).

Since probing of existing *egl-20* alleles had not identified any DNA polymorphisms, I designed a screen using trimethylpsoralen mutagenesis to isolate *egl-20* mutations which fail to complement *egl-20(n585)* [see Materials and Methods]. Trimethylpsoralen activated by UV light generally produces deletions larger than 2kb, which are easily detectable on Southern blots (Yandell *et al.*, 1994). *egl-20(n585)* is viable, fertile, and Egl in trans to a deficiency for the region, (see Chap. 2 and this Chapter, Materials and Methods), so this screen should be able to identify deletions of the *egl-20* locus. This screen was begun by Wendy Gilbert, who also constructed the starting strain for the mutagenisis, when she was a rotation student working with me in the lab. She screened 2000 F1's and did not find any new *egl-20* alleles. This screen is currently being continued by Gregg Jongeward.

Generation of transgenic animals carrying cosmid and YAC genomic clones

At the time that I initiated the cloning of *egl-20*, genomic DNA from the entire *fem-3* to *mec-3* interval was contained in a series of overlapping cosmid and YAC (yeast artificial chromosome) clones. In parallel with the RFLP mapping of *egl-20*, I began generating transgenic animals which carried extrachromosomal arrays containing cosmids or YAC's with genomic DNA from this interval. Transgenic animals were generated by injecting cosmids and YAC's both singly and in pools into the syncytial gonad of *egl-20* mutants. In this way I hoped to identify clones which would rescue the *egl-20* mutant phenotype, and thus indicate the physical location of the *egl-20* gene.

Since *egl-20* initially mapped to such a large interval, I injected cosmids both singly and in pools (two pools the kind gift of Tom Barnes). I eventually began to inject YAC clones in an attempt to narrow down the field. As my RFLP mapping finally appeared to suggest that *egl-20* might map to a gap in

the cosmid contig, I injected both the cosmids flanking the gap and a YAC clone that spanned it. I was unable to obtain either transient rescue (F1's) or stable rescue (F2's) with any cosmids or YAC's (Fig. 6.2).

Discussion

The *egl-20* gene is required for such dissimilar but fundamental processes as activating Hox genes, polarizing cells correctly along the A/P axis, and determining where migrating cells stop. Learning the sequence of the *egl-20* gene and its pattern of expression would help distinguish between the many models proposed for its function. (For a more complete discussion of models of *egl-20* function, see Discussions in Chapters 2, 4, and 5). Significant homologies to known genes might suggest a potential mechanism. Does *egl-20* affect expression of the Hox gene *mab-5* by directly binding to the *mab-5* gene as a transcription factor, or does it function more indirectly by signalling the QL cell externally? If the *egl-20* gene were expressed in cells other than QL or its descendants, this would be the first implication that cell signalling might be involved in regulating the migrations of these cells. To answer these questions, and others, I initiated the cloning of the *egl-20* gene.

Status of *egl-20* cloning

Using a combination of genetic and molecular techniques, I mapped the *egl-20* gene to a small interval on the physical map between RFLP's on the cosmids C28D4 and W02D1 (Fig. 6.1). This interval included a break in the cosmid contig spanned by genomic DNA cloned into Yeast Artificial Chromosomes (YAC's). I was unable to either obtain transformation rescue with YAC's or cosmids (Fig. 6.2) or identify a DNA polymorphism associated

with an *egl-20* allele. This suggested that *egl-20* might either be unable to rescue by transformation, or might be mismapped. Since there are no reports of mutations that were never able to be rescued by transformation, it seemed likelier that I had not tried hard enough with the existing clones, that *egl-20* was mismapped or that the clones I was working with were deleted.

The cloning of the *egl-20* gene is being continued by Gregg Jongeward and Jennifer Whangbo. It seems likely that a continuation of this approach of RFLP mapping, transformation rescue attempts and mapping relative to cloned genes in the region, combined with a screen for trimethylpsoralen-induced (deletion) alleles, should lead to the identification of the *egl-20* sequence.

What might *egl-20* encode?

Genes have been identified both in *C. elegans* and in other species such as *Drosophila* and mice that are required for the same type of developmental processes as *egl-20*. **Hox gene Activators.** Many Hox gene activators have been identified in *Drosophila, C. elegans* and mice. Some of these genes are transcription factors, such as Kr in mice or pair rule genes such as *fushi tarazu* or *even-skipped* in flies. However, signalling molecules like *decapentaplegic*, a TGF-B family member, or *wingless*, a segment polarity gene, have also been shown to activate expression of Hox genes in the fly (Tremml and Bienz, 1992; Thuringer and Bienz, 1993). Sequenced genes which regulate expression of the Hox gene *mab-5* in *C. elegans* are of all types: *pal-1* is a putative transcription factor, homologous to the *Drosophila* gap gene *caudal* (Waring and Kenyon, 1991), *lin-22* is homologous to the *Drosophila* neurogenic gene *Hairy* (Wrischnik, 1995), and *lin-17*appears to be an integral membrane protein homologous to the *Drosophila* tissue polarity gene *frizzled* (H. Sawa

and R. Horvitz, pers. comm.). **Cell Polarity Genes.** Many genes which regulate A/P cell polarity in the fly or the worm are also known. Segment polarity genes, such as *wingless* and *patched*, and tissue polarity genes such as *frizzled* and *disheveled* have been shown to regulate the A/P polarity of cells in the fly eye (Ma and Moses, 1995; Wehrli and Tomlinson, 1995; Zheng *et al.*, 1995) and epidermis (reviewed in Peifer and Bejsovec, 1992; Gubb, 1993; Theisen *et al.*, 1994). The *C. elegans frizzled* homolog, *lin-17* (Sternberg and Horvitz, 1988), and *wingless* paralog, *lin-44* (Herman and Horvitz, 1994; Herman *et al.*, 1995), perform similar functions in the worm hypodermis and nervous system. **Genes involved in a system of positional information.** Less is known about these genes, although the gap, pair rule and segment polarity genes appear to help establish such a system in the developing *Drosophila* embryo. Later, in the developing *Drosophila* eye, temporal gradients of segment and tissue polarity gene expression may provide positional information which then orients cells correctly along the two major axes of the eye (Ma and Moses, 1995; Wehrli and Tomlinson, 1995; Zheng *et al.*, 1995). Positional information in the optic tectum of vertebrates may be provided by Eph receptor ligands such as RAGS, ELF-1 and Mek4 (Cheng *et al.*, 1995; Drescher *et al.*, 1995).

It is difficult to imagine one known protein that takes on the many different roles of the *egl-20* gene product. One possible way to reconcile *egl-20*'s many different functions is to assume that one function is primary and the others are merely consequences of this main activity. For example, *egl-20* could be part of a system of positional information that is upstream of Hox gene expression and cell polarity. Another likely possibility is that *egl-20* could be homologous to a segment or tissue polarity gene. Not only do some segment and tissue polarity genes appear to affect both Hox gene activation

and A/P cell polarity, but they may be able to provide positional information. In any case, whether *egl-20* is homologous to a known gene or is completely new, learning its sequence, expression pattern and mechanism of action will provide insight into the connection between Hox genes, cell polarity, and guidance of migrating cells.

Acknowledgements

I would like to thank Gian Garriga for his kind gift of the outcrossed MT3979 strain. I would also like to thank John Collins for the Tc3 and Tc5 probes, pTR10 and pTW23, respectively, and the Emmons lab (via Bob Klein of the Meyer lab) for the Tc6 probe, pCE1061. I would especially like to thank Tom Barnes for generously sharing unpublished information, his pools of cosmid DNA and his transgenic line with the partial *daf-14* rescuing activity. I am greatly indebted to Alan Coulson and the *C. elegans* genome project for generating the physical map of the *egl-20* chromosomal region and the many, many cosmids and YAC's which they sent. I would also like to thank Bruce Wang for being such a patient and encouraging teacher of molecular biology and Lisa Wrischnik for all her help with YAC's and pulse-field gels. I would also like to thank other members of the Kenyon lab, especially Craig Hunter, for many helpful discussions.

full genotype	**relevant genotype**	**% QL desc. Ant.**	**n**
egl-20(n585)/ egl-20(n585)	***egl-20/egl-20***	100%	50
eDf19/ unc-24(e138) egl-20(n585)	***eDf19/egl-20***	100%	25
dpy-13(e184)mDf7/ unc-24(e138) egl-20(n585) mec-3(e1338)	***mDf7/egl-20***	18%	50
eDf18/unc-24(e138) egl-20(n585)	***eDf18/egl-20***	0%	7
eDf19/ unc-24(e138) dpy-20(e1282)	***eDf19/+***	9%	123
unc-24(e138) egl-20(n585)/+	***egl-20/+***	7%	100
dpy-13(e184) mDf7/nT1	***mDf7/+***	0%	47
eDf18/ unc-24(e138) dpy-20(e1282)	***eDf18/+***	5%	65

Table 6.1 The deficiency *eDf19*, but not the deficiencies *eDf18* and *mDf7*, deletes the *egl-20* locus. The *eDf19* deficiency chromosome fails to complement *egl-20(n585)* and, like *egl-20(n585)*, is haploinsufficient for the QL.(d) Mig defect. QL descendants which were at or anterior to V4.p were scored as anterior.

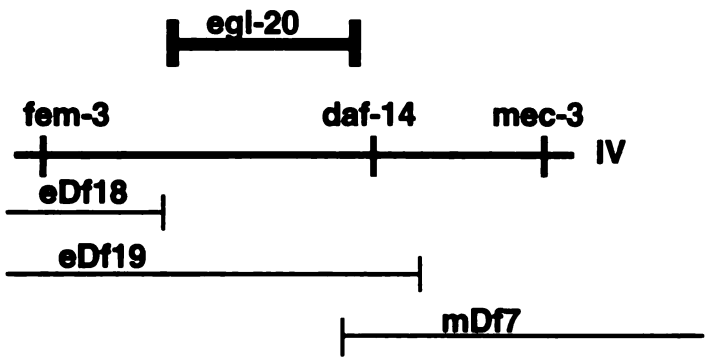

Fig. 6.1. Genetic map of the *egl-20* region of LGIV. The regions of LGIV deleted by the deficiencies *eDf18*, *eDf19* and *mDf7* are shown below. *eDf19*, but not *eDf18* or *mDf7*, delete the *egl-20* locus. *egl-20* maps between the cloned genes *fem-3* and *daf-14*, a distance of x map units.

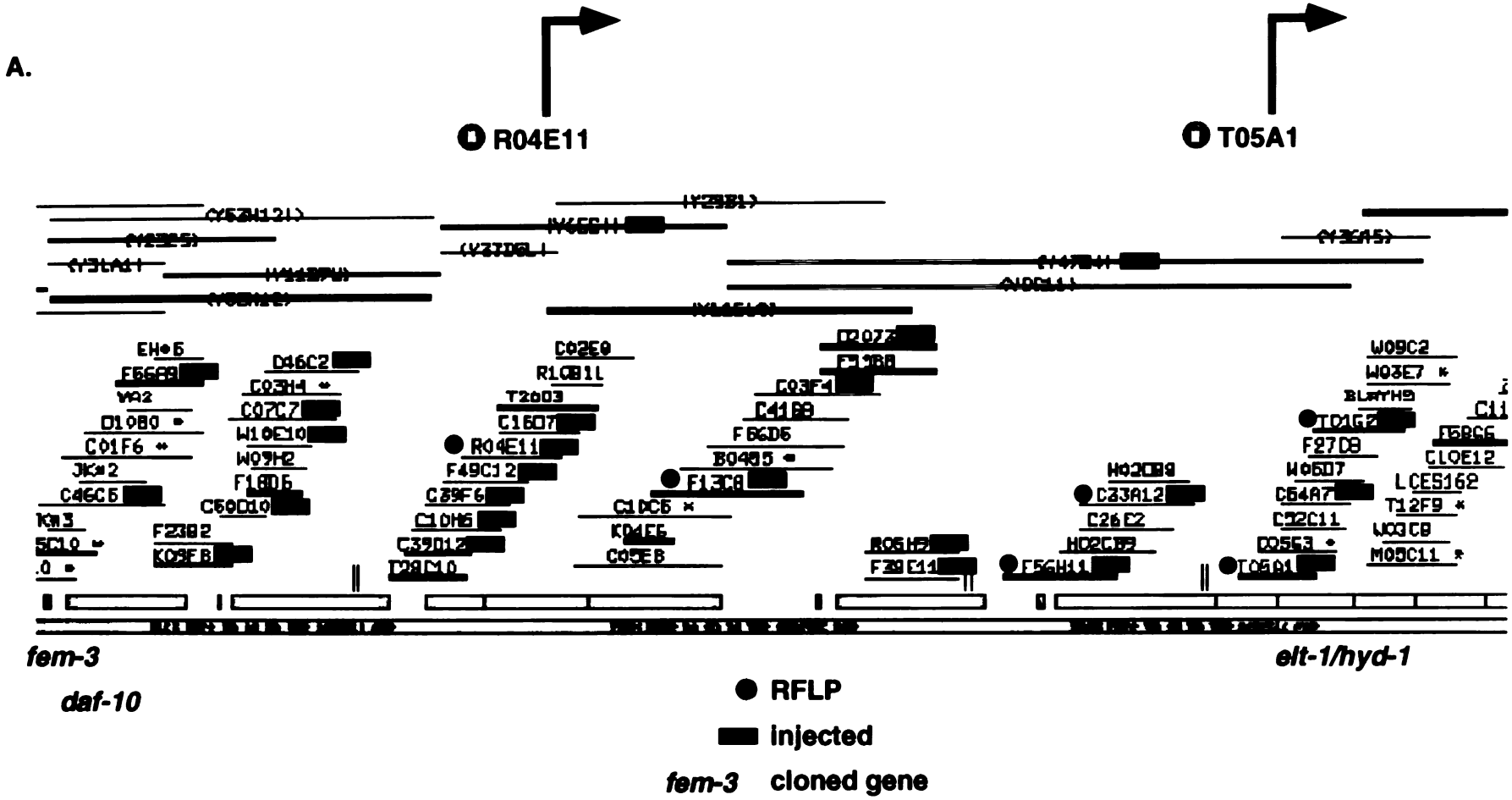

Fig. 6.2. The physical map of the *egl-20* region, from *fem-3* to *mec-3* (see Fig. 6.1), showing the overlapping cosmid and Yac clones of *C. elegans* genomic DNA. Cloned genes are colored pink, cosmids and Yac's tested for transformation rescue are labelled green, and cosmids containing N2/RW7000 RFLP's are marked with a blue circle. Blue arrows above the RFLP's indicate the direction of the *egl-20* gene relative to the tested polymorphism. A. The left half of the cosmid contig. B. The middle portion of the cosmid contig. C. The right half of the cosmid contig.

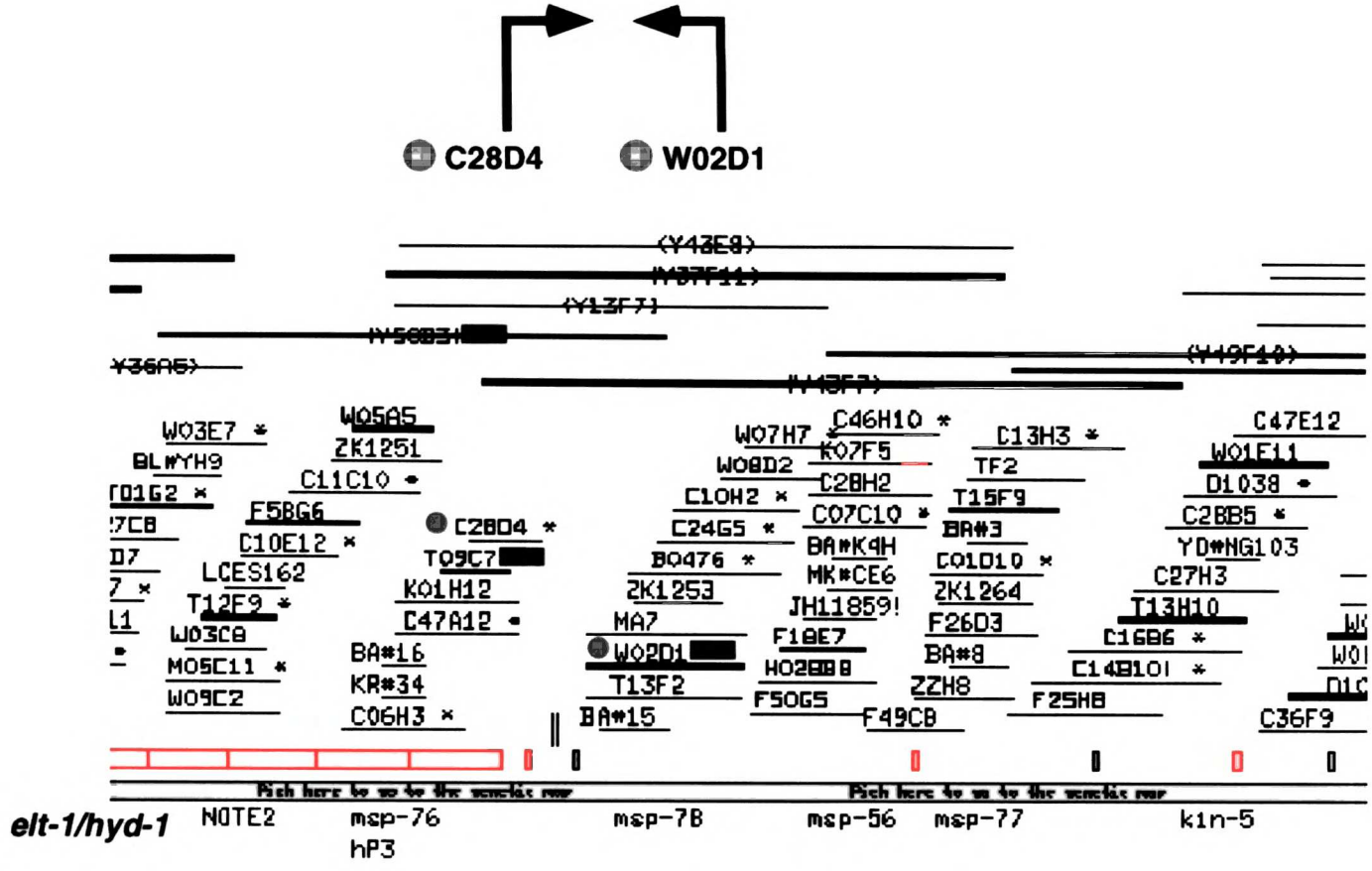

● RFLP

▬ injected

fem-3 cloned gene

Fig. 6.2B

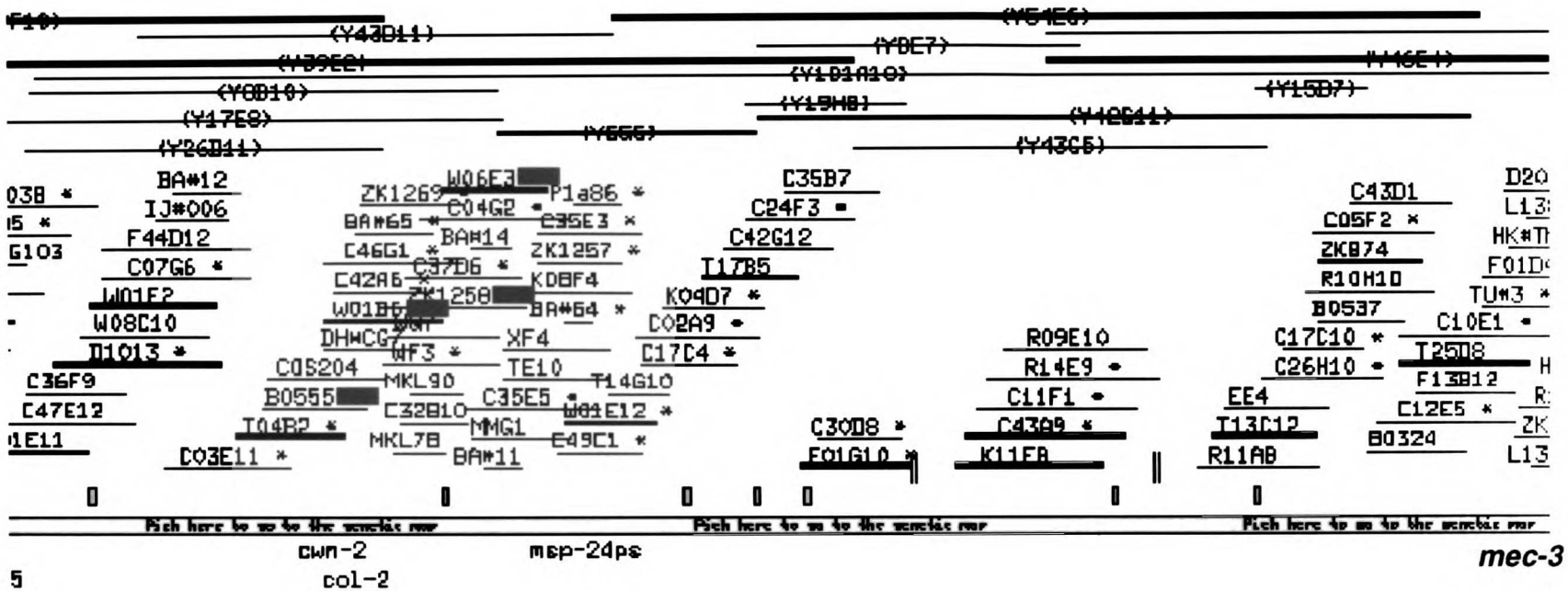

● RFLP

▬ injected

fem-3 cloned gene

Fig. 6.2C

Chapter 7: Discussion and Future Directions

Summary

The *C. elegans egl-20* gene plays a role in several different aspects of development. I have shown that *egl-20* functions to guide migrating cells to their final positions, to regulate Hox gene expression in two different cell types, and to orient the polarity of certain epidermal cells along the A/P axis. In addition, I have examined the interaction of *egl-20* with other genes. I have found that three genes, *mig-14*, *lin-17* and *mig-1* interact with *egl-20* to regulate both neural cell migration and anterior/posterior (A/P) polarity of epidermal cells. Analysis of the role of these genes in cell polarity suggests that they may be components of a cell-cell signalling pathway. These results have been described in more detail in chapters 2 through 6, so only the basic conclusions will be summarized here.

Summary of Chapters

In Chapter 2 I characterized the effects of *egl-20* on the migration of the descendants of the Q neuroblasts. I showed that *egl-20* is required for two different aspects of cell migration: activation of the Hox gene *mab-5* and *mab-5*-independent regulation of final position. In collaboration with Lee Honigberg and Naomi Robinson in the lab, I showed that *egl-20* acts at the same step as *mig-14*, *mig-1* and *lin-17* to regulate expression of the Hox gene *mab-5* within the migrating QL descendants. Curiously, mutations in these genes do not generally affect expression of *mab-5*: aside from a lack of expression in QL and its descendants, the remainder of the pattern is wild-type. This observation is consistent with a model in which *mab-5* expression is regulated by many different tissue-specific regulators. In addition to its effect on *mab-5* expression, *egl-20* is required for determining the final

position of migrating Q descendants along the A/P axis. Together, Lee Honigberg and I have shown that mutations in *egl-20* and *mig-14* cause migrating QR descendants to stop at positions posterior to normal, even if they must migrate in the opposite direction to do so. This finding is consistent with a model in which *egl-20* and *mig-14* specify the position that Q descendants migrate to, and not their direction of migration.

Chapter 3 presents an analysis of migration defects in double mutant combinations between mutations in different *mab-5* activators: *egl-20, mig-1, lin-17* and *lin-22*. I did not observe any novel phenotypes in these double mutants, suggesting that these genes may not have redundant functions in other tissues. I did, however, uncover some interesting interactions the regulation of Q descendant and HSN migration. I found that although an *egl-20* mutation shifted the final positions of the QR descendants towards the posterior in *mig-1* and *lin-17* mutants (i.e., *egl-20* was epistatic), the change in direction of QL descendant migration in *egl-20* mutants was NOT epistatic to mutations in *mig-1* and *lin-17*. I also found that in *mig-1* mutants, *mab-5* can promote posterior migration in an *egl-20*-independent way. Surprisingly, I was unable to detect expression of *mab-5* in the QL daughters in *mig-1; egl-20* double mutants, even though *mab-5* was able to keep the QL descendants in the posterior in 12% of these double mutants. I also observed that the HSN neuron can migrate too far into the anterior in *lin-17* mutants. The migration of HSN is shortened in *egl-20* mutants (Desai *et al.*, 1988), but I show that this defect can be partially suppressed by a *lin-17* mutation. This analysis raises two questions: 1. How do these genes regulate cell migration? 2. How is a position-specific gene like *mab-5* regulated in an organism that appears to favor lineal control and local cell signals to regulate Hox gene expression?

In Chapter 4 I show that mutations in the *egl-20* gene prevent *mab-5* from being activated in the V6 cell in response to seam-cell signalling. Normally, activity of the *C. elegans* caudal homolog, *pal-1*, in V6 activates *mab-5* expression independently of cell signals. *egl-20* mutations could block *mab-5* expression in V6 in response to extracellular signals either by creating a new signalling center in a neighboring cell, or by removing a component in V6 required for *mab-5* expression. In the course of this analysis, I also uncovered a role for *pal-1* in regulating the migrations of the Q descendants. Since *pal-1* mutations reduce *mab-5* expression in QL, and dominantly enhance the effect of *mab-5* mutations on the direction of QL descendant migration (Salser and Kenyon, unpublished data), it seems likely that *pal-1* is required to activate *mab-5* expression in QL and its descendants as well as in the V6 lineage. It will be interesting to learn more about the relationship between the homeobox gene caudal and *egl-20* in Hox gene regulation. In *Drosophila, caudal* appears to function upstream of the Hox genes: are *pal-1* and *egl-20* components of a conserved pathway for Hox gene activation? Further analysis of these genes and their interactions will address this question.

Chapter 5 focuses on another aspect of *egl-20* biology: the ability of *egl-20* mutations to reverse the A/P polarity of epidermal seam cells, in particular that of V5. In the wild-type, all six V cells, including V5 divide to produce a posterior daughter which develops as a seam cell, like its mother, and an anterior daughter which fuses with a large epidermal syncytium. In *egl-20* mutants, V5 can divide with reversed polarity: the anterior daughter can develop as a seam cell and the posterior daughter as a syncytial cell. Thus, wild-type *egl-20* activity is required for the V5 cell to divide with wild-type polarity. I have shown that this reversal is influenced by the presence of posterior neighbors: when posterior seam cells are ablated, V5 divides with

wild-type polarity, and when anterior neighbors are ablated, it always divides with reverse polarity. These findings suggest that there are at least two mechanisms for determining the A/P polarity of V5 in *egl-20* mutants: one which involves signals from neighboring seam cells and one which is seam-cell independent. Somewhat surprisingly, experiments by Jennifer Whangbo in the lab have demonstrated that the A/P polarity of seam cells in wild-type animals is unaffected by neighbor ablation. Thus, the *egl-20*-dependent signalling pathway may be redundant with another polarity determining mechanism in wild-type or may only exist in *egl-20* mutants. By analyzing genes which enhance or suppress this polarity reversal, Jennifer Whangbo and I have identified several candidates for genes involved in the signal/response pathway: *lin-17*, the *C. elegans* homolog of the *Drosophila* tissue polarity gene *frizzled*, *lin-18*,*mig-1*, and *mig-14*. Four of these genes, *egl-20*, *mig-14*, *mig-1* and *lin-17*, all regulate the same step of cell migration, activation of the Hox gene, *mab-5*. In addition, *egl-20* and *mig-14* also act to determine the stopping points of these migrating cells along the A/P axis. Together, these observations suggest that stationary and migratory cells may share a system for determining position and orientation along the anterior/posterior axis.

Identifying the sequence of the *egl-20* will help to answer many questions about *egl-20* function, and the sequence of events in the *egl-20*-dependent pathways. In Chapter 6 I presented the progress to date on the cloning of the *egl-20* gene. Through a combination of genetic and physical mapping, I have shown that *egl-20* maps to a small interval covered by a single YAC clone. Further mapping and transformation rescue experiments, that are currently being carried out be Gregg Jongeward and Jennifer Whangbo in the lab, should succeed in identifying the *egl-20* sequence. A screen to identify new

egl-20 alleles containing deletions large enough to be visualized on a Southern blot might help in the cloning by creating a large physical change in the DNA associated with the *egl-20* locus. The many experiments that the *egl-20* sequence would make possible are described in detail below.

Future Directions

Although we have learned much about the role of the *egl-20* gene in *C. elegans* development, these findings raise many additional questions. In the following six sections, I will try to present some of the many questions raised by observations and analysis of the *egl-20* mutant phenotype.

I. Cloning

Perhaps one of the biggest questions about *egl-20* unanswered at this time is: What does the *egl-20* gene encode? The sequence of the *egl-20* gene could be very informative. Motifs or homologies could suggest a mechanism for *egl-20* action. For example, does *egl-20* act in the nucleus, or is it secreted? Might it be a cytoplasmic kinase which responds to cell signals, or part of the transcription machinery?

In addition, cloning the gene would provide a useful tool. Analysis of the sequence of mutant alleles would allow us to determine which of the strong alleles, if any, are null. Antibodies, in situ hybridization and fusions to reporter genes would indicate where *egl-20* is expressed, and when. Since no free duplication covering the *egl-20* locus exists at this time, a rescuing array containing cosmid DNA from the *egl-20* region could be used instead to do mosaic analysis. Analysis of such an array in a wild-type background might also identify phenotypes resulting from overexpression of the*egl-20* gene. Knowing the sequence of the *egl-20* gene it would be possible to use different

promoters to misexpress the *egl-20* gene. What would be the effect of expressing *egl-20* in QR and its neighbors? Would the QR descendants now migrate towards the posterior? Analysis of the normal *egl-20* expression pattern together with the effects of over- and misexpression could answer many questions about the mode and mechanism of *egl-20* function.

II. Cell Migration

How does *egl-20* function to regulate QL and QR descendant migration?

One wild-type function of the *egl-20* gene is to activate the Hox gene *mab-5* in the migrating neuroblast QL and its descendants. In Chapter 2, I described three other genes that are also required for *mab-5* activation, *mig-14*, *mig-1* and *lin-17*. Double mutant analysis of these genes was informative (see Chapter 3), but did not provide enough information to order these genes into a pathway. Cloning the *egl-20* gene would make it possible to do molecular epistasis between *egl-20* and the other *mab-5* activation genes, just as we did for *mab-5*. For example, *mig-14* and *egl-20* have virtually identical phenotypes; is this because *mig-14* is required for *egl-20* expression?

egl-20 also has another *mab-5*-independent effect of migration of the Q descendants: it directs the Q descendants to migrate to positions shifted anterior to where they would otherwise migrate (see Chapter 2). How does *egl-20* determine the stopping points of migrating cells along the A/P axis? Determining the localization of the *egl-20* gene product, EGL-20, should help to distinguish between models. Analysis of other genes with the same phenotype, such as *mig-14*, and identification and analysis of suppressors and enhancers of this *egl-20* positioning phenotype may suggest a mechanism.

Similarly, mosaic analysis and expression studies may suggest a role for local cell signals in *mab-5* activation in the QL neuroblast.

How do mutations in *pal-1* and *mig-1* act to alter the migrations of the QL descendants?

mig-1. In the course of analyzing the *egl-20* Mig defect, I observed interesting effects of mutations in *mig-1* and *pal-1* on the migrations of cells in the QL lineage. Analysis of the *mig-1; egl-20* double mutant (Robinson, 1995; and this thesis, Chapter 3) demonstrated that posterior-directed migration of QL descendants in this strain required *mab-5* activity. However, I was unable to detect *mab-5* expression in QL or its daughters. Can *mab-5* function non-autonomously to direct QL descendant migration in *mig-1; egl-20* mutants? Or do mutations in *mig-1* render QL more sensitive to low levels of *mab-5*? How does a mutation in *mig-1* compensate for the loss of *egl-20*? It seems unlikely that mutations in *mig-1* render QL more sensitive to low levels of MAB-5, since the frequency of cells which express faintly or not at all, correlates with the frequency of QL descendants which migrate towards the anterior (Chapter 2). An increased sensitivity to MAB-5 could be tested by giving *mig-1; egl-20* mutants low level heat shocks, which are unable to induce sufficient expression of a hs-*mab-5* fusion gene to reverse the direction of Q descendant migration. If *mig-1* mutants are more sensitive, shorter or cooler heat shocks might be sufficient to rescue the QL descendant migration defect in *mig-1; egl-20* mutants. Non-autonomy of *mab-5* would be much harder to test. *mab-5* mosaic analysis in a *mig-1; egl-20* mutant would answer the question most directly. Unfortunately, since less than 15% of QL descendants migrate towards the posterior in *mig-1; egl-20* mutants, many mosaics of each class would have to be analyzed before a non-autonomous

role for *mab-5* could be demonstrated. Also, since many cells which are neighbors of QL are closely related to QL by lineage, it would be difficult to get enough losses to determine a requirement for *mab-5* outside QL. A more risky, but perhaps easier approach, would be to use single-cell heatshock to activate *mab-5* in different cells in a *mig-1; egl-20* mutant, and see whether any of them allowed the QL descendants to remain in the posterior. Perhaps the best approach will be to wait for the cloning of the *mig-1* gene to see where it acts and whether any homologies suggest a mechanism for gene function.

pal-1. Observation of the *pal-1* mutant phenotype suggests that it grossly resembles that of *mab-5* and *egl-20*: the QL descendants migrate to anterior positions in *pal-1* mutants (Chapter 4). Observation of the migrations of QL and its descendants in bulged *pal-1* mutants should indicate whether this *pal-1* mutation affects the same step of the migrations as *mab-5*. Since the wild-type function of *pal-1* is to activate *mab-5* in V6 (Salser and Kenyon, 1996), and since *mab-5* expression is reduced in QL in *pal-1* mutants (S. Salser and C. Kenyon, unpublished data), it seems likely that the *pal-1* QL descendant migration defect is due to a reduction of *mab-5* expression in QL. What is the relationship between *pal-1* and *egl-20* in QL? Since *pal-1* is cloned, molecular epistasis should indicate whether *egl-20* affects expression of *pal-1*. Since *pal-1* has many effects on embryonic development and *egl-20*'s effects so far appear to be predominantly post-embryonic, it may be that *pal-1* affects expression of *egl-20*. Similarly, does *egl-20* normally act downstream of *pal-1* in V6, or is *egl-20* part of a bypass pathway? The cloning of the *egl-20* gene will provide a way to monitor *egl-20* expression and test these possibilies.

What is the role of *egl-20* in other cell migrations?

Mutations in *egl-20* alter the final positions of the HSN neurons, the distal tip cells (DTC's) of the somatic gonad, the M mesoblast and the most anterior male sensory ray (or rays). Since the known *egl-20* mutations appear to reduce or eliminate gene function (see Chapter 2), the wild-type function of *egl-20* must allow these cells to migrate normally.

HSN. *egl-20* affects migration of the Q descendants by regulating expression of the Hox gene *mab-5* and determining the final positions of these cells perhaps by altering their response to global positional information or local cell signals. How might *egl-20* affect the migrations of these other cells? HSN requires activity of the Hox gene *egl-5*, might *egl-20* act by activating *egl-5* expression in HSN? In *egl-5* mutants, in addition to not migrating the full distance, the HSN neurons do not differentiate properly and fail to make the neurotransmitter seratonin. *egl-20* mutants, in contrast, synthesize seratonin at apparently wild-type levels (Desai *et al.*, 1988). In addition, in some *egl-20* mutants the HSN neurons express an integrated *egl-5*-lacZ fusion gene (data not shown). However, HSN neurons which do not migrate as far as wild-type are located in a region of the body, the posterior, which contains many *egl-5*-expressing cells (Wang *et al.*, 1993). Since the HSN nucleus is quite small, it is difficult to determine whether the cell is blue because it expresses *egl-5*, or just because dye from neighboring *egl-5*-expressing cells has diffused onto it. Antibodies to EGL-5 may be able to resolve this problem. If *egl-20* mutants do not affect *egl-5* expression, how does *egl-20* affect HSN migration? Several other genes, including *mig-1*, *mig-14* and *lin-17*, are required for wild-type migration of the HSN neurons. Genetic and molecular epistasis of genes required for HSN migration, but not differentiation, may ultimately help determine a pathway for regulation of HSN migration.

DTC. The migrations of the DTC's of the somatic gonad are variably affected in *egl-20* mutants (see Appendix). Mutations in other genes required for Q descendant migration, such as *mig-5*, a putative disheveled homolog (C-B Guo and E. Hedgecock, pers. comm.) and *mig-14* (Kiyoji Nishiwaki, pers. comm.) also affect the migrations of the DTC's. How do these genes interact to direct the migrations of the DTC's? *egl-5* is required for posterior migration of the linker cell (which performs a function analogous to the DTC's in the male gonad); might *egl-20* and *mig-14* regulate DTC migration by regulating Hox gene expression? *egl-20* and *mig-14* may tune the response of migrating Q descendants to positional information. How do the migrating DTC's determine where to turn?

Rays 1 (and 2). Baird *et al.*, (1991) have shown that the ray precursors migrate into the tail as a sheet of cells connected by adherens junctions. In males, V5 produces a single sensory ray, a neural structure used in male mating, and epidermal seam cells which produce alae, cuticular ridges (Sulston and Horvitz, 1977). The ray precursors are born in the body, but migrate into the tail attached to the V6-derived ray precursors (Baird *et al.*, 1991). Since these cells appear to move as a sheet, the V5-derived ray precursor may need to be born next to the descendants of V6 in order to migrate at all. In *egl-20* mutants, the most anterior ray does not always migrate into the tail and is sometimes separated from the tail by epidermal cells (indicated by the patch of cuticular ridges, or alae, they produce).

At a lower frequency, the second most anterior ray also fails to migrate. Polarity reversals have been observed in the V6 lineage as well (see Chapter 5). However, since V6 makes only rays and no alae, a polarity reversal in the V6 lineage cannot separate a ray precursor from other ray precursors. Each ray has a unique identity determined by the combination of Hox genes it

expresses (Chow and Emmons, 1994; Salser and Kenyon, 1996). One possibility is that only certain ray precursors can adhere to each other. If polarity reversals place certain ray precursors, which are not normally adjacent, next to each other, they may be unable to adhere properly to each other, thus preventing the unadherent ray precursor from being pulled with the row of migrating ray precursors. Such an event would also have the effect of leaving even more anterior rays stranded in the body as well. Alternatively, *egl-20* may affect the ability of these rays to migrate independently from their ability to adhere to each other. More extensive lineage analysis of V6 and V5 in *egl-20* mutants, correlated with the ability of specific ray precursors to migrate, may help to address this question. Similarly, analysis of *mab-5* expression at the time of ray precursor development, could determine whether the pattern of Hox gene expression, and thus of ray identity, has been altered.

M. The M mesoblast migrates down the left side of the worm from the head to the gonad where it crosses over to the right side (Sulston *et al.*, 1983). In *egl-20* mutants, M is slightly anterior to wild-type, but is always found on the right side of the animal. In addition, a non-nuclear-localized *mab-5*-GFP fusion shows that the shape of M in *egl-20* mutants can be abnormal (data not shown), much as it is in *mab-5*- mutants (Zipkin and Kenyon, unpublished data). Since M migrates prior to elongation of the embryo, *egl-20* mutations may affect which neighbors M adheres to during elongation, rather than the migration itself. Perhaps the location of *egl-20* expression or the subcellular localization of EGL-20 will suggest a mechanism for how *egl-20* mutations can affect M position.

Other migrations. I have examined the effect of the *egl-20(n585)* mutation on many other cell migrations, most of which are unaffected (see Chapter 2). However, I have not examined the effect of *egl-20* mutations on the

migrations of the sex myoblasts (SM's) in males or hermaphrodites, or the short migrations of the descendants of P1.a and P2.a (Salser and Kenyon, 1993 and 1994). The migrations of the sex myoblasts require *mab-5* activity in males. We have observed misplaced SM's in *egl-20* mutant males (see discussion of M lineage, below). Might *egl-20* function in a similar way in both SM's and QL descendants? Analysis of the migrations themselves, and expression of Hox genes in the SM's could clarify *egl-20*'s role in cell migration.

Many axons migrate both during embryonic and post-embryonic development of the *C. elegans* nervous system. Cell migration and axon guidance share many important features. Many tools have been developed over the past years to visualize the axons of specific neurons. *egl-20* mutations affect several cell migrations. Might they affect axon guidance as well? *egl-20* is not particularly uncoordinated, but mutant hermaphrodites are egg-laying defective (Egl) and mutant males mate very poorly. These behavioral defects can be partially explained by defects in the migration of the HSN neurons in hermaphrodites and in the development of the spicules and anterior rays in males. However, the behavioral defects in *egl-20* mutants appear to be more severe than expected. For example, *mig-14(mu71)* mutants have a more penetrant HSN migration defect than *egl-20(n585)* mutants, and yet *mu71* mutants are only occasionally Egl (Lee Honigberg and Cynthia Kenyon, unpublished data), while more than 98% of *n585* mutants are Egl (data not shown).

III. Polarity Reversals

How is the V5 reversal regulated?

I have shown that in *egl-20* mutants, signals from neighboring seam cells help orient the A/P polarity the epidermal cell, V5. However, we were unable to uncover any evidence that seam cells contribute to determining the A/P polarity of V5 in wild-type. How does wild-type *egl-20* activity determine the polarity of V5? Does it act in V5 to allow it to ignore seam cell signalling, or does it act in the neighboring seam cells to block signal production? Another possibility is that it could act in other nearby cells, such as hyp7 or posterior P cells, to signal V5 to ignore seam-cell signals. Mosaic analysis and expression studies should distinguish between these possibilities.

All *egl-20* alleles appear to be temperature sensitive for the polarity reversal phenotype (see Chapter 5). Since most of these alleles are not temperature sensitive for other other phenotypes, this suggests that at high temperatures *egl-20+* is needed to stabilize a process. At lower temperatures, this process proceeds almost normally in the absence of *egl-20*. Genes required for this temperature-sensitive process could be identified by either screening for mutations which enhance the *egl-20* phenotype (perhaps by mutagenizing a weaker allele, such as *mu27*, and screening at low temperatures), or by screening for mutations which have polarity defects on their own, at low temperatures.

Mutations in *mig-1*, *lin-17* and *mig-14* appear to modulate the seam-cell-dependent signal/response pathway in *egl-20* mutants. Where do these gene products act? *lin-17* has recently been cloned (H. Sawa and Horvitz, pers. comm.); mosaic analysis and expression studies (currently ongoing) should prove very informative. Mutations in *mig-1* and *lin-17* have opposite effects on the *egl-20*-dependent V5 reversal; which is epistatic? The answer to this question will have to wait until null alleles of *lin-17* and *mig-1* have been identified. Do those alleles also modulate the seam-cell-dependent pathway?

Mutations in *mab-5* and *mig-13* enhance or suppress, respectively, the reversal of V5 in *egl-20* mutants. However, at 25°C, where these phenotypes were examined, both *mab-5; egl-20* and *egl-20; mig-13* have significant levels of sterility and lethality. Perhaps these mutations do not actually modulate the frequency of polarity reversals, but rather survival. If the more affected animals (i.e. those with V5 reversals) die, then a large percentage of survivors would have wild-type V5 divisions and the mutation would appear to suppress. Conversely, a mutation might stress the developing *egl-20* mutant enough to mimic a temperature increase, and appear to enhance the *egl-20* phenotype. By examining the effect of these mutations at low temperatures, where decreased survival is not a problem, it might be possible to distinguish between an effect on survival, and an effect on the reversal itself.

How are later reversals regulated?

Mutations in *egl-20* can also affect later divisions of the V cells (see Chapter 5). However, not all lineages are affected equally. There is a weak A/P bias in the lineages affected: V6 is affected most frequently, while V1 was wild-type in all mutants examined. However, the most posterior branch of the V6 lineage was rarely affected: virtually all polarity reversals were observed in the seam cell adjacent to V5, V6.pa. What makes some cells more likely to reverse? Curiously, the control sides of ablated worms, or of unablated worms which were on the azide pad next to ablated worms, had a higher frequency of polarity reversals late in the V cell lineages than unexposed worms (data not shown). Exposure to azide or a laser microbeam may increase the stress level, and perhaps the heat shock response, of ablated worms. If wild-type *egl-20* activity is required to stabilize a process at high temperatures, then its loss would be more strongly felt under these

conditions. It would be interesting to test other conditions which increase stress or induce heat shock, to determine whether such conditions increase the need for *egl-20* activity in general.

All analyses of late V lineage reversals were carried out in hermaphrodites. The V6 cell in males produces five sensory rays, each with a unique identity. If *egl-20* mutations caused polarity reversals in L2 or L3 in males, the pattern of rays in the tail might be altered. Perhaps this misorganization of sensory structures contributes to the inability of *egl-20* males to mate.

Does *egl-20* regulate the polarity of cell divisions in other tissues?

In addition to reversing the polarity of cells in the lateral epidermis, *egl-20* mutations can also reverse the polarity of cells in the Q lineage (see Chapter 2). *egl-20* may have a more general effect on cell polarity, but few other lineages have been examined in *egl-20* mutants. *egl-20* mutants have a number of defects that are not fully explained: in particular, the male mating defect and the egg-laying defect. Polarity reversals in the developing male tail can lead to crumpled spicules (Chamberlin and Sternberg, 1995), a defect variably found in *egl-20* mutants. Examination of postembryonic divisions in other tissues, such as the ventral hypodermis, the ventral nerve cord, the M lineage and the male tail, may uncover a requirement for *egl-20* outside the lateral epidermis and the Q lineage.

IV. Does *egl-20*(+) activate *mab-5* expression in theV5 lineage in response to neighbor ablation?

L1/L2. In wild-type animals, the ectoblast V5 responds to ablation of neighboring seam cells by producing only epidermal cells in L2, instead of

producing a neuronal structure, the postdeirid (see Chapter 4). In *egl-20* mutants, as in *mab-5* mutants, V5 continues to produce a postdeirid even after neighboring cells are ablated. Salser and Kenyon (unpublished data) have shown that *mab-5* is activated in V5 after ablation of its posterior neighbor, V6. *egl-20* mutations prevent V6 from activating *mab-5* in response to T ablation in *pal-1* mutants (see Chapter 4). Is the wild-type function of *egl-20* to activate *mab-5* in V5 in response to loss of neighboring seam cells? To test this, we attempted to look at expression of *mab-5-GFP* in wild-type V5 cells after ablation of posterior neighbors, but were unsuccessful. This *egl-20* phenotype may be temperature sensitive, or the many copies of the *mab-5* promoter may act as a sink for certain crucial factors. The only way to answer this question may be by probing *mab-5* expression in *egl-20* mutants directly, using anti-*mab-5* antibodies. This technique may prove difficult, however, since antibodies detected only weak expression in a few animals following neighbor ablation (S. Salser and C. Kenyon, unpublished data). This expression may be too weak to clearly detect a loss of staining.

L3/L4. V5 in wild-type and V6 in *pal-1* mutants can both be induced to make 5 rays by ablating one posterior (or several anterior) neighbors. After neighbor ablation, *mab-5* is activated in V5 or V6 and appears to be expressed by all its progeny. Mutations in *egl-20*, however, permit the production of at most 2 or occasionally 3 rays even when the postdeirid is not made (see Chapter 4). Ectopic rays in *lin-22* mutants are dependent on activity of the Hox genes *egl-5* and *lin-39* as well as *mab-5* (Wrischnik, 1995). Are the V rays produced in *egl-20* mutants *mab-5*-dependent? If they are, then *mab-5* is able to get turned on in *egl-20* mutants in at least part of the V5 or V6 lineage after neighbor ablation. anti-MAB-5 antibodies would have to be used to detect late expression, since the integrated *mab-5*-GFP fusion currently in use, muIs16, is

not expressed in the V cells after L2. What genes are responsible for this late activation of *mab-5* in the V lineages? It would be interesting to test the possibility that other genes required to activate *mab-5* in Q cells also act late in descendants of V5 or V6 to activate *mab-5* expression after neighbor ablation.

V. What is the role of *egl-20* in the M lineage?

The M mesoblast divides postembryonically to produce body muscles, coelomocytes, and the sex myoblasts (SM's). The SM's then migrate, anteriorly in hermaphrodites and posteriorly in males, where they divide and give rise to sex-specific muscles, which include the vulval and uterine muscles in hermaphrodites and the diagonal muscles and spicule erector muscles in males (Sulston and Horvitz, 1977). *egl-20* hermaphrodites are Egl (Trent *et al.*, 1983) and males mate poorly, if at all (data not shown). In wild-type animals, the HSN neuron produces seratonin and is required for egg-laying (Trent *et al.*, 1983; Desai *et al.*, 1988; Desai and Horvitz, 1989). The HSN cell body is misplaced in *egl-20* mutants (Desai *et al.*, 1988), however, this is probably not the only cause of the Egl defect, since in some mutants in which the cell body is misplaced, the HSN axon can often migrate and branch correctly, and still regulate egg-laying (Garriga *et al.*, 1993). Also, Trent and Horvitz (1983) found that addition of either exogenous seratonin, which compensates for the loss of HSN, or imiprimine, which prevents reuptake of seratonin and possibly dopamine, were unable to reproducibly induce egg-laying in *egl-20(n585)* mutants. These observations suggested that *egl-20* mutants might be defective in a part of the egg-laying system other than HSN.

SM's. In hermaphrodites the SM's migrate towards the anterior, where they are attracted by the gonad (reviewed in (Garriga and Stern, 1994). In

males, the SM's migrate towards the tail. In *mab-5* mutants, the SM's in males reverse direction and migrate towards the middle of the body, as they do in hermphrodites (Kenyon, 1986). In spot checks of a few animals, we have observed SM's located anterior of the gonad in *egl-20* mutant males. *egl-20* acts upstream of *mab-5* in the QL lineage to determine the direction of cell migration; might it regulate *mab-5* expression in the male SM's as well? If it does, it must not be the only factor, since the *mab-5* mutant phenotype is much more penetrant than that of *egl-20*. Analysis of *mab-5* expression in the SM's in *egl-20* mutant males would help to answer this question. However, the SM's in the *egl-20* mutant were farther anterior than SM's in *mab-5* mutant males (i.e. anterior to the gonad). Why was this SM located so far anterior? In *egl-20* mutants M itself is located anterior to wild-type. Perhaps this SM was actually born in that position and will migrate back to the tail. However, M is not much anterior to wild-type, so it is unlikely that this shift in M position could entirely account for the anterior SM's. Mutations in *egl-20* cause polarity reversals in other lineages (see Chapter 5), perhaps a reversal in the M lineage can cause an SM to be born farther anterior in the lineage. Following the M lineage and SM migration in *egl-20* mutant males should help distinguish between these possibilities.

Much is known about the egg-laying system in *C. elegans*, but virtually nothing about the nature of the *egl-20* mutant defect. Could there be a defect in the M lineage in *egl-20* mutant hermaphrodites? In the few hermaphrodites examined, the positions of the SM's appeared wild-type. However, it would be interesting to examine more to see if some were occasionally positioned further anterior in *egl-20* hermaphrodites, as they can be in males. The position and orientation of the vulval muscles under polarized light appeared grossly normal in *egl-20* mutants, but this analysis

was incomplete: few animals were examined and the uterine muscles were not checked. *lin-39* is expressed in the SM's, but it's role in SM development is unknown. It would be interesting to examine *lin-39* expression in the M lineage in *egl-20* mutants to see whether the pattern is disrupted.

Analysis of the M lineage in *egl-20* mutants would likely be quite informative, but perhaps the best way to learn more about the nature of the Egl defect in *egl-20* mutants, would be to screen for mutations which suppress the Egl defect. Identifying interacting genes in this way might suggest a pathway or mechanism that might be involved. Also, genes identified in this way might also play a role in other *egl-20*-dependent processes such as Q descendant migration, HSN migration, orientation of cell polarity and Hox gene regulation.

Coelomocytes. Hermaphrodites produce two M-derived coelomocytes, one on the left and one on the right side of the body (Sulston and Horvitz, 1977). In *egl-20* mutants, over half the sides examined are missing a coelomocyte; what happened? In *mab-5* mutants, there are several defects in the M lineage and the coelomocytes are never made (Kenyon, 1986). Could *egl-20* mutations variably affect *mab-5* expression in the M lineage as well? If the coelomocytes are not made, what is made instead? Are both coelomocytes always coordinately affected, or can *egl-20* mutations independently affect different sublineages? Simply following the divisions of M in an *egl-20* mutant could answer many of these questions. Analysis of *mab-5* expression could also prove informative.

In addition to affecting production of M-derived coelomocytes, *egl-20* mutations have a second effect on these coelomocytes: in *egl-20* mutants, these coelomocytes can be found in positions far anterior to wild-type (see Appendix). This is reminiscent of the effect of *egl-20* mutations on SM's in

males. Again, anterior coelomocytes could be a result of the anterior position of M or polarity reversals within the M lineage. However, these coelomocytes are shifted quite far anteriorly, so it seems difficult to imagine how either a shift in M's position or a polarity reversal could account for such a great difference in position. Alternatively, the coelomocytes or one of their ancestors might actively migrate towards the anterior. Since the SM's are close relatives of the coelomocytes, perhaps a common ancestor had the ability to migrate. Again, to distinguish between these possibilities, it is essential to follow the lineage of M in *egl-20* mutants. Learning how *egl-20* acts to position M descendants correctly along the A/P axis might shed more light on how *egl-20* positions Q descendants, and vice versa.

egl-20 mutations affect both the production and placement of M-derived coelomocytes in hermaphrodites. Males produce only one M-derived coelomocyte from a different part of the lineage. Is the production and placement of this coelomocyte defective as well? It will be interesting to examine the phenotype of *egl-20* males in more detail.

Analysis of the effects of *egl-20* mutations on the M lineage could answer many questions about cell polarity, cell migration, positional information and cell signals. I think this is the most important question to be addressed after identifying the *egl-20* sequence.

VI. What other genes interact with *egl-20*?

In a Nomarski screen for mutations affecting migrations of cells in the Q lineages, Deborah Cowing identified a recessive mutation, *mu112*, which partially failed to complement the weak *egl-20* allele, *mu39* (see Appendix). Preliminary mapping experiments, however, suggested that *mu112*, unlike *egl-20*, may not map to LGIV (data not shown). The *mu112* mutation has a

phenotype similar to that of *egl-20*: the QL descendants migrate to anterior positions. *mu112*, like *egl-20(mu39)*, is only partially penetrant. *mu112* might enhance the phenotype of strong *egl-20* allele such as *n585* even more. Mutations in *lin-17* suppress many *egl-20* phenotypes. Might the *mu112* mutation also enhance the polarity reversal phenotype in homozygous *egl-20* mutants? It will be interesting to learn more about the gene that *mu112* mutates; does it map to a known gene?

Since *egl-20* mutations are dosage sensitive, it may be possible to identify other interacting genes by screening for mutations which enhance or suppress the phenotype of *egl-20* mutants. *egl-20(n585)* is to be weakly semi-dominant for the QL descendant Mig phenotype, but reported to be fully recessive for the Egl phenotype (Trent *et al.*, 1983). Perhaps this dissecting scope phenotype could be used to screen for enhancers. Enhancers of the Egl phenotype might be mutations in genes that interact closely with the *egl-20* gene product, and thus might enhance other *egl-20* mutant phenotypes as well.

Conclusion

The roles I have identified for *egl-20* in Q descendant migration, orientation of cell polarity and Hox gene regulation are just the beginning. As described above, *egl-20* mutations have many additional phenotypes in the descendants of M, and in certain other migrations. Clearly *egl-20*'s activities are broad, affecting many different aspects of *C. elegans* development. Since *egl-20* affects many important cell biological events, such as cell migration and cell polarity, it will be interesting to see whether its function is conserved in other animals. Further analysis, both genetic and molecular, should help clarify the role of *egl-20* in these fundamental developmental processes.

References

Ahn, J. and Fire, A. (1994). A Screen for Genetic Loci Required for Body-Wall Muscle Development During Embryogenesis in *Caenorhabditis elegans*. *Genetics* **137,** 483-98.

Amon, A. (1996). Mother and daughter are doing fine: Asymmetric cell division in yeast. *Cell* **84,** 651-654.

Anderson, P. and Brenner, S. (1984). A selection for myosin heavy-chain mutants in the nematode C elegans. *Proceedings of the National Academy of Sciences USA* **81,** 4470-4474.

Anton, E., Weskamp, G., Reichardt, L. and Matthew, W. (1994). Nerve growth factor and its low-affinity receptor promote Schwann cell migration. *Proceedings of the National Academy of Sciences of the United States of America,* **91,** 2795-9.

Austin, J. and Kenyon, C. (1994). Cell contact regulates neuroblast formation in the *Caenorhabditis elegans* lateral epidermis. *Development* **120,** 313-324.

Baird, S. E., Fitch, D. H. A., Kassem, I. A. A. and Emmons, S. W. (1991). Pattern formation in the nematode epidermis: determination of the arrangement of peripheral sense organs in the *C. elegans* male tail. *Development* **113,** 515-526.

Behar, T. N., Schaffner, A. E., Tran, H. T. and Barker, J. L. (1994). Correlation of gp140trk expression and NGF-induced neuroblast chemotaxis in the embryonic rat spinal cord. *Brain Research* **664,** 155-66.

Brenner, S. (1974). The genetics of *C. elegans*. *Genetics* **77,** 71-94.

Burrus, L. W. (1994). wnt-1 as a short-range signalling molecule. *Bioessays* **16,** 155-7.

Chalfie, M. and Sulston, J. (1981). Developmental genetics of the mechanosensory neurons of *C. elegans*. *Dev. Biol.* **82,** 358-370.

Chamberlin, H. M. and Sternberg, P. W. (1993). Multiple cell interactions are required for fate specification during male spicule development in *Caenorhabditis elegans*. *Development* **118,** 297-324.

Chamberlin, H. M. and Sternberg, P. W. (1995). Mutations in the *Caenorhabditis elegans* gene vab-3 reveal distinct roles in fate specification and unequal cytokinesis in an asymmetric cell division. *Dev. Biol.* **170,** 679-89.

Chen, W.-T. (1992). Membrane proteases: roles in tissue remodeling and tumour invasion. *Current Oinion in Cell Biology* **4,** 802-809.

Cheng, H. J., Nakamoto, M., Bergemann, A. D. and Flanagan, J. G. (1995). Complementary gradients in expression and binding of ELF-1 and Mek4 in development of the topographic retinotectal projection map. *Cell* **82,** 371-81.

Chisholm, A. (1991). Control of cell fate in the tail region of *C. elegans* by the gene egl-5. *Development* **111,** 921-32.

Chow, K. L. and Emmons, S. W. (1994). HOM-C/Hox genes and four interacting loci determine the morphogenetic properties of single cells in the nematode male tail. *Development* **120,** 2579-2593.

Clark, E. and Brugge, J. (1995). Integrins and signal transduction pathways: the road taken. *Science* **268,** 233-239.

Clark, S. G., Chisholm, A. D. and Horvitz, H. R. (1993). Control of Cell fates in the central body region of *C. elegans* by the homeobox gene *lin-39*. *Cell* **74,** 43-55.

Colamarino, S. A. and Tessier-Lavigne, M. (1995). The axonal chemoattractant netrin-1 is also a chemorepellent for trochlear motor axons. *Cell* **81,** 621-9.

Collins, J., Saari, B. and Anderson, P. (1987). Activation of a transosable element in the germline but not the soma of *C. elegans*. *Nature* **328,** 726-728.

Costa, M., Weir, M., Coulson, A., Sulston, J. and Kenyon, C. (1988). Posterior pattern formation in *C. elegans* involves position-specific expression of a gene containing a homeobox. *Cell* **55,** 747-56.

Cowing, D. and Kenyon, C. (1992). Expression of the homeotic gene *mab-5* during *Caenorhabditis elegans* embryogenesis. *Development* **116,** 481-490.

Desai, C., Garriga, G., McIntire, S. L. and Horvitz, H. R. (1988). A genetic pathway for the development of the *Caenorhabditis elegans* HSN motor neurons. *Nature* **336,** 638-46.

Desai, C. and Horvitz, H. R. (1989). *Caenorhabditis elegans* mutants defective in the functioning of the motor neurons responsible for egg laying. *Genetics* **121,** 703-21.

Devore, D. L., Horvitz, H. R. and Stern, M. J. (1995). An FGF receptor signalling pathway is required for the normal cell migrations of the sex myoblasts in *C. elegans* hermaphrodites. *Cell* **83,** 611-20.

Dibb, N., Brown, D., Karn, J., Moerman, D., Bolten, S. and Waterston, R. (1985). Sequence analysis of mutations that affect the synthesis, assembly and enzymatic activity of unc-54 myosin heavy chain of C elegans. *J. Mol. Biol.* **183,** 543-551.

Dimilla, P., Stone, J., Quinn, J., ALbelda, S. and Lauffenburger, D. (1993). Maximal migration of human smooth muscle cells on fibronectin and type IV collagen occurs at an intermediate attachment strength. *J. Cell Biol.* **122,** 729-737.

Dodd, J. and Schuchardt, A. (1995). Axon guidance: a compelling case for repelling growth cones. *Cell* **81,** 471-474.

Donovan, M., Miranda, R., Kraemer, R., McCaffrey, T., Tessarollo, L., Mahadeo, D., Sharif, S., Kaplan, D., Tsoulfas, P., Parada, L. and al., e. (1995). Neurotrophin and neurotrophin receptors in vascular smooth muscle cells. Regulation of expression in response to injury. *American Journal of Pathology* **147,** 309-24.

Drescher, U., Dremoser, C., Handwerker, C., Loschinger, J., Noda, M. and Bonhoeffer, F. (1995). In vitro guidance of retinal ganglion cell axons by RAGS, a 25 kDa tectal protein related to ligands for Eph receptor tyrosine kinases. *Cell* **82,** 359-70.

Drubin, D. G. and Nelson, W. J. (1996). Origins of cell polarity. *Cell* **84,** 335-344.

Emmons, S. W. (1988). The Genome. In *The Nematode Caenorhabditis elegans,* (ed. W. B. Wood), pp. 47-79. Cold Spring Harbor, New York: Cold Spring Harbor Laboratory.

Ferguson, E. and Horvitz, H. (1985). Identification and characterization of 22 genes that affect the vulval cell lineages of the nematode *C. elegans. Genetics* **110,** 17-72.

Fire, A., Harrison, S. W. and Dixon, D. (1990). A modular set of lacZ fusion vectors for studying gene expression in *Caenorhabditis elegans. Gene* **93,** 189-98.

Fixsen, W. D. 1985. The genetic control of hypodermal lineages during nematode develoment. Ph.D., Massachusetts Institue of Technology,

Francis, R. and Waterston, R. H. (1991). Muscle cell attachment in *Caenorhabditis elegans. J Cell Biol* **114,** 465-79.

Garriga, G., Desai, C. and Horvitz, H. R. (1993). Cell interactions control the direction of outgrowth, branching and fasciculation of the HSN axons of *Caenorhabditis elegans. Development* **117,** 1071-87.

Garriga, G. and Stern, M. J. (1994). Hams and Egls: genetic analysis of cell migration in *Caenorhabditis elegans*. *Current Opinion in Genetics and Development* **4,** 575-80.

Gavis, E. R. (1995). Pattern formation. *Gurken* meets *torpedo* for the first time. *Current Biology* **5,** 1252-4.

Gettner, S. N. 1994. Betapat-3, a *C. elegans* integrin beta subunit. Ph.D., University of California, San Francisco,

Giancotti, F. and Ruoslahti, E. (1990). Elevated levels of the a5b1 fibronectin receptor suppresses the transformed phenotype of chinese hamster ovary cells. *Cell* **60,** 849-859.

Godin, I., Wylie, C. and Heasman, J. (1990). Genital ridges exert long-range effects on mouse primordial germ cell numbers and direction of migration in culture. *Development* **108,** 357-363.

Gubb, D. (1993). Genes controlling cellular polarity in *Drosophila*. *Development* **Supplement,** 269-277.

Hamelin, M., Scott, I. M., Way, J. C. and Culotti, J. G. (1992). The *mec-7* beta-tubulin gene of *Caenorhabditis elegans* is expressed primarily in the touch receptor neurons. *EMBO Journal* **11,** 2885-93.

Hawkins, R. L. and Seeds, N. W. (1989). Protease inhibitors influence the direction of neurite outgrowth. *Developmental Brain Research* **45,** 203-209.

Hedgecock, E. M., Culotti, J. G. and Hall, D. H. (1990). The *unc-5, unc-6* and *unc-40* genes guide circumferential migrations of pioneer axons and mesodermal cells on the epidermis in *C. elegans*. *Neuron* **4,** 61-85.

Hedgecock, E. M., Culotti, J. G., Hall, D. H. and Stern, B. D. (1987). Genetics of cell and axon migrations in *Caenorhabditis elegans*. *Development* **100,** 365-82.

Herman, M. A. and Horvitz, H. R. (1994). The *Caenorhabditis elegans* gene *lin-44* controls the polarity of asymmetric cell divisions. *Development* **120,** 1035-47.

Herman, M. A., Vassilieva, L., Horvitz, H. R., Shaw, J. E. and Herman, R. K. (1995). The *C. elegans* gene *lin-44*, which controls the polarity of certain asymmetric cell divisions, encodes a Wnt protein and acts cell nonautonomously. *Cell* **83,** 101-10.

Hodgkin, J., Edgley, M., Riddle, D. L. and Albertson, D. G. (1988). Appendix 4, Genetics. In *The Nematode Caenorhabditis elegans*, (ed. W. B. Wood), Cold Spring Harbor, New York: Cold Spring Harbor Laboratory.

Horvitz, H. and Herskowitz, I. (1992). Mechanisms of asymmetric cell division: two Bs or not two Bs, that is the question. *Cell* **68,** 237-55.

Hotary, K. B. and Robinson, K. R. (1990). Endogenous electrical currents and the resultant voltage gradients in the chick embryo. *Dev. Biol.* **140,** 149-160.

Howard, K. (1990). The Blastoderm Prepattern. *Seminars in Cell Biology* **1,** 161-72.

Hursh, D. A., Padgett, R. W. and Gelbart, W. M. (1993). Cross regulation of decapentaplegic and Ultrabithorax transcription in the embryonic visceral mesoderm of *Drosophila*. *Development* **117,** 1211-22.

Huttenlocher, A., Sandborg, R. R. and Horwitz, A. F. (1995). Adhesion in cell migration. *Current Opinion in Cell Biology* **7,** 697-706.

Hyman, A. A. (1989). Centrosome movement in the early divisions of *Caenorhabditis elegans*: a cortical site determining centrosome position. *J Cell Biol* **109,** 1185-93.

Ingham, P. (1991). Segment Polarity Genes and Cell Patterning within the *Drosophila* body segment. *Current Opinion in Genetics and Development* **1,** 261-7.

Ishii, N., Wadsworth, W. G., Stern, B. D., Culotti, J. G. and Hedgecock, E. (1992). UNC-6, a laminin-related protein, guides cell and pioneer axon migrations in *C. elegans*. *Neuron* **9,** 873-81.

Jacobson, L. A., Jen, J. L., Hawdon, J. M., Owens, G. P., Bolanowski, M. A., Emmons, S. W., Shah, M. V., Pollock, R. A. and Conklin, D. S. (1988). Identification of a putative structural gene for cathepsin D in *Caenorhabditis elegans*. *Genetics* **119,** 355-63.

Kennedy, T. E., Serafini, T., de la Torre, J. R. and Tessier-Lavigne, M. (1994). Netrins are diffusible chemotropic factors for commissural axons in the embryonic spinal cord. *Cell* **78,** 425-35.

Kenyon, C. (1986). A gene involved in the development of the posterior body region of *C. elegans*. *Cell* **46,** 477-487.

Klingensmith, J. and Nusse, R. (1994). Signaling by wingless in *Drosophila*. *Dev. Biol.* **166,** 396-414.

Klymkowsky, M. W. and Parr, B. (1995). The Body language of cells: the intimate connection between cell adhesion and behavior. *Cell* **83,** 5-8.

Krasnow, R. E. and Adler, P. N. (1994). A single *frizzled* protein has a dual function in tissue polarity. *Development* **120,** 1883-1893.

Kropf, D. L., Kloareg, B. and Quatrano, R. S. (1988). Cell wall is required for fixation of the embryonic axis in *Fucus* zygotes. *Science* **239,** 187-190.

Krumlauf, R. (1994). Hox Genes in Vertebrate Development. *Cell* **78,** 191-201.

Lawrence, P. A. (1992). *The making of a fly*. Oxford: Blackwell Scientific Publications

Lawrence, P. A. and Morata, G. (1994). Homeobox Genes: Their Function in *Drosophila* Segmentation and Pattern Formation. *Cell* **78,** 181-190.

Ma, C. and Moses, K. (1995). *wingless* and *patched* are negative regulators of the morphogenetic furrow and can affect tissue polarity in the developing *Drosophila* compound eye. *Development* **121,** 2279-2289.

Marczynski, G. T. and Shapiro, L. (1995). The control of asymmetric gene expression during Caulobacter cell differentiation. *Archives of Michrobiology* **163,** 313-21.

McCaig, C. D. (1988). Nerve guidance: A role for bio-electric fields? *Progress in Neurobiology* **30,** 449-468.

Monard, D. (1988). Cell-derived proteases and protease inhibitors as regulators of neurite outgrowth. *Trends in Neurosciences* **11,** 541-4.

Montell, D. J. (1994). Moving right along: regulation of cell migration during *Drosophila* development. *Trends Genet.* **10,** 59-62.

Orlando, V. and Paro, R. (1995). Chromatin multiprotein complexes involved in the maintenance of transcription patterns. *Current Opinion in Genetics and Development* **5,** 174-9.

Park, W. J., Liu, J. and Adler, P. N. (1994). The frizzled gene of *Drosophila* encodes a membrane protein with an odd number of transmembrane domains. *Mechanisms of Development* **45,** 127-37.

Peifer, M. and Bejsovec, A. (1992). Knowing your neighbors: cell interactions determine intrasegmental patterning in *Drosophila. Trends Genet.* **8,** 243-249.

Pirrotta, V. (1995). Chromatin complexes regulating gene expression in *Drosophila. Current Opinion in Genetics and Development* **5,** 466-72.

Podbilewicz, B. and White, J. G. (1994). Cell Fusions in the developing epithelia of *C. elegans. Dev. Biol.* **161,** 408-424.

Porter, B. E., Weis, J. and Sanes, J. R. (1995). A motoneuron-selective stop signal in the synaptic protein S-laminin. *Neuron* **1995,**

Quatrano, R. S., Brawley, S. H. and Hogsett, W. E. (1979). In *Determinants of Spatial Organization,* (ed. S. Subtelny and I. R. Koenigsberg), New York: Academic Press.

Rhyu, M. S. and Knoblich, J. A. (1995). Spindle orientation and asymmetric cell fate. *Cell* **82,** 523-6.

Robinson, N. T. 1995. Genetic Analysis of Neuroblast Migration in *Caenorhabditis elegans*. Ph.D., University of California, San Francisco,

Rosenquist, T. A. and Kimble, J. (1988). Molecular cloning and transcript analysis of *fem-3,* a sex-determination gene in *Caenorhabditis elegans. Genes Dev.* **2,** 606-616.

Salser, S. and Kenyon, C. (1991). Activation of a *C. elegans Antennapedia* homolog within migrating cells controls their direction of migration. *Nature* in press.

Salser, S., Loer, C. and Kenyon, C. (1993). Multiple HOM-C gene interactions specify cell fates in the nematode central nervous system. *Genes Dev.* **7,** 1714-1724.

Salser, S. J. and Kenyon, C. (1996). A *C. elegans* Hox Gene Switches ON, OFF, ON, and OFF Again to Regulate Proliferation, Differentiation, and Morphogenesis. *Development* **in press,**

Seedorf, K. (1995). Intracellular signalling by growth factors. *Metabolism: Clinical and Experimental* **44,** 24-32.

Serafini, T., Kennedy, T. E., Galko, M. J., Mirazayan, C., Jessel, T. M. and Tessier-Lavigne, M. (1994). The netrins define a family of axon outgrowth promoting proteins homologous to *C. elegans* UNC-6. *Cell* **78,** 409-424.

Shaller, D., Wittmann, C., Spicher, A., Muller, F. and Tobler, H. (1990). Cloning and analysis of three new homeobox genes from the nematode *Caenorhabditis elegans*. *Nucleic Acids Res.* **18,** 2033-6.

Shupbach, T. and Roth, S. (1994). Dorsoventral patterning in *Drosophila* oogenesis. *Current Opinion in Genetics and Development* **4,** 502-7.

Simon, J. (1995). Locking in stable states of gene expression: transcriptional control during *Drosophila* development. *Current Opinion in Cell Biology* **7,** 376-85.

Slack, J. M. (1994). Inducing factors in Xenopus early embryos. *Current Biology* **4,** 116-26.

Smith, L. G., Hake, S. and Sylvester, A. W. (1996). The *tangled-1* mutation alters cell division orientations throughout maize leaf development without altering leaf shape. *Development* **122,** 481-89.

Sternberg, P. W. and Horvitz, H. R. (1988). *lin-17* mutations of *Caenorhabditis elegans* disrupt certain asymmetric cell divisions. *Dev Biol* **130,** 67-73.

Stringham, E. G. and Candido, E. P. (1993). Targeted single-cell induction of gene products in *Caenorhabditis elegans*: a new tool for developmental studies. *J. Exp. Zool.* **266,** 227-33.

Sulston, J., Du, Z., Thomas, K., Wilson, R., Hillier, L., Staden, R., Halloran, N., Green, P. and Theirry-Mieg, J. (1992). The *C. elegans* genome sequencing project: a beginning. *Nature* **356,** 37-41.

Sulston, J. and Hodgkin, J. (1988). Methods. In *The Nematode Caenorhabditis elegans*, (ed. W. B. Wood), pp. 587-605. Cold Spring Harbor, New York: Cold Spring Harbor Laboratory.

Sulston, J. and Horvitz, H. (1977). Post-embryonic cell lineages of the nematode, *C elegans*. *Dev. Biol.* **56,** 110-156.

Sulston, J., Schierenberg, E., White, J. and Thomson, J. (1983). The embryonic cell lineage of the nematode *C elegans*. *Dev. Biol.* **100,** 64-119.

Sulston, J. and White, J. (1980). Regulation and cell autonomy during postembryonic development of *C. elegans*. *Dev. Biol.* **78,** 577-597.

Tamkun, J. W. (1995). The role of *brahma* and related proteins in transcription and development. *Current Opinion in Genetics and Development* **5,** 473-7.

Teragawa, C. and Bode, H. (1990). Spatial and temporal patterns of interstitial cell migration in *Hydra vulgaris*. *Dev. Biol.* **138,** 63-81.

Tessier-Lavigne, M. (1995). Eph receptor tyrosine kinases, axon repulsion, and the development of topographic maps. *Cell* **82,** 345-8.

Theisen, H., Prucell, J., Bennett, M., Kansagara, D., Syed, A. and Marsh, J. L. (1994). *dishevelled* is required during *wingless* signalling to establish both cell polarity and cell identity. *Development* **120,** 347-360.

Thuringer, F. and Bienz, M. (1993). Indirect autoregulation of a homeotic *Drosophila* gene mediated by extracellular signalling. *Proc. Natl. Acad. Sci. USA* **90,** 3899-903.

Tremml, G. and Bienz, M. (1992). Induction of labial expression in the *Drosophila* endoderm: response elements for dpp signalling and for autoregulation. *Development* **116,** 447-56.

Trent, C., Tsung, N. and Horvitz, H. (1983). Egg-laying defective mutants of the nematode C elegans. *Genetics* **104,** 619-647.

Vinson, C. and Adler, P. N. (1987). Directional non-cell autonomy and the transmission of polarity information by the *frizzled* gene of *Drosophila*. *Nature* **329,** 549-551.

Waddle, J. A., Cooper, J. A. and Waterston, R. H. (1994). Transient localized accumulation of actin in *Caenorhabditis elegans* blastomeres with oriented asymmetric divisions. *Development* **120,** 2317-2328.

Wang, B. B., Müller-Immergluck, M. M., Austin, J., Robinson, N. T., Chisholm, A. and Kenyon, C. (1993). A Homeotic Gene Cluster Patterns the Anteroposterior Body Axis of *C. elegans*. *Cell* **74,** 29-42.

Waring, D. A. and Kenyon, C. (1990). Selective silencing of cell communication influences anteroposterior pattern formation in *C. elegans*. *Cell* **60,** 123-31.

Waring, D. A. and Kenyon, C. (1991). Regulation of cellular responsiveness to inductive signals in the developing *C. elegans* nervous system. *Nature* **350,** 712-5.

Waring, D. A., Wrischnik, L. and Kenyon, C. (1992). Cell signals allow the expression of a pre-existent neural pattern pattern in *C. elegans*. *Devel. Biol.* **in press,**

Way, J., Run, J. and Wang, A. (1992). Regulation of anterior cell-specific *mec-3* expression during asymmetric cell division in *C. elegans*. *Developmental Dynamics* **194,** 289-302.

Way, J. C. and Chalfie, M. (1988). *mec-3*, a homeobox-containing gene that specifies differentiation of the touch receptor neurons in *C. elegans*. *Cell* **54,** 5-16.

Way, J. C., Wang, L., Run, J. Q. and Hung, M. S. (1994). Cell polarity and the mechanism of asymmetric cell division. *Bioessays* **16,** 925-31.

Wehrli, M. and Tomlinson, A. (1995). Epithelial planar polarity in the developing *Drosophila* eye. *Development* **121,** 2451-2459.

White, J., Southgate, E., Thomson, J. and Brenner, S. (1986). The structure of the nervous system of the nematode *C. elegans*. *Philosophical Transactions of the Royal Society of London* **314B,** 1-340.

Wightman, B., Clark, S. G., Taskar, A. M., Forrester, W. C., Maricq, A. V., Bargmann, C. I. and Garriga, G. (1996). The *C. elegans* gene *vab-8* guides posteriorly directed axon outgrowth and cell migration. *Development* **122,** 671-682.

Williams, B. D., Schrank, B., Huynh, C., Shownkeen, R. and Waterston, R. H. (1992). A genetic mapping system in *Caenorhabditis elegans* based on polymorphic sequence-tagged sites. *Genetics* **131,** 609-624.

Wrischnik. 1995. The role of the *lin-22* gene in patterning the *C. elegans* lateral ectoderm. Ph.D., University of California, San Francisco,

Xie, G. Y., Jia, Y. and Aamodt, E. (1995). A *C. elegans* mutant screen based on antibody or histochemical staining. *Genetic Analysis: Biomolecular Engineering* **12,** 95-100.

Yandell, M. D., Edgar, L. G. and Wood, W. B. (1994). Trimethylpsoralen induces small deletion mutations in *Caenorhabditis elegans*. *Proceedings of the National Academy of Sciences USA* **91,** 1381-1385.

Zheng, L., Zhang, J. and Carthew, R. W. (1995). *frizzled* regulates mirror-symmetric pattern formation in the *Drosophila* eye. *Development* **121,** 3045-3055.

Appendix A: A Comparison of the HSN and Q descendant Mig phenotypes in different *egl-20* alleles

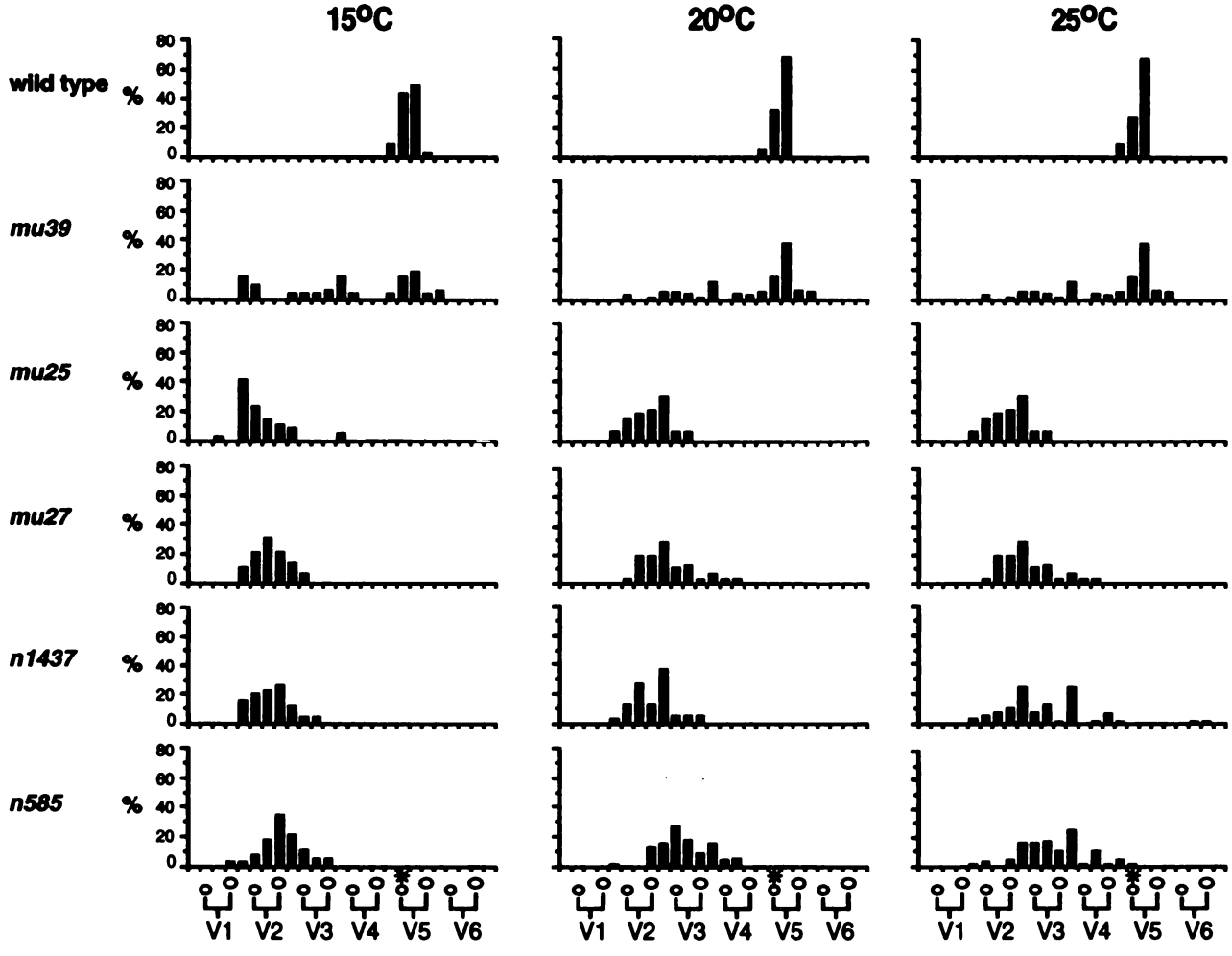

Fig. A.1. Position of the QL.pa daughters, PVM and SDQL, in different *egl-20* alleles at different temperatures. Position was determined relative to the positions of the Vn.p and Vn.a cells, indicated below, as described in Chapter 2. The asterisk indicates the birthplace of QL. More than 24 animals of each genotype were examined.

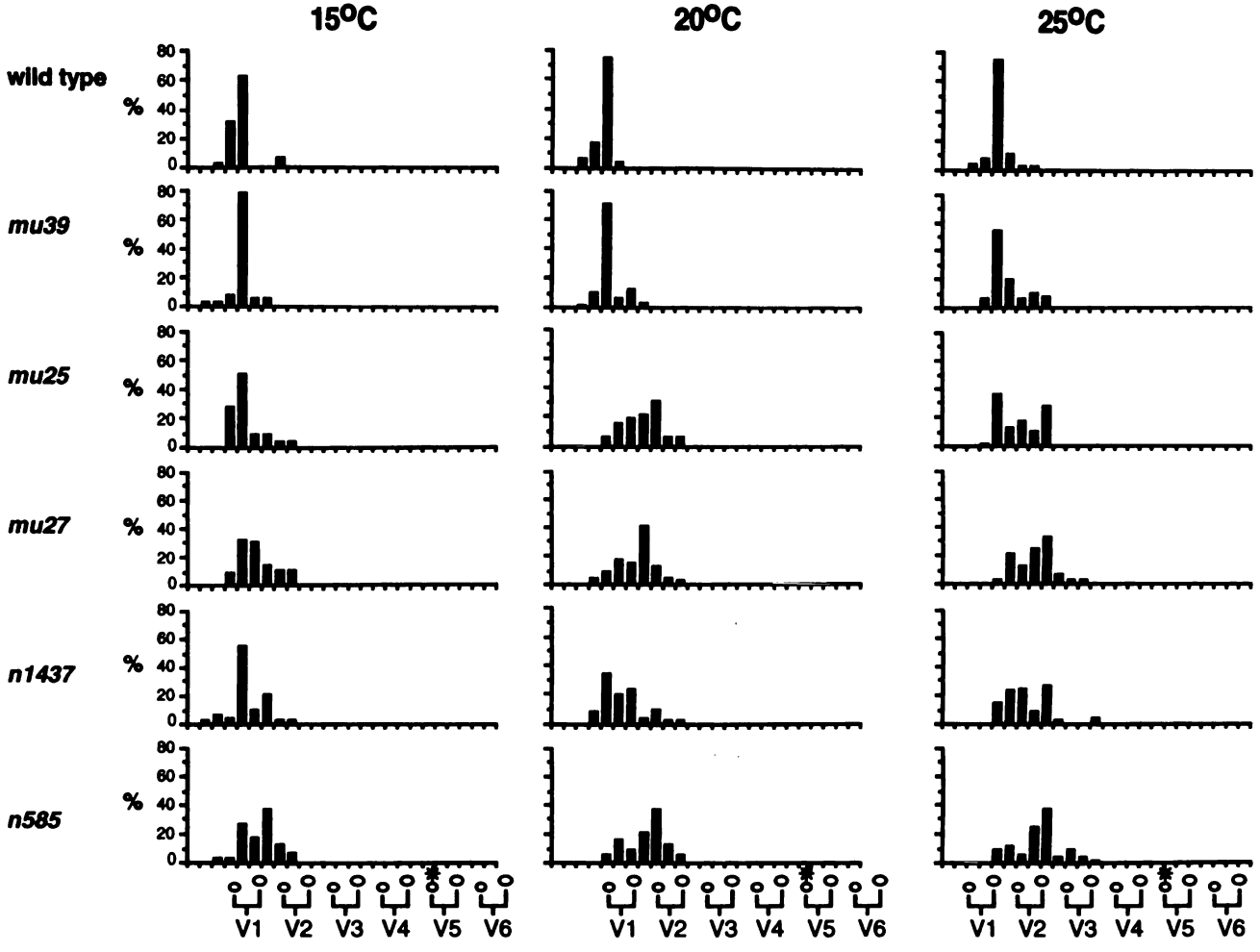

Fig. A.2. Position of the QR.pa daughters, AVM and SDQR, in different *egl-20* alleles at different temperatures. Position was determined relative to the positions of the Vn.p and Vn.a cells, indicated below, as described in Chapter 2. The asterisk indicates the birthplace of QR. More than 24 animals of each genotype were examined.

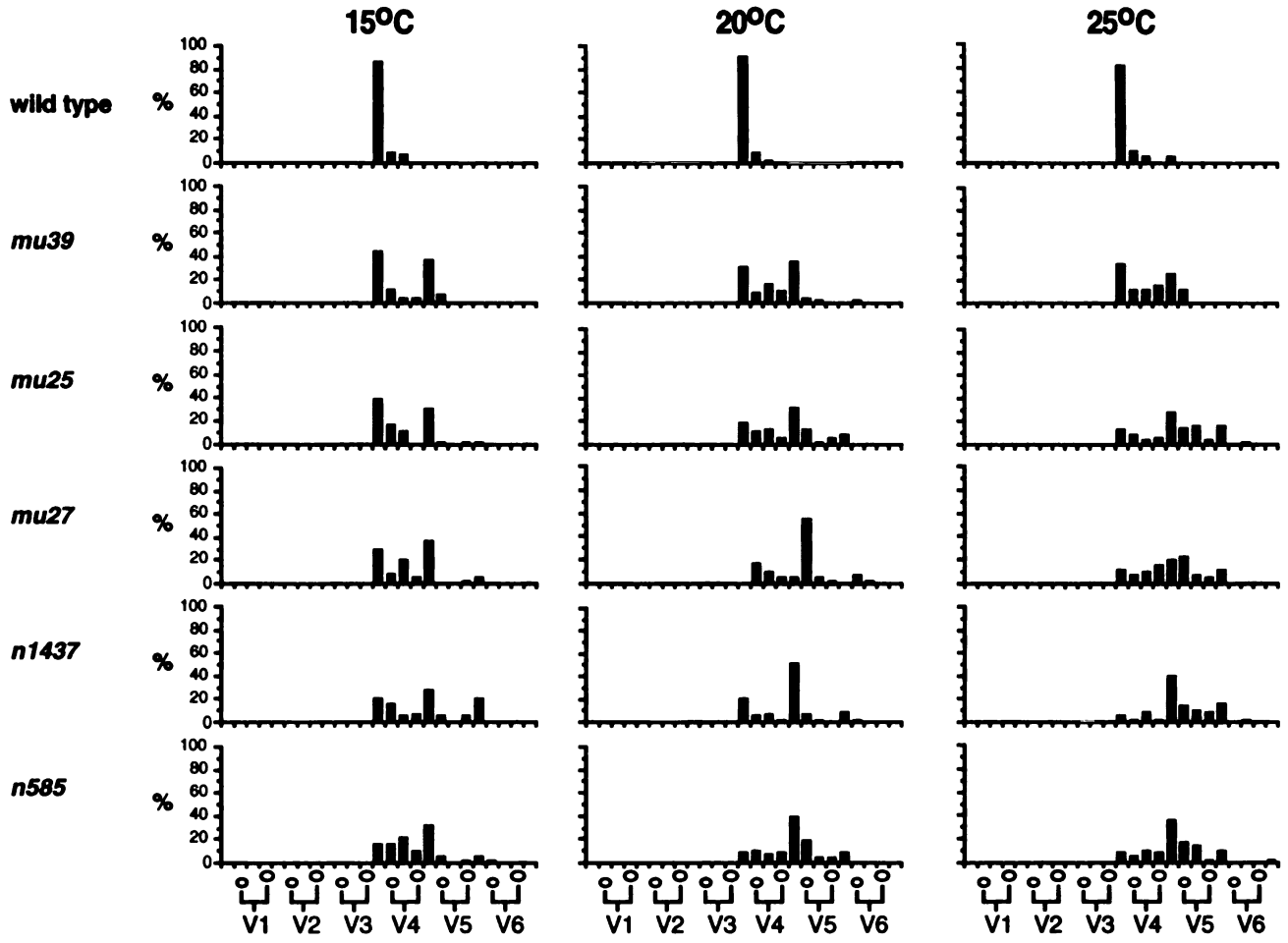

Fig. A.3. Position of the HSN neuron in different *egl-20* alleles at different temperatures. Position was determined relative to the positions of the Vn.p and Vn.a cells, indicated below, as described in Chapter 2. More than 25 animals of each genotype were examined.

Appendix B: A Comparison of the distal tip cell migrations in wild-type and *egl-20* mutant worms.

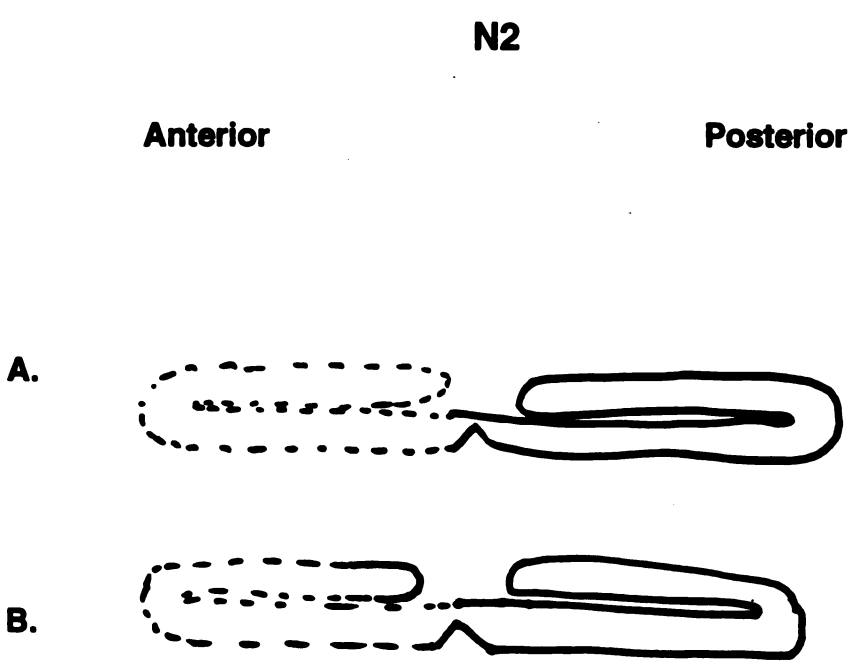

B.1. Migrations of the distal tip cells (DTC's) in wild-type (N2) L4 hermaphrodites grown at 25°C. The dashed line indicates the portion of the gonad on the right side of the worm. The solid line indicates the portion of the gonad on the left side. A. A normal gonad: the anterior gonad arm is on the right side of the worm and the posterior gonad arm is on the left side. B. A gonad in which the tip of the anterior arm has crossed over to the left side. This phenotype was observed in 3/20 (15%) of wild-type hermaphrodites raised at 25°C. More severe defects were observed in 2/20 wild-type worms (10%; data not shown).

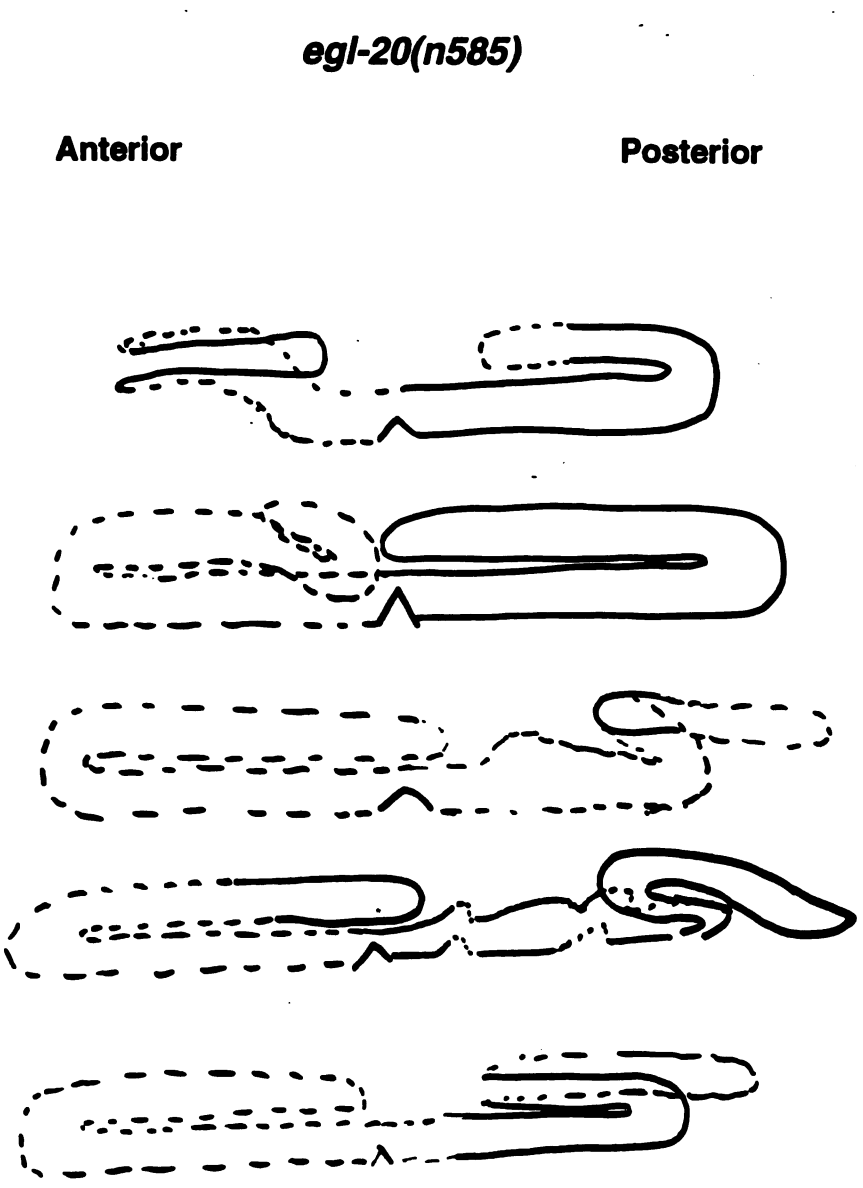

B.2. Abnormal migration of the DTC's in five L4 *egl-20* mutant hermaphrodites grown at 25°C. Migration defects of this severity were observed in 13/24 (54%) of *egl-20* mutant hermaphrodites. (Compare to 10% in wild-type, Fig. B.1) The dashed line indicates the portion of the gonad on the right side of the worm. The solid line indicates the portion of the gonad on the left side.

Appendix C: Production and position of the M-derived coelomocyte in wild-type and mutant worms

genotype	% cc+	(n)	% 2 cc's/side
wild-type	100%	30	0%
egl-20(n585)	53%	43	5%
lin-17(n671)	84%	25	12%
mig-1(e1787)	86%	29	3%

Table C.1. Mutations in *egl-20, lin-17* and *mig-1* affect the production of M-derived coelomocytes (cc's) in hermaphrodites. The M mesoblast produces two coelomocytes, one on the left and one on the right. Only one side of each worm was examined. No difference in frequency was observed between the left and the right sides. In some animals two M-derived coelomocytes were observed on one side (see far right column), suggesting that in some animals one coelomocyte had slipped over to the other side. However, this frequency was too low to account for all the missing coelomocytes. The data in this table are from animals raised at 25°C. The frequency of missing coelomocytes in *egl-20(n585)* mutants at 20°C was not significantly different: 58% of hermphrodites were missing an M-derived coelomocyte (n= 38).

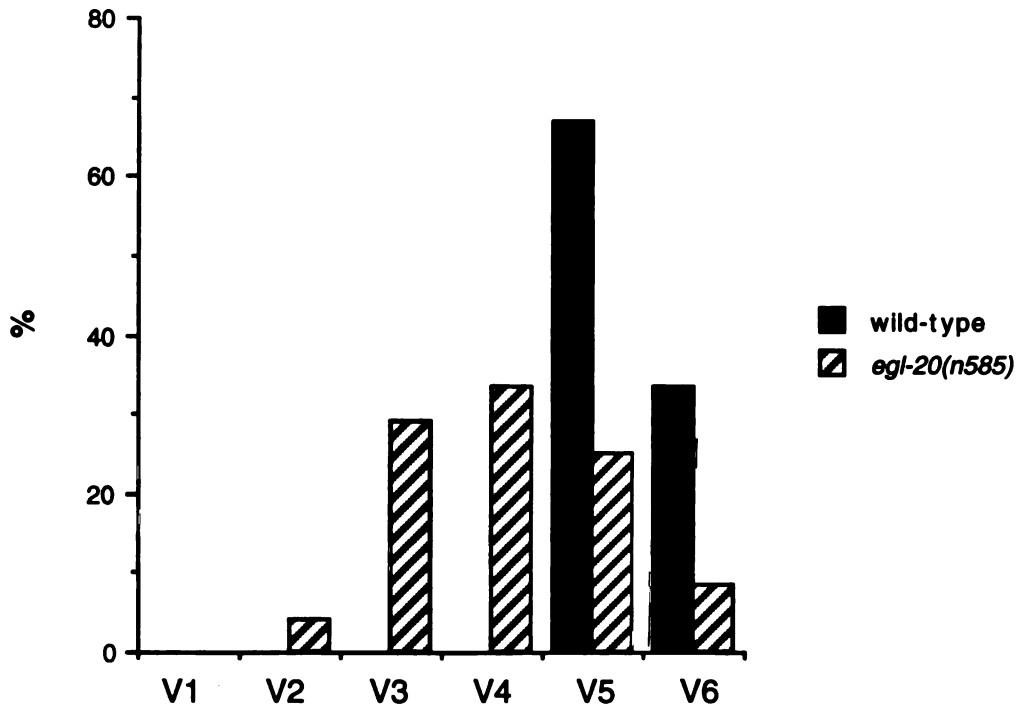

Fig. C.1. M-derived coelomocytes can be found in more anterior positions in *egl-20* mutants. Positions of M-derived coelomocytes were determined relative to the descendants of the six V cells (x-axis). Coelomocyte positions were determined in L4 or L3 hermaphrodites raised at 25°C. Wild-type, n=30; *egl-20*, n=43.

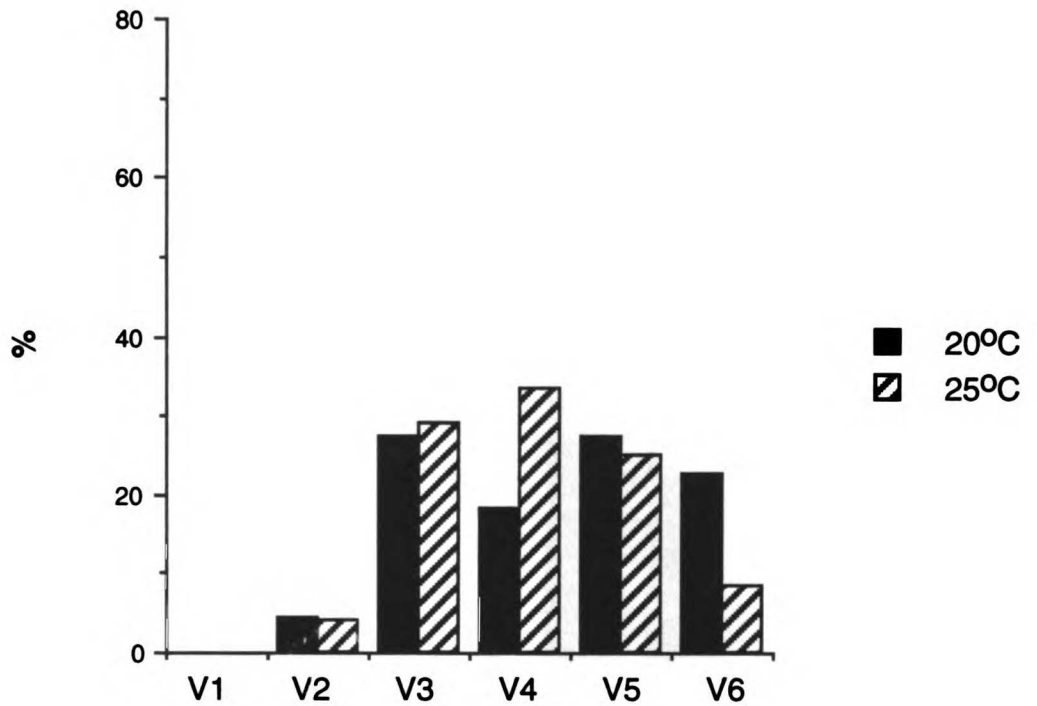

Fig. C.2. Position of the M-derived coelomocytes in *egl-20* mutants is similar at 20 and 25°C. Coelomocyte position was determined relative to the descendants of the six V cells (x-axis) in L4 or L3 hermaphrodites. n=43 for animals raised at 25°C, and n=38 for animals raised at 20°C.

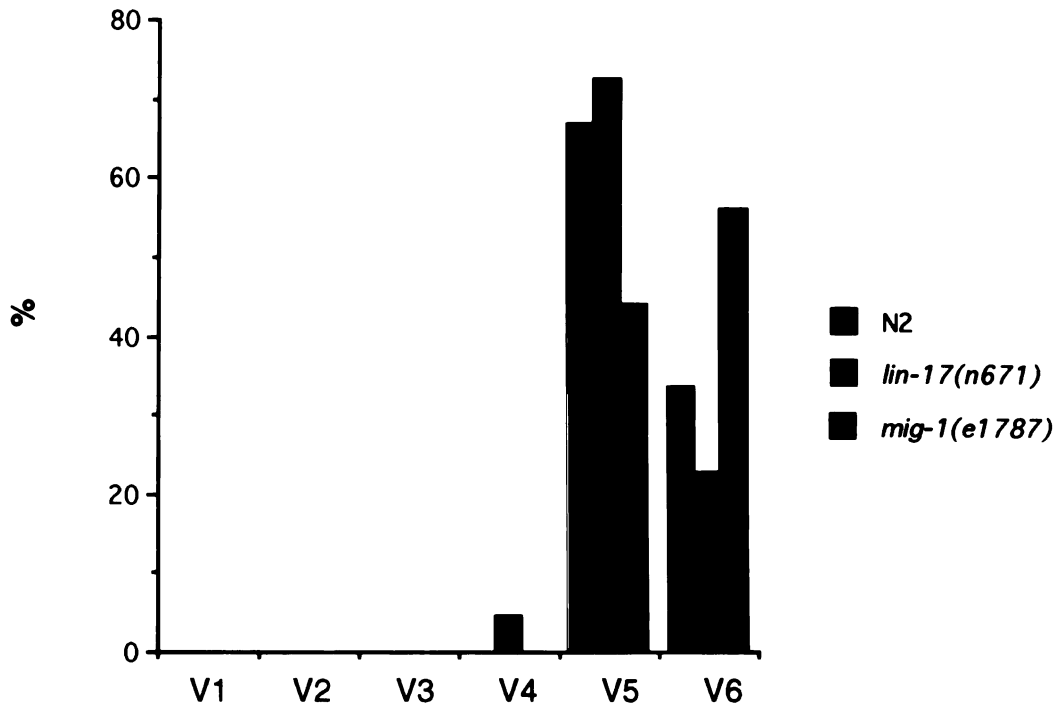

Fig. C.3. Mutations in *lin-17* and *mig-1* do not alter the position of M-derived coelomocytes along the A/P axis in hermaphrodites. Position of M-derived coelomocytes were determined relative to the descendants of the six V cells (x-axis). Coelomocyte positions were determined in L4 or L3 hermaphrodites raised at 25°C. $n \geq 25$ for all genotypes.

Appendix D: *mab-5* expression in *egl-20(mu39)* and *unc-40(e271)* mutants

	A.				B.	
	***mab-5* Ab staining in QL.a and QL.p**				**Position of QL.pa desc.**	
genotype	**% bright**	**% faint**	**% none**	**(n)**	**% posterior**	**(n)**
wild type	**98**	2	0	(94)	**100**	(50)
egl-20(n585)	**0**	0	100	(27)	**4**	(50)
egl-20(mu39)	**71**	29	0	(24)	**34**	(25)
unc-40(e271)	**38**	41	21	(29)	**48**	(51)JA

Table D.1. Frequency of *mab-5* Ab staining in the QL daughters in *egl-20(mu39)* and *unc-40(e271)* mutants.

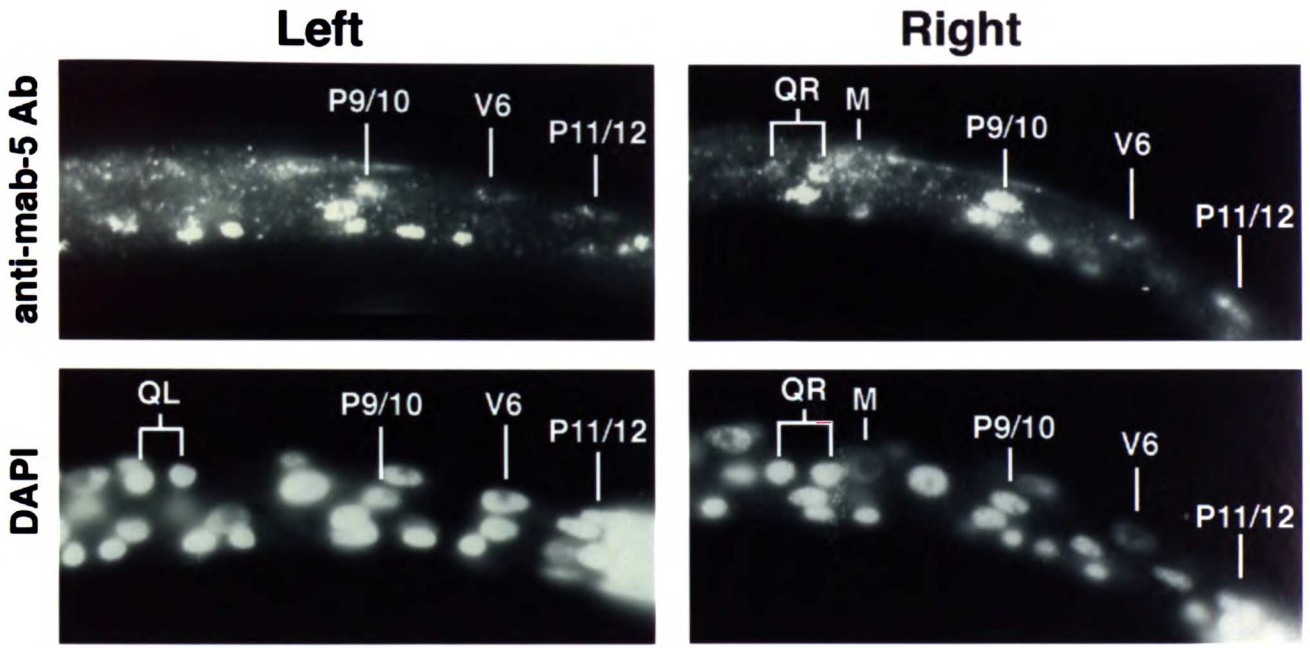

Fig. D.1. In unc-40(e271) mutants, the daughters of QL sometimes fail to express mab-5, whereas the daughters of QR sometimes ectopically express mab-5. Staining shown is of 3-6 hour old unc-40 mutants raised at 25 degrees C. The staining protocol is as described in Chapter 2.

Appendix E: The *mu112* mutation partially fails to complement the *egl-20(mu39)* mutation

Background:

mu112 was isolated by Deborah Cowing in a clonal screen for animals with misplaced Q descendants. The mutagen was EMS (Brenner, 1974). The *mu112* phenotypes, after one outcross, are: anterior migration of QL descendants (33%) and a broader distribution of QR.pa positions than wild-type (D. Cowing and C. Kenyon, unpublished data). The *mu112* phenotypes have only been analyzed at 25 degrees.

Together, Deborah Cowing and Lee Honigberg have shown that *mu112* fully complements *mig-14(mu71)* at 25 degrees (D. Cowing, L. Honigberg and C. Kenyon, unpublished data).

Results

mu112 partially fails to complement the weak *egl-20* allele, *mu39*.

genotype	%QL.d cells Anterior	(n)
mu39/mu39	66%	(25)
mu39/+	0%	(114)
mu112/mu112	34%	(22)
mu112/+	0%	(31)
mu39/mu112	13%	(30)

Table E.1. *mu112* partially fails to complement the weak *egl-20* allele, *mu39*. The *mu112* data in this graph is from Deborah Cowing in the lab, the *mu39* data is mine, and the *mu112/mu39* complementation test was done jointly. All the data in this table are from worms grown at 25°C.

Preliminary mapping experiments suggest that *mu112* may not be linked to the center of LGIV.

To test whether *mu112* maps the the cluster on LGIV, where the *egl-20* gene is located, I crossed males heterozygous for *unc-24(e138) dpy-20(e1282)* to *mu112* hermaphrodites. F1 hermaphrodites which segregated Unc Dpy progeny were kept. F2 progeny from these hermphrodites which were either Unc Dpy or non-Unc non-Dpy were cloned out. The position of the QL descendants was then scored in the progeny of each Unc Dpy clone. The position of the QL descendants was also scored in the progeny of non-Unc non-Dpy clones which did not segregate any Unc Dpy animals, and were thus presumably homozygous for the *mu112* LGIV.

phenotype	Mig	non-Mig
Unc Dpy	2	4
non-Unc non-Dpy	1	1

Table E.2. *mu112* appears to be unlinked to *unc-24* and *dpy-20*. More than 10 animals were scored from each F2 clone. The *mu112* Mig phenotype is not fully penetrant. In addition, anteriorly migrating QL descendants stop only a short distance anterior to wild-type. Hence it was difficult to accurately score the *mu112* phenotype. Often, only one cell was mutant out of 15 worms, and that cell was only in V4. Since this position was never seen in wild-type animals, (see Chapter 2, Table 1), these worms were scored as non-Mig.

Conclusions

Our data show that *mu112* and *egl-20(mu39)* do not fully complement one another. The two possible explanations for this are that *mu112* and *mu39* are allelic, or that *mu112* is an unlinked non-complementing mutation. Since *mu112* fully complements the *mig-14(mu71)* mutation, whose phenotype is very similar to that of the strong *egl-20* alleles, its inability to complement *mu39* is more striking. More careful mapping will be needed in order to be certain that *mu112* does NOT map to the LGIV cluster.

Together, these observations raise several questions, which are discussed in more detail in Chapter 7. Would *mu112* fail to complement a strong *egl-20* allele? Would the presence of the *mu112* mutation affect other *egl-20* mutant phenotypes, such as the HSN mig defect or the V5 polarity reversal?

Appendix F: The *lin-17* migration defect is temperature-sensitive

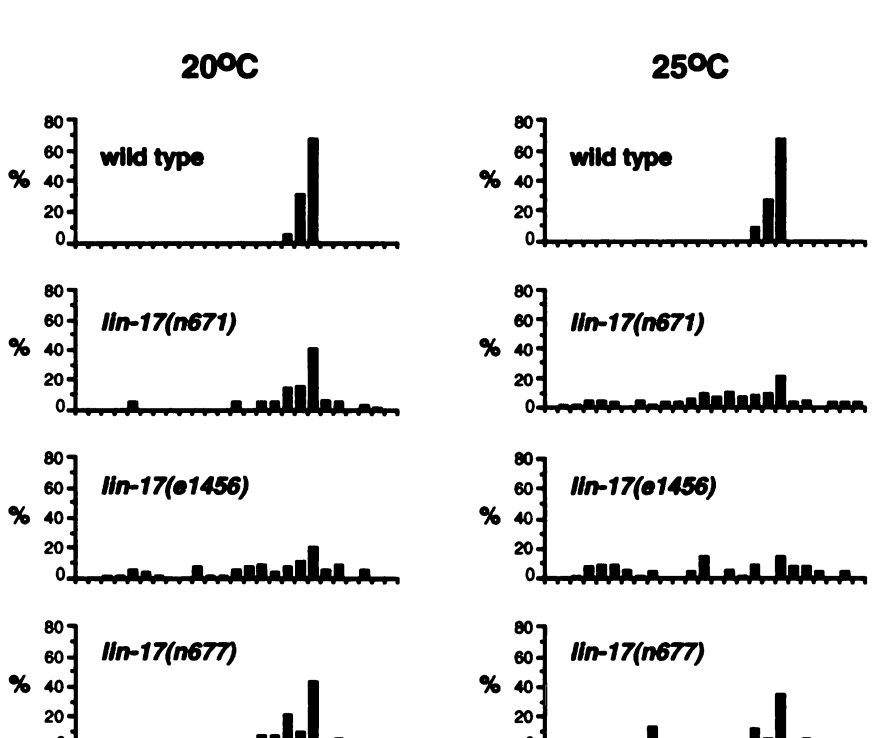

F.1 The *lin-17* mutant QL descendant migration defect is temperature-sensitive. Position was determined relative to the positions of the Vn.p and Vn.a cells, indicated below, as described in Chapter 2. The asterisk indicates the birthplace of QL. More than 24 animals of each genotype were examined.

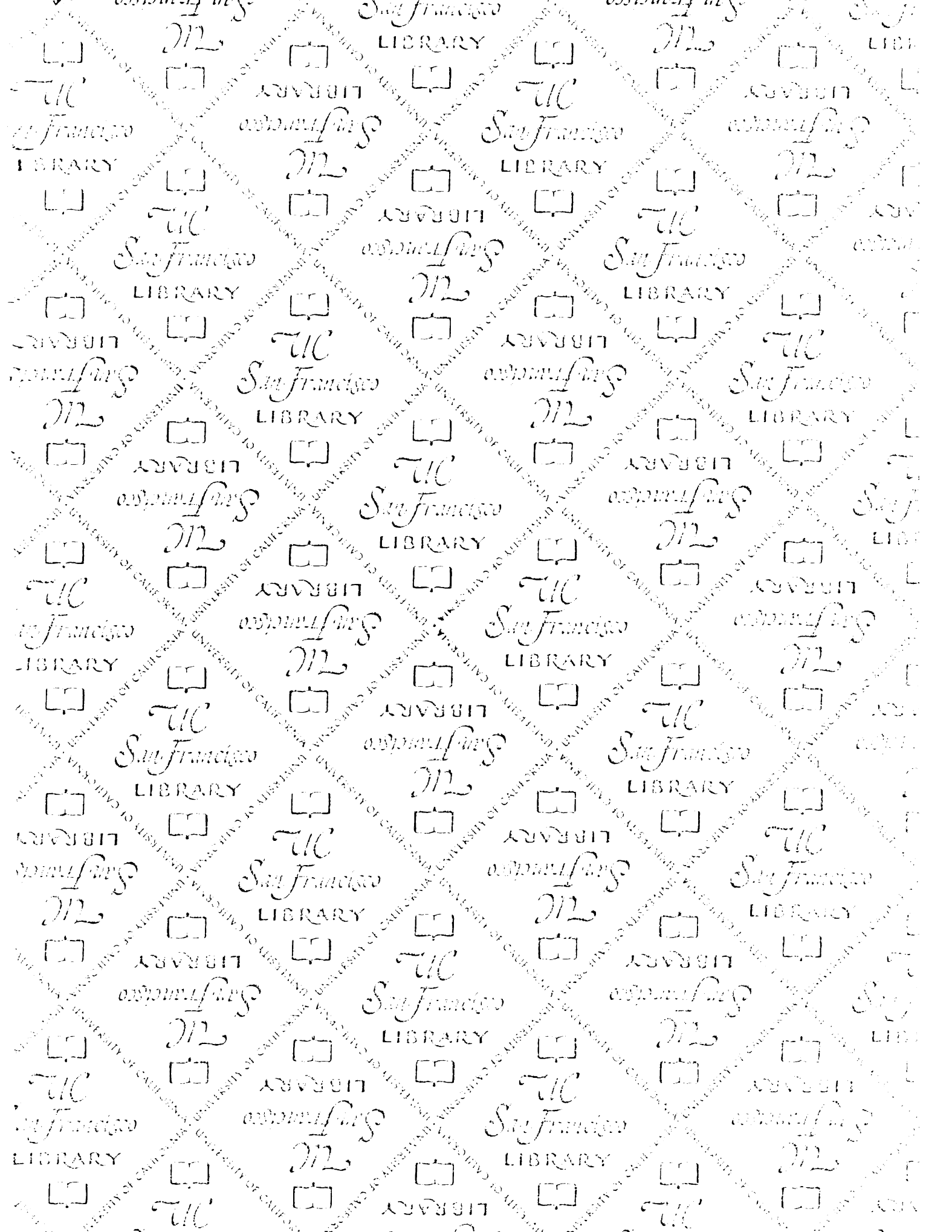
UC
San Francisco
LIBRARY
UNIVERSITY OF CALIFORNIA, SAN FRANCISCO